UNIVERSITY OF CALIFORNIA, SAN DIEGO

Solution Biophysical Characterization of the Thrombin-Thrombomodulin Interation

A dissertation submitted in partial satisfaction of the

requirements for the degree of Doctor of Philosophy

in

Chemistry

by

Nicholas Adam Treuheit

Committee in charge:

Professor Elizabeth A. Komives, Chair
Professor James Halpert
Professor J. Andrew McCammon
Professor Susan Taylor
Professor Jerry Yang

2013

The dissertation of Nicholas Adam Treuheit is approved, and it is acceptable in quality and form for publication on microfilm:

_____

_____

_____

_____

_____

Chair

University of California, San Diego

2013

DEDICATION

I dedicate this work to my Dad for getting the ball rolling,

to my Mom for helping me become someone that I like,

and to my brother and sister for teaching me strength, patience, and humility.

TABLE OF CONTENTS

LIST OF ABBREVIATIONS

Å	Angstrom
ABE1	Anion Binding Exosite 1
ABE2	Anion Binding Exosite 2
D	Dalton
DSC	Differential Scanning Calorimetry
EDTA	Ethylenediaminetetraacetic Acid
EGF-like	Epidermal Growth Factor-like
EGRCK	D-Glu-Gly-Arg chloromethylketone
FPLC	Fast Protein Liquid Chromatography
HSQC	Heteronuclear Single Quantum Coherence
ITC	Isothermal Titration Calorimetry
$k$ex	Rate constant for exchange
k_a	Association rate constant
K_a	Association equilibrium constant
k_d	Dissociation rate constant
K_d	Dissociation equilibrium constant
MALDI-TOF	Matrix-Assisted Laser Desorption Ionization with Time of Flight Detection
NMR	Nuclear Magnetic Resonance
PDB	Protein Data Bank
PPACK	D-Phe-Pro-Arg chloromethylketone

Q-TOF MS	Quadrapole Time-of- Flight Mass Spectrometer
TCEP	tris-carboxyethylphosphine
TFA	Trifluoroacetic Acid
TM	Thrombomodulin
TM45	The fourth and fifth EGF-like domains of thrombomodulin
TM456	The fourth, fifth and sixth EGF-like domains of thrombomodulin
TM456m	The fourth, fifth and 23 residues of the sixth EGF-like domain of TM
TM456t	The fourth, fifth, and 30 residues of the sixth EGF-like domain of TM
TMEGF56	The fifth and sixth EGF-like domains of thrombomodulin

LIST OF FIGURES

LIST OF TABLES

ACKNOWLEDGEMENTS

I think that it is an impossible effort to try and thank and acknowledge everyone that has helped me accomplish what is finally culminating here, but the effort to do is still an incredibly worthwhile and important endeavor. I want to thank my family, without whom I would never have been able to get all the way here. Mom and Dad are, were, and always will be relentlessly supportive. I read once that it is a parent's job to fill their child up with love before they send them out into the world and I knew it a long time ago, but by that metric I have the best parents that a person could hope for. My brother Alex is one of my best friends, closest confidants, and one of two people that has the ability to immediately and constantly irritate me. I wouldn't trade it for the world. My sister Shannon has the patience of a saint, growing up with essentially three evil brothers, she is an incredible mother and she sets the kind of example that I hope to emulate some day.

My advisor, Betsy Komives, is one of the three principle influences responsible for guiding me toward becoming the scientist that I am today. Her constant thirst and excitement for knowledge is infectious. She not only taught me the right ways to approach science and experimental discovery, she also helped me with the single most important lesson I picked up in graduate school: how to weather failure and what you can learn from it.

Finally, I want to thank my fellow lab workers, without whom my grad school experience would have been entirely different and sorely lacking in fun and happiness. Mela Mulvihill either taught me or was right with me for the bulk of what I learned

working in Betsy's lab, and she was relentless in her efforts to avoid laughing at fantastic jokes. She was an invaluable release valve for everything and single-handedly made 80% of my graduate work better. Brian Fuglestad was one of my best friends outside of lab in addition to being my project partner for thrombin, we had any number of invaluable discussions about out projects, at all hours of the day, and shared more laughs than I care to remember. Vera Alverdi helped to provide as unique of an experience as I have had, she always had something nice to say, and she could answer anything about everything. And she did. Muneera Smith taught me everything about thrombin, thrombomodulin, and ITC when I joined the lab and she might be the single most pleasant person I know. Finally, I know that it doesn't do them justice, but Maj Ghassemian,Stephanie Truhlar, Mike Guttman, Carla Cervantes, Ingrid DeVries, Jorge Lamboy, Amy Davenport, Dana Dominguez, Tomas Stonehouse, Lindsey Handley, Holly Dembinski, Jesse Meyer are all my friends and each made the lab a pleasant place to be.

Chapter II, in full, is a reprint that the dissertation author was the principal researcher and author of. The material appears in *Biochemistry*. (**Treuheit, N.A.,** Smith, M., and Komives, E. A., Thermodynamic compensation upon binding to exosite 1 and the active site of thrombin, *Biochemistry* (2011) 50(21))

VITA

2007 Bachelors of Science, Chemistry, UC Berkeley, Berkeley, CA

2009 Masters of Science, Chemistry, University of California, San Diego

2013 Doctor of Philosophy, Chemistry, University of California, San Diego

PUBLICATIONS

Treuheit, N.A., Beach, M.A., Komives, E.A. " Design and activity of improved thrombomodulin fragments" (in preparation).

Treuheit, N.A., Beach, M.A., Komives, E.A., (2011) Thermodynamic Compensation upon Binding to exosite 1 and the Active Site of Thrombin. *Biochemistry*. 50, 4590-4596.

FIELDS OF STUDY

Major Field: Biochemistry

Studies in Biochemistry and Biophysics

Professor Elizabeth A. Komives

HONORS AND AWARDS

2008-2011 Cell and Molecular Genetics Training Grant, trainee

2007-2009 Molecular Biophysics Training Grant, affiliate

ABSTRACT OF THE DISSERTATION

Solution Biophysical Characterization of the Thrombin-Thrombomodulin Interaction

by

Nicholas Adam Treuheit

Doctor of Philosophy in Chemistry

University of California, San Diego, 2013

Professor Elizabeth A. Komives, Chair

The final step of the blood coagulation cascade is the activation of thrombin. Active thrombin cleaves fibrinogen to create fibrin which polymerizes into clots. Regulation of thrombin is imperative to maintaining normal hemostasis. The blood contains a high concentration of prothrombin, which must be proteolytically cleaved at two sites to generate active α-thrombin. Very little α-thrombin is ever generated, and this is rapidly captured by either thrombomodulin (TM) and/or antithrombin III. This work investigates the dynamics of thrombin by ITC and H/D exchange mass spectrometry, characterizes new and improved fragments of TM, and beings preliminary work with potential biologically useful TM fusion proteins for *in vivo* use.

In Chapter I, I introduce the coagulation cascade and parts that thrombin and

thrombomodulin play in maintaining hemostasis.

Chapter II describes the work that I did using ITC and DSC to characterize the affects of various ligands binding to thrombin and how that binding allosterically altered the active site, ABEI, and even change the thermal stability of thrombin.

In Chapter III, I summarize the work done trying to make new constructs of TM with improved activity and binding affinity toward thrombin without the negative impact on protein stability and present two new constructs that show significant improvement overall.

Chapter IV is our most recent HD exchange mass spectrometry work looking at the effects of TM456t binding to both human and bovine thrombin, and how much this binding changes regions all throughout the protein. The results there show significant dynamic change in the entire molecule.

And finally, Chapter V highlights our first attempts at using TM as part of a fusion protein designed to target activated platelets by the $\alpha_{IIb}\beta_3$ integrin, potentially bringing a strong anticoagulant to sites of blood clots.

Chapter I

Introduction

A. Regulation of blood coagulation

The circulatory system is a critical component in the maintenance of life. It allows for the circulation of blood, bringing oxygen and nutrients to vital organs, and removing waste and carbon dioxide. There exist a number of controls to help maintain blood hemostasis and alleviate the two major, life-threatening problems that can occur: thrombosis (excess clotting) and hemophilia (excess bleeding). α-Thrombin or Thrombin (Factor II and IIa for pro- and active enzyme forms), is chiefly responsible for helping activate platelets and forming blood clots, in addition to contributing to deactivation of its own upstream proteases.

Thrombin is generated at the culmination of the blood coagulation cascade (Figure 1.1), but there are two different pathways for producing thrombin. "Shallow" activation of the endothelium triggers the intrinsic pathway, initiated by the exposure of subendothelial collagen to the blood stream, allowing Factor XII to be activated and cascade down to thrombin activation. (Furie & Furie, 2008) More extensive damage to the endothelium causes the Tissue Factor, TF, to be released into the blood, triggering the second, extrinsic pathway. TF leads to the activation of Factor VII, which proceeds to activation Factor X, and Factor Xa is directly responsible for activating thrombin. Thrombin is a pivotal component for maintaining the balance between thrombosis and hemostasis because it functions as both a procoagulant and anticoagulant in the cascade. Free thrombin proteolyzes soluble fibrinogen into fibrin, which then polymerizes to create the matrix necessary to stabilize a blood clot. Also, it participates in a positive feedback loop by catalyzing further activation of blood

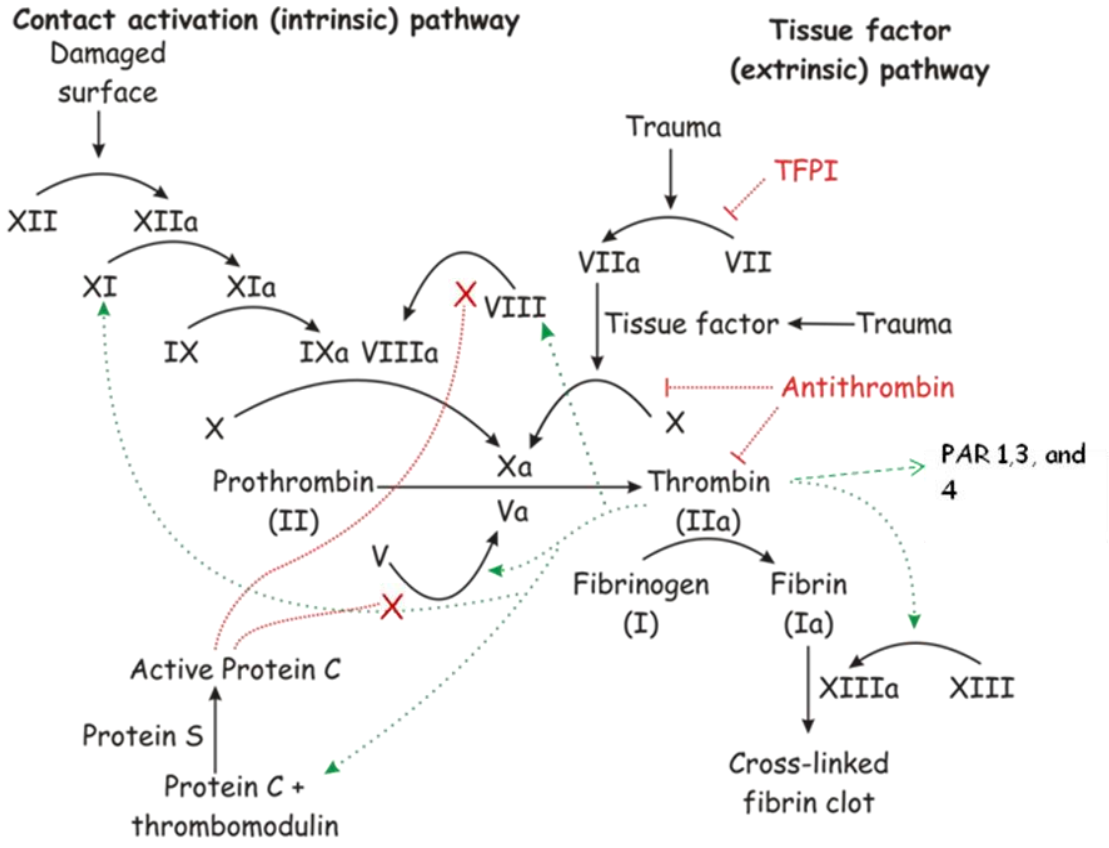

Figure 1.1: The dual action protease thrombin (Factor IIa) and its zymogen prothrombin (Factor II) reside in the center of the coagulation cascade. This figure was adapted from www.wikipedia.org.

factors XI, VIII, and V; its own upstream proteases (Esmon, 2000). Furthermore, thrombin can cleave Protease Activated Receptors (PARs) 1, 3, and 4 on the surface of platelets as part of the activation process, whereby activated platelets are recruited to a forming clot, or thrombus, along with fibrin (Macfarlane, *et al.*, 2001). This procoagulation activity must be tightly controlled to prevent potential damage caused by floating emboli, which can lead to blocked blood flow in extremities (deep vein thrombosis) or in the brain (stroke). This is accomplished through the interaction of thrombin and thrombomodulin (TM), the protein that drives the anticoagulant activity of thrombin. When TM binds to thrombin it completely blocks fibrinogen binding and subsequent cleavage (procoagulant) and promotes thrombin-mediated cleavage of protein C (Esmon, 2000). Additionally, activated protein C deactivates two upstream activators of thrombin; Factors Va and VIIIa (Walker, *et al.*, 1979, Suzuki, *et al.*, 1983, Fulcher, *et al.*, 1984). Ultimately, free thrombin activity is blocked by anti-thrombin III, a potent inhibitor of thrombin *in vivo* (Rosenberg & Lam, 1979, Fenton, 1986).

The importance of these protein interactions simply cannot be overstated. Thrombosis is uncontrolled clotting, typically the result of a piece of a thrombus coming free in the bloodstream, that ultimately blocks the flow of the circulatory system and it is the leading cause of heart attacks and strokes. Furthermore, some diseases cause a loss of control in the coagulation cascade, resulting in uncontrolled blood clotting throughout the body, also known as Disseminated Intravascular Coagulation (DIC). Additionally, specific human coagulation diseases such as heterozygous Protein C deficiency and the Factor V Lieden mutation, which leads to

Protein C resistant Factor V, lead to highly increased risk of thrombosis (Griffin, *et al.*, 1981, Zoller, *et al.*, 1994). Thus, given the importance and relevance of these proteins to human health, studying the thrombin-thrombomodulin interaction can achieve a greater understanding of this critical step in the anticoagulant pathway and possibly find a handle with which to exert control over the system itself. Greater control over the coagulation pathway would offer unparalleled protection from bleeding disorders and could significantly reduce medical mortality rates.

B. The thrombin-thrombomodulin interaction

If the activity of thrombin upon fibrinogen and platelets is the centerpiece of the coagulation cascade, then the thrombin-TM complex and its interaction with Protein C is central to the anti-coagulation pathway. TM is a large (~78 kD), multidomain, transmembrane protein located primarily on the surface of blood vessels which allows for ready access to free thrombin. Its domains consist of an amino terminal lectin-like domain, which has been shown to have anti-inflammatory activity both by itself and through its interaction with a proinflammatory protein, HMGB1 (Abeyama, *et al.*, 1995). The lectin domain is followed by a region containing six Epithelial Growth Factor (EGF)-like domains. The various EGF domains appear to serve a variety of purposes, where all six have been shown to stimulate growth of fibroblasts and EGF3-6 are needed to activate Thrombin-Activatable Fibrinolysis Inhibitor (TAFI) (Hamada, *et al.*, 1995, Bajzar, *et al.*, 1996). However, the portion of TM responsible for cofactor activity in connection with thrombin is the part containing

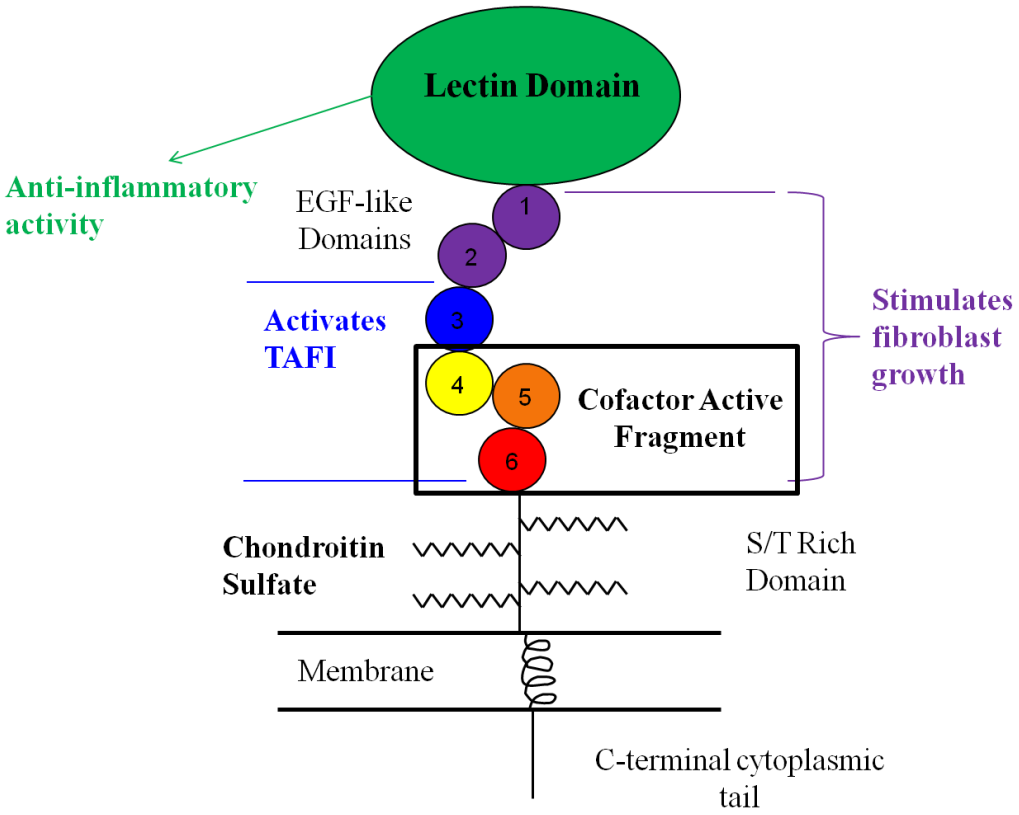

Figure 1.2: Schematic diagram of full, natural Thrombomodulin. N-terminal lectin domain (green), followed by six EGF-like domains (purple, blue, yellow, orange, and red), completed by the S/T domain, transmembrane domain, and the C-terminal cytoplasmic tail.

EGF-like domains 4, 5, and 6 (Zushi, *et al.*, 1989). This is followed by a serine and threonine rich region, a transmembrane domain, and a small cytoplasmic tail. See Figure 1.2 for a schematic of full length TM and a map of the uses of its various domains.

Alanine scanning mutagenesis experiments helped to reveal critical residues in both TM and thrombin that are involved in generating aPC (Nagashima & Lundh, 1993, Hall, *et al.*, 1999). A crystal structure of the thrombin-TM complex indicated that the binding site for TM is Anion-Binding Exosite I (ABEI) and that the 5^{th} EGF-like domain accounts for all of the direct contacts with thrombin (Fuentes-Prior, *et al.*, 2000). This helped identify the residues in TM that have direct binding contacts with thrombin, and they all exist solely in the 5^{th} domain. A key observation from combining these two studies is that a number of residues in the 4^{th} domain of TM are required for cofactor activity, but do not make any direct contacts with thrombin. Also, the 6^{th} EGF-like domain appears to contribute to a fraction of the binding interface compared to the 5^{th} domain, but eliminating it decreases the binding affinity of TM for thrombin by 10-fold {White, 1995 #14}. Deleting the 4^{th} EGF-like domain yields constructs with no protein C cofactor activity (Kurosawa, *et al.*, 1987, Stearns, *et al.*, 1989, Zushi, *et al.*, 1989, Tsiang, *et al.*, 1992, White, *et al.*, 1995). Additionally, the 4^{th} domain increases the affinity of the 5^{th} domain for thrombin by 20-fold, but it cannot bind or activate thrombin by itself. Thus TM45, a fragment containing only EGF 4 and 5, is the smallest cofactor active fragment of TM, and the addition of the 6^{th} domain increases the affinity for thrombin by an additional 10-fold without affecting k_{cat} (White, *et al.*, 1995).

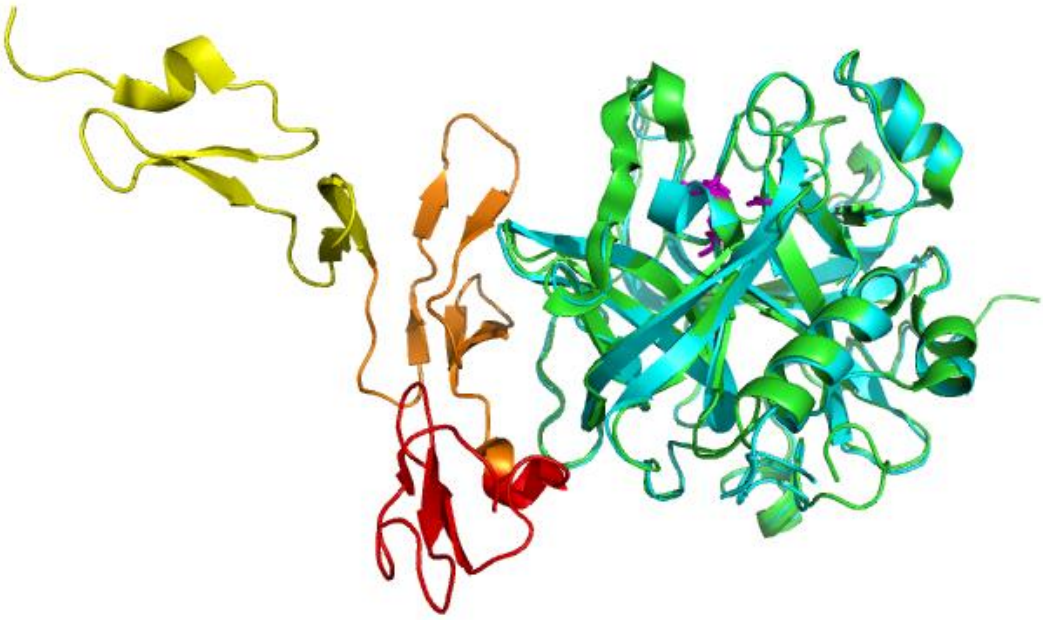

Figure 1.3: An overlay of the crystal structure of PPACK-bound thrombin (Green, PDB 1PPB) with the crystal structure of TM456-bound thrombin (TMEGF4: Yellow, EGF5: Orange, EGF6: Red, thrombin: Cyan, PDB 1DX5).

The specific mechanism for the effect of TM upon thrombin-mediated activation of PC is still not well understood. Figure 1.3 helps to illustrate the difficulty in finding the specific effects or changes in thrombin upon binding by TM. In this overlay of "free" and TM-bound thrombin, the differences in their crystal structures are essentially non-existent. The active site and secondary structural elements are almost entirely unchanged, and small changes are likely the result of small crystal packing adjustments. The lack of any conformational change can at least partly be explained by the requirement for covalent inhibition at the active site serine of thrombin before crystallization will occur. This seems to lock the active site into a "closed" conformation that eliminates any extra molecular motion that may exist in solution.

Based upon the observed absence of change in thrombin upon binding of TM, the argument can be made that TM simply provides a docking site for protein C, which allows for more favorable substrate presentation and improved activation (Yang & Rezaie, 2003). However, this hypothesis alone is insufficient to account for a number of other experiments using fluorescence, kinetic binding, structural, and amide H/D exchange that show subtle conformational changes in thrombin upon binding to TM. It has been shown that TM1-6 elicited a different fluorescent change in the active site of thrombin upon binding when compared to TM56 binding, suggesting an allosteric effect by TM binding upon the thrombin active site (Ye, *et al.*, 1991). Additionally, the association rates of a number of thrombin inhibitors increase dramatically when TM is complexed with thrombin versus thrombin alone (Rezaie, *et al.*, 1995, van de Locht, *et al.*, 1997, Myles, *et al.*, 1998, Rezaie, *et al.*, 1998, De

Cristofaro & Landolfi, 1999). Furthermore, Arg35 in thrombin has been shown to interfere with the thrombin-protein C interations and appears to be twisted away by thrombomodulin binding to thrombin (Rezaie & Yang, 2003). Finally, it was shown recently by H/D exchange mass spectrometry that only the cofactor active fragment TM45 complexed with thrombin could alter the deuterium exchange rate of 2 different regions near the thrombin active site compared to thrombin alone. The cofactor inactive fragment, TM56, does not affect thrombin-PC activity and it did not cause the decreased deuterium exchange near the active site that was observed in the TM45-thrombin complex (Koeppe, 2005). Taken together, these findings suggest that TM does more than simply provide a docking site for PC. The H/D exchange effects point to a more dynamic allosteric effect of TM binding that cannot be captured in crystal structures.

In order to better grasp the subtle effects of TM binding on the structure and activity of thrombin, it is necessary to continue finding solution-based experimental methods that will supplement established crystallographic data. The research presented here will attempt to get a better understanding of the changes in thrombin by looking at specific thermodynamic changes resulting from binding of a variety of thrombin ligands using ITC and DSC. Furthermore, new constructs and mutations of TM show strong improvement protein stability and cofactor activity. Not only do these constructs provide improved proteins for use in understanding the thrombin-TM interactions, but they create opportunities for expanding kinetic and NMR experiments to continue developing our understanding of the structural dynamics of thrombin in solution. We then use these constructs to improve upon previous H/D exchange mass

spectrometry experiments, finding previously unseen peptides showing more widespread molecular motion than before. Finally, these new protein constructs may serve as the foundation for new anti-coagulant drugs when paired with specific targeting proteins, potentially creating new, more efficient treatments for DIC, stroke, and other blood clotting disorders.

D. References

[1] Abeyama K, Stern DM, Ito Y, *et al.* (1995) The N-terminal domain of thrombomodulin sequesters high-mobility group-B1 protein, a novel antiinflammatory mechanism. *J Clin Invest* **115**: 1267-1274.

[2] Bajzar L, Morser J & Nesheim M, Prendergast, F., et al. (1996) TAFI, or Plasma Procarboxypeptidase B couples the coagulation and fibrinolytic cascades through the thrombin-thrombomodulin comples. *J Biol Chem* **271**: 16603-16608.

[3] De Cristofaro R & Landolfi R (1999) Allosteric modulation of BPTI interaction with human alpha- and zeta-thrombin. *Eur J Biochem* **260**: 97-102.

[4] Esmon CT (2000) Regulation of blood coagulation. *Biochim Biophys Acta* **1477**: 349-360.

[5] Fenton JW (1986) Thrombin. *Ann N Y Acad Sci* **485**: 5-15.

[6] Fuentes-Prior P, Iwanaga Y, Huber R, *et al.* (2000) Structural basis for the anticoagulant activity of the thrombin-thrombomodulin complex. *Nature* **404**: 518-525.

[7] Fulcher CA, Gardiner JE, Griffin JH & Zimmerman TS (1984) Proteolytic inactivation of human factor VIII procoagulant protein by activated human protein C and it analogy with factor V. *Blood* **63**: 486-489.

[8] Furie B & Furie BC (2008) Mechanisms of Thrombus Formation. *N Engl J Med* **259**: 938-949.

[9] Griffin JH, Evatt B, Zimmerman TS, Kleiss AJ & Wideman C (1981) Deficiency of protein C in congenital thrombotic disease. *J Clin Invest* **68**: 1370-1373.

[10] Hall SW, Nagashima M, Zhao L, Morser J & Leung LLK (1999) Thrombin interacts with thrombomodulin, protein C, and thrombin-activatable fibrinolysis inhibitor via specific and distinct domains. *J Biol Chem* **274**: 25510-25516.

[11] Hamada H, Ishii H, Sakyo K, Horie S, Nishiki K & Kazama M (1995) The epidermal growth factor-like domain of recombinant human thrombomodulin exhibits mitogenic activity for Swiss 3T3 cells. *Blood* **86**: 225-233.

[12] Koeppe JR, Seitova, A., Mather, T., Komives, E. (2005) Thrombomodulin tightens the thrombin active site loops to promote protein C activation. *Biochemistry* **44**: 14784-14791.

[13] Kurosawa S, Galvin JB, Esmon NL & Esmon CT (1987) Proteolytic formation and properties of functional domains of thrombomodulin. *J Biol Chem* **262**: 2206-2212.

[14] Macfarlane SR, Seatter MJ, Kanke T, Hunter GD & Plevin R (2001) Proteinase-Activated Receptors. *Am Soc Pharmacol Exptl Therap* **53**: 246-282.

[15] Myles T, Church F, Whinna H, Monard D & Stone SR (1998) Role of thrombin anion-binding exosite-I in the formation of thrombin-serpin complexes. *J Biol Chem* **273**: 31203-31208.

[16] Nagashima M & Lundh E (1993) Alanine-scanning mutagenesis of the epidermal growth factor-like domains of human thrombomodulin identifies critical residues for its cofactor activity. *J Biol Chem* **268**: 2888-2892.

[17] Rezaie AR & Yang L (2003) Thrombomodulin allosterically modulates the activity of the anticoagulant thrombin. *Proc Natl Acad Sci USA* **100**: 12051-12056.

[18] Rezaie AR, He X & Esmon CT (1998) Thrombomodulin increases the rate of thrombin inhibition by BPTI. *Biochemistry* **37**: 693-699.

[19] Rezaie AR, Cooper ST, Church FC & Esmon CT (1995) Protein C inhibitor is a potent inhibitor of the thrombin-thrombomodulin complex. *J Biol Chem* **270**: 25336-25339.

[20] Rosenberg RD & Lam L (1979) Correlation between structure and function of heparin. *Proc Natl Acad Sci USA* **76**: 1218-1222.

[21] Stearns DJ, Kurosawa S & Esmon CT (1989) Microthrombomodulin. Residues 310-486 from the epidermal growth factor precursor homology domain of thrombomodulin will accelerate protein C activation. *J Biol Chem* **264**: 3352-3356.

[22] Suzuki K, Stenflo J, Dahlback B & Teodorsson B (1983) Inactivation of human coagulation factor V by activated protein C. *J Biol Chem* **258**: 1914-1920.

[23] Tsiang M, Lentz SR & Sadler JE (1992) Functional domains of membrane-bound human thrombomodulin. EGF-like domains four to six and the serine/threonine-rich domain are required for cofactor activity. *J Biol Chem* **267**: 6164-6170.

[24] van de Locht A, Bode W, Huber R, Le Bonniec BF, Stone SR, Esmon CT & Stubbs MT (1997) The thrombin E192Q-BPTI complex reveals gross structural rearrangements: implications for the interaction with antithrombin and thrombomodulin. *EMBO J* **16**: 2977-2984.

[25] Walker FJ, Sexton PW & Esmon CT (1979) The inhibition of blood coagulation by activated Protein C through the selective inactivation of Factor V. *Biochim Biophys Acta* **571**: 333-342.

[26] White CE, Hunter MJ, Meininger DP, White LR & Komives EA (1995) Large-scale expression, purification and characterization of small fragments of thrombomodulin: the roles of the sixth domain and of methionine 388. *Protein Eng* **8**: 1177-1187.

[27] Yang L & Rezaie AR (2003) The Fourth Epidermal Growth Factor-like Domain of Thrombomodulin Interacts with the Basic Exosite of Protein C. *J Biol Chem* **278**: 10484-10490.

[28] Ye J, Esmon NL, Esmon CT & Johnson AE (1991) The active site of thrombin is altered upon binding to Thrombomodulin. *J Biol Chem* **266**: 23016-23021.

[29] Zoller B, Svensson PJ, He X & Dahlbäck B (1994) Identification of the same factor V gene mutation in 47 out of 50 thrombosis-prone families with. *J Clin Invest* **94**: 2521-2524.

[30] Zushi M, Gomi K, Yamamoto S, Maruyama I, Hayashi T & Suzuki K (1989) The last three consecutive epidermal growth factor-like structures of human thrombomodulin comprise the minimum functional domain for protein C-activating cofactor activity and anticoagulant activity. *J Biol Chem* **264**: 10351-10353.

Chapter II

Thermodynamic Compensation upon Binding to Exosite I and the Active Site of Thrombin

A. Introduction

Thrombin is a dual-action protease that serves a pivotal function in the coagulation cascade where it participates in cleavage of fibrinogen to form blood clots but it also activates protein C initiating anticoagulation. Thrombomodulin (TM) binding to thrombin, inhibits fibrinogen binding, and increases the catalytic activity toward protein C (Esmon, 2000). The cofactor active portion of TM includes only the fourth, fifth, and sixth EGF-like domains(Stearns, *et al.*, 1989, Hayashi, *et al.*, 1990). The residues responsible for binding to thrombin are contained in the fifth and sixth domains, and residues in the fourth domain are necessary for protein C activation (Kurosawa, *et al.*, 1988, White, *et al.*, 1995, Koeppe, 2008).

TM binding to thrombin has been shown to greatly increase the binding rate of various inhibitors to thrombin (Rezaie, *et al.*, 1995, van de Locht, *et al.*, 1997, Myles, *et al.*, 1998, Rezaie, *et al.*, 1998, De Cristofaro & Landolfi, 1999) and the k_a for protein C binding has been shown to be 1000-fold higher for the TM-thrombin complex compared to thrombin alone (Xu, *et al.*, 2005). TM binds at exosite 1, a site well removed from the active site, where a number of different proteins such as fibrinogen and hirudin are known to bind (Myles, *et al.*, 1998, Ayala, 2001). However, TM binding did not measurably alter the structure of thrombin (Fuentes-Prior, *et al.*, 2000) possibly due to the presence of an irreversible inhibitor, L-Gly-Gly-Arg chloromethyl ketone (GGACK), in the active site of thrombin which dramatically decreases the dynamics of the complex (Koeppe & Komives, 2006). In addition, different changes in the spectra of fluorescent dyes bound to the active site of

thrombin were observed depending on whether cofactor-active or inactive fragments of TM were bound at exosite 1 (Ye, *et al.*, 1991). More recently, H/D exchange experiments have been used to probe changes in the backbone dynamics of thrombin when bound to TMEGF45 and TMEGF56 (Koeppe, *et al.*, 2005). Two regions, one that was part of a β-strand connecting exosite 1 to the active site, retained more deuterium when bound to TMEGF45 compared to TMEGF56. Figure 1a highlights exosite 1 and the active site of thrombin as well the β-strand that connects them. Although all of these results suggest an allosteric linkage between exosite 1 and the active site, thermodynamic coupling between these two binding sites has not been directly demonstrated.

Thermodynamic measurements give powerful insights for understanding the interactions of receptors and their ligands, and isothermal titration calorimetry (ITC) is a tool that can be used to directly measure all the thermodynamic properties of a binding event. Interactions between a monoclonal antibody and thrombin, as well as between TM and thrombin have been examined previously by ITC, but the TM-thrombin interaction appears to be entirely entropic and so it could not be studied further with this method (Baerga-Ortiz, *et al.*, 2004). Recently, ITC was used to examine the binding of ligands to the thrombin active site and to exosite 2 (Kamath, *et al.*, 2010). Here, we have probed the thermodynamic coupling between exosite 1 and the active site using ITC.

In order to further investigate the effects of various ligands binding to thrombin, we used an analog of dansyl-L-arginine-(3-ethyl-1,5-pantanediyl) amide (DAPA) (Nesheim, *et al.*, 1979) that functions as a reversible active site inhibitor and

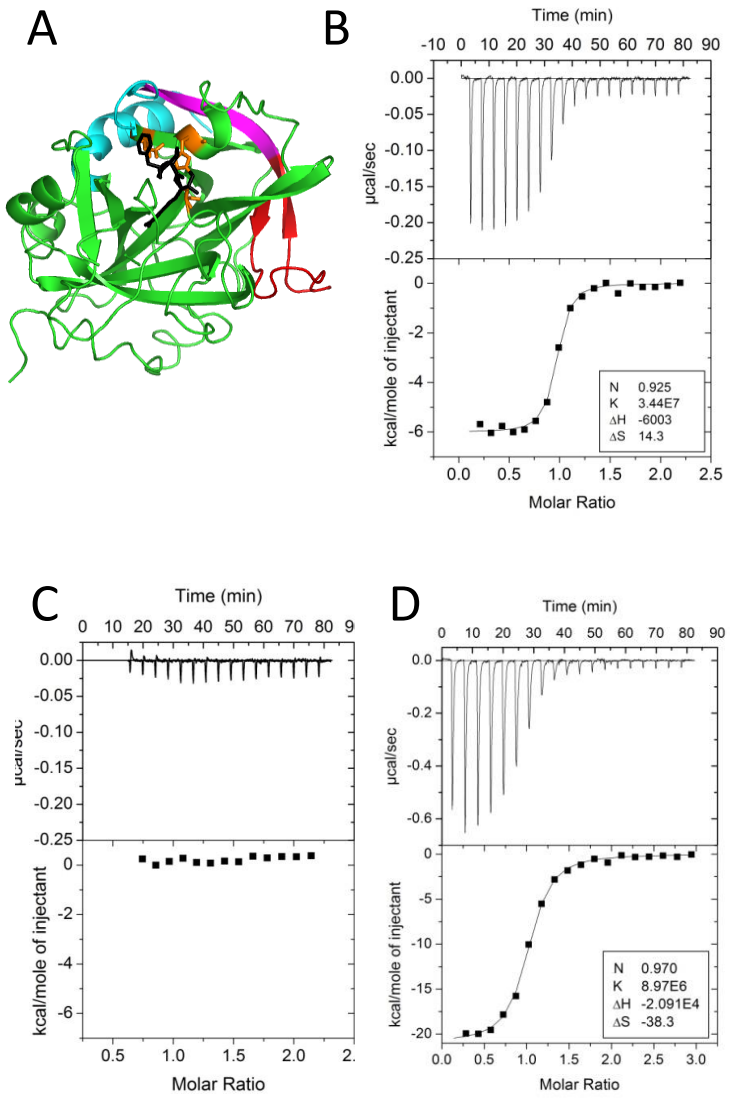

Figure 2.1: (A) Crystal structure of PPACK thrombin (PDB 1PPB (Bode, *et al.*, 1989)). The catalytic triad is highlighted in orange, exosite 1 is shown in red, with the β-strand linking exosite 1 to the active site highlighted in purple, and the two peptides with reduced H/D exchange in the presence of TMEGF45 shown in cyan. The covalently bound PPACK is colored black. ITC binding curves are shown for addition of 15 µL injections of a 70 µM solution of DAPA (B), or a 13 µM solution of TMEGF56 (C), or a 70 µM solution of the thrombin aptamer (D) to thrombin (6.5 µM in the cell).

a DNA aptamer that binds at exosite 1 (Wu, *et al.*, 1992, Macaya, *et al.*, 1995). Both of these ligands bind with high affinity and a significant change in enthalpy. The effects of different ligands binding alone and in combination reveal thermodynamic coupling between exosite 1 and the active site. Binding at the active site changes the thermodynamic signature of exosite 1 ligands and conversely binding at exosite 1 changes the thermodynamic signature of active site ligands.

B. Materials and Methods

1. Preparation of Thrombin

Bovine thrombin was purified from a barium citrate eluate (prepared from bovine plasma) according to previously published methods (Ni, *et al.*, 1990). The eluate powder (5g) was redissolved overnight in 200 mL of 100 mM EDTA, 10 mM sodium citrate, and 150 mM NaCl containing 11.1g of ammonium sulfate and 30mg of benzamidine. Following resuspension, the concentration of ammonium sulfate was increased from 10 to 40%. After centrifugation at 10,000g for 20 min, the supernatant was kept, brought to 70% ammonium sulfate, and centrifuged. The pellet, containing prothrombin, was dissolved in 5 mL of 50 mM Tris (pH 7.5) and 150 mM NaCl and loaded onto a G-25 Sephadex gel filtration column (2.5 cm x 100 cm) to remove the ammonium sulfate, and the fraction containing the protein was collected. The prothrombin was activated by incubating it with 2.0 mg/mL *Echis carinatus* venom (Miami Serpentarium), 10 mM $CaCl_2$, and 1 mg/mL PEG-8000 for 45 min at 37^{o}C. The mixture was loaded onto a second G-25 Sephadex (2.5 cm x 100 cm) equilibrated

in 25 mM KH_2PO_4 (pH 6.5) and 100 mM NaCl, and the protein fraction was collected. Finally, the G-25 fraction containing active thrombin was loaded onto a MonoS FPLC 16/10 column (Amersham/GE Healthcare) equilibrated with buffer A [25 mM KH_2PO_4 (pH 6.5) and 100 mM NaCl]. The thrombin was eluted with a linear gradient of buffer B [25 mM KH_2PO_4 (pH 6.5) and 500 mM NaCl] over the course of 90 minutes. Purified, active α-thrombin was identified by fibrinogen clotting. Active fractions were stored in 1 mL aliquots with 10 mM benzamidine at -80^{o}C for up to two weeks. For PPACK thrombin, 1 mL fractions of active α-thrombin were added to 1.1 μmol lyphoilized aliquots of PPACK and allowed to shake for 3 hours at room temperature before storing at -80^{o}C.

2. Preparation of TMEGF45

TMEGF45 was expressed in *Pichia pastoris* yeast as described previously (White, *et al.*, 1995). The protein was first purified by anion-exchange chromatography (QAE Sephadex followed by HiLoad 26/10 Q Sepharose) followed by reverse-phase HPLC as described previously (Wood & Komives, 1999). HPLC fractions with specific activities above 3 x 10^4 nmol apC/min/mg TM were lyophilized and stored at -20^{o}C. The lyophilized fractions were finally reconstituted in DI H_2O and purified by HiLoad 16/60 Superdex 75 size-exclusion chromatography (Amersham/GE Healthcare) in 50 mM Bis-tris propane (pH 7.4), 150 mM NaCl.

Table 2.1: Results from isothermal titration calorimetry experiments exploring binding at exosite 1 and the active site of thrombin. Values are the average of three independent experiments.

in cell	in syringe	K_a ($x10^7$ M^{-1})	N	ΔH (kcal/mol)	-T Δ S (kcal/mol)	Δ G (kcal/mol)
Without calcium						
thrombin	DAPA	4.5 ± 2.5[1]	0.9 ± 0.1	-5.9 ± 0.3	-4.4 ± 0.6	-10.3 ± 0.4
thrombin	aptamer	0.9 ± 0.2	0.96 ± 0.1	-20.2 ± 0.8	10.5 ± 0.9	-9.7 ± 0.2
thrombin	TM56	No heat observed				
apt-thromin	DAPA	5.8 ± 0.37	1.11 ± 0.1	-4.2 ± 0.3	-6.4 ± 0.7	-10.6 ± 0.4
ppack-thrombin	aptamer	0.8 ± 0.1	0.98 ± 0.02	-17.7 ± 1.1	8.3 ± 1.2	-9.4 ± 0.8
TM45-thrombin	DAPA	5.0 ± 1.8	0.86 ± 0.02	-4.5 ± 0.2	-6.0 ± 0.4	-10.5 ± 0.2
With 2.5 mM calcium						
thrombin	DAPA	4.5 ± 0.5	0.9 ± 0.1	-6.2 ± 0.04	-4.2 ± 0.1	-10.4 ± 0.1
thrombin	aptamer	1.5 ± 0.2	0.87 ± 0.04	-22.4 ± 0.1	12.6 ± 1.0	-9.8 ± 0.1
apt-thromin	DAPA	5.6 ± 2.1	1.06 ± 0.08	-4.8 ± 0.2	-5.7 ± 0.4	-10.5 ± 0.3
ppack-thrombin	aptamer	1.4 ± 0.6	0.9 ± 0.1	-21.0 ± 0.3	11.3 ± 0.004	-9.7 ± 0.3
TM45-thrombin	DAPA	5.9 ± 2.2	1.00 ± 0.06	-5.0 ± 0.1	-5.5 ± 0.2	-10.5 ± 0.2

3. Preparation of DAPAme

Due to the lack of availability of 4-ethylpiperidine, required for the synthesis of DAPA as described in (Nesheim, *et al.*, 1979), a modification of the synthesis using readily available starting materials was developed that uses 4-methylpiperidine instead. Dansyl arginine HCl (75 mg, 0.169 mmol) and N,N-carbonyldiimidazole (180 mg, 1.11 mmol) were added to 600 μL of DMSO and allowed to stir for 2 min. Then 180 μL of 4-methylpiperidine was added and the reaction was allowed to stir for 4 hours at room temperature in the dark. The reaction was quenched with 2 mL of 150 mM NaCl and extracted twice with ethyl acetate. The ethyl acetate layer containing the crude DAPAme was evaporated over the course of an hour with a directed stream of N_2, leaving a yellow oil which was resuspended in warm 0.1% TFA, 15% acetonitrile (ACN) and immediately injected on a Waters C18 reverse phase column (19 mm x 300 mm) equilibrated with 0.1% TFA/10% ACN. Defame was eluted by a gradient of 0-50% ACN over 30 minutes at a flow rate of 10 mL. Fractions were collected and analyzed by MALDI-MS; DAPAme has a molecular weight of 489.3 g/mol. Fractions containing only DAPAme were lyophilized out of H_2O and stored at -80^0C for up to 3 months in 4.2 nmol aliquots. Concentration of DAPAme was determined by the absorbance at 330 nm (ε = 4010 cm L $unit^{-1}$ mol^{-1}).

4. DNA Aptamer

The15 base thrombin-binding DNA aptamer, GGTTGGTGTGGTTGG, was ordered from Integrated DNA Technologies. Samples were lyophilized in 43 nmol

aliquots and stored at -20^{o}C until needed. Immediately before use, the samples were reconstituted in 600 μL of ITC buffer. Concentration was determined by the absorbance at 260 nm (ε = 143300 cm L unit^{-1} mol^{-1}).

5. ITC Experiments

Immediately before ITC, all proteins were re-purified by HiLoad 16/60 Superdex 75 size-exclusion chromatography (Amersham/GE Healthcare) equilibrated in 50 mM Bis-tris propane (pH 7.4), 150 mM NaCl, (and 2.5 mM $CaCl_2$ for the experiments in calcium-containing buffer). Protein concentrations were determined by BCA assay (Pierce Chemicals). Collected fractions were concentrated to 6.5 μM and stored at -20^{o}C for the day until they were used. DAPAme and thrombin aptamer samples were reconstituted in 50 mM Bis-tris propane (pH 7.4), 150 mM NaCl, (and 2.5 mM $CaCl_2$ for the experiments in calcium-containing buffer) to final concentrations of 65-70 μM. For TMEGF45-thrombin experiments, 13 nmol of re-purified thrombin were combined with 65 nmol of re-purified TMEGF45 and concentrated to a final volume of 2 mL, yielding a final concentration of 6.5 μM thrombin and a 5-fold excess of TMEGF45, ensuring that the thrombin was >99% bound with the TMEGF45 (Mandell, *et al.*, 2001).

All ITC experiments were performed on a VP-ITC calorimeter (MicroCal, Inc). The volume of the calorimetric cell in the VP-ITC is 1.4 mL and all titrations detailed in this paper were conducted by adding the titrant in steps of 10 μL. All experiments were performed at 25^{o}C with a 180 second initial delay. In order to avoid bubble formation in the calorimetric cell during stirring, all solutions were thoroughly degassed. The heat evolved during each injection of ligand was obtained by

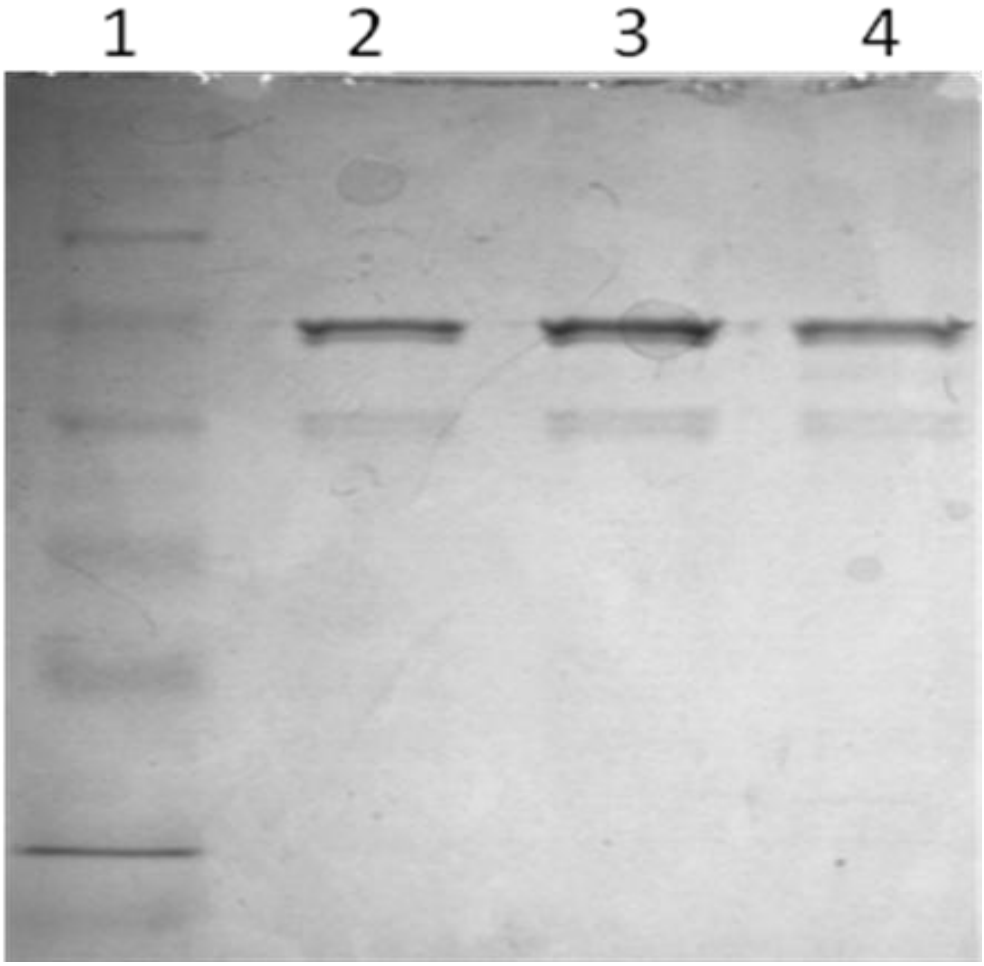

Figure 2.2: SDS-PAGE sample with fresh, SEC purified thrombin in ITC buffer. Lane 1 contains protein ladder, lane 2 contains thrombin immediately after collection from SEC, lane 3 is a sample from the ITC after an entire thrombin + DAMPA titration, and lane 4 is a sample from the ITC after a thrombin + aptamer titration.

integrating the calorimetric signal. The heat associated with binding of a ligand to the protein in the cell was obtained by subtracting the heat of dilution from the heat of reaction. Heats of dilution due to mismatch between the syringe and cell solutions were insignificant in all experiments. The individual heats were plotted as a function of the molar ratio, and nonlinear regression of the data was performed using the ORIGIN software supplied with the instrument according to a single binding site model, which provided the enthalpy change (ΔH) and the binding constant (K_A).

6. Differential Scanning Calorimetry (DSC) Experiment

Immediately before DSC, all proteins were re-purified by HiLoad 16/60 Superdex 75 size-exclusion chromatography (Amersham/GE Healthcare) equilibrated in 25 mM PIPES pH 6.5, and 150 mM NaCl. Samples containing 25 μM thrombin, 75 μM TMEGF45, 50 μM DAPAme or 50 μM aptamer were degassed for 10 minutes prior to DSC analysis. All melting experiments were performed on a VP-DSC calorimeter from MicroCal Inc with an active cell volume of 0.5 mL. Melting experiments were performed over a range of 25-90^{0}C with a scan rate of 90^{0}C/hour and sets of experiments were always preceded by an initial buffer scan followed by dynamic loading of samples during a thermal downscan.

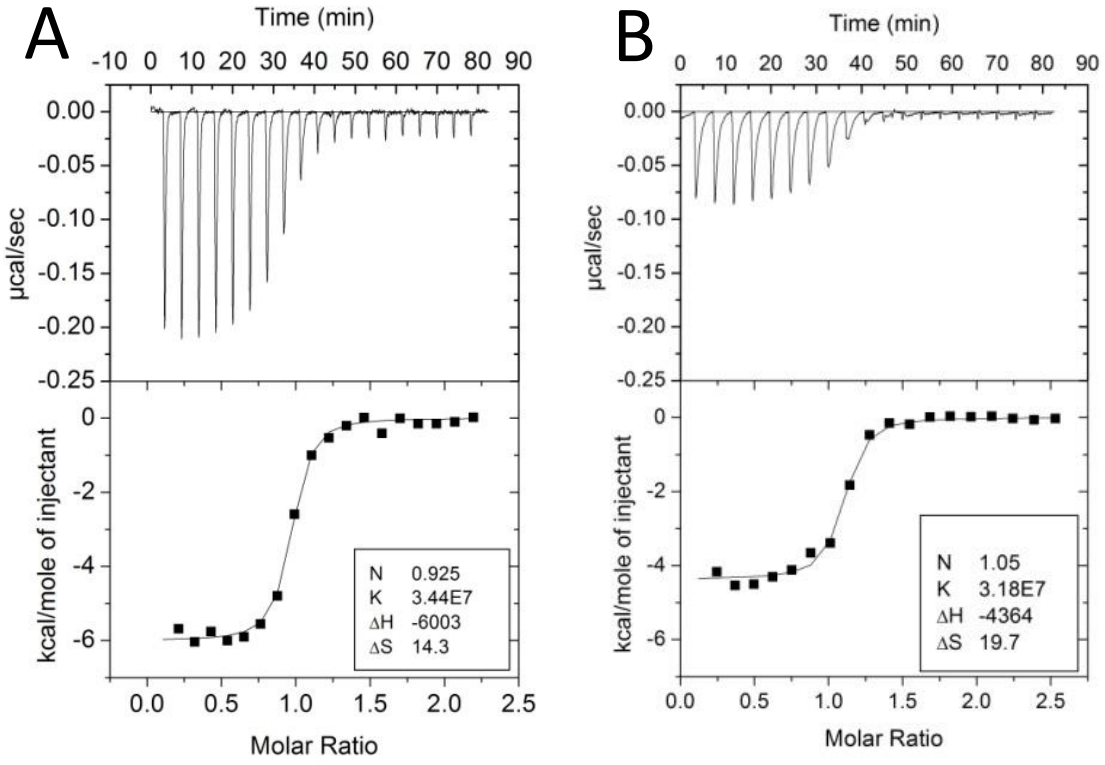

Figure 2.3: ITC binding curves for the addition of 15 µL injections of a 70 µM DAPA solution binding to thrombin alone (6.5 µM in the cell) (A) and DAPA binding to a thrombin-aptamer complex (6.5 µM thrombin with 20 µM aptamer) (B).

C. Results

1. Binding of ligands to the active site and to exosite 1 of thrombin

With the goal of probing how ligand binding at exosite 1 might affect the thermodynamics of binding at the active site, we tested various ligands that were known to bind at each of these sites. The fluorescent ligand, DAPA, which has often been used for active site titration (Nesheim, *et al.*, 1979), has exothermic binding with a ΔH of -6 kcal/mol and an equilibrium binding dissociation constant of 22 nM. Due to uneven quality of commercially-available DAPA, an analog, DAPAme was synthesized that gave an essentially identical thermodynamic signature (Figure 2.1B, Table 1). For the rest of the manuscript, DAPAme will be referred to simply as DAPA. Experiments were all performed at 25^{o}C in order to minimize autocatalytic degradation of thrombin. SDS-PAGE analysis of the thrombin re-obtained from the ITC cell after an experiment in which DAPA binding was measured showed that the thrombin had not been significantly autolyzed (Figure 2.2). Thus, the binding of DAPA gives a convenient thermodynamic signature of binding to the active site of thrombin (Kamath, *et al.*, 2010).

We previously showed that TMEGF45 shows no change of heat when it binds to thrombin, thus making it a poor choice of ligand for probing binding to exosite 1 (Baerga-Ortiz, *et al.*, 2004). Here we show that TMEGF56, which binds 10-fold more strongly to thrombin than TMEGF45, also does not release heat upon binding to thrombin (Figure 1C). This same preparation of TMEGF56 bound tightly to thrombin

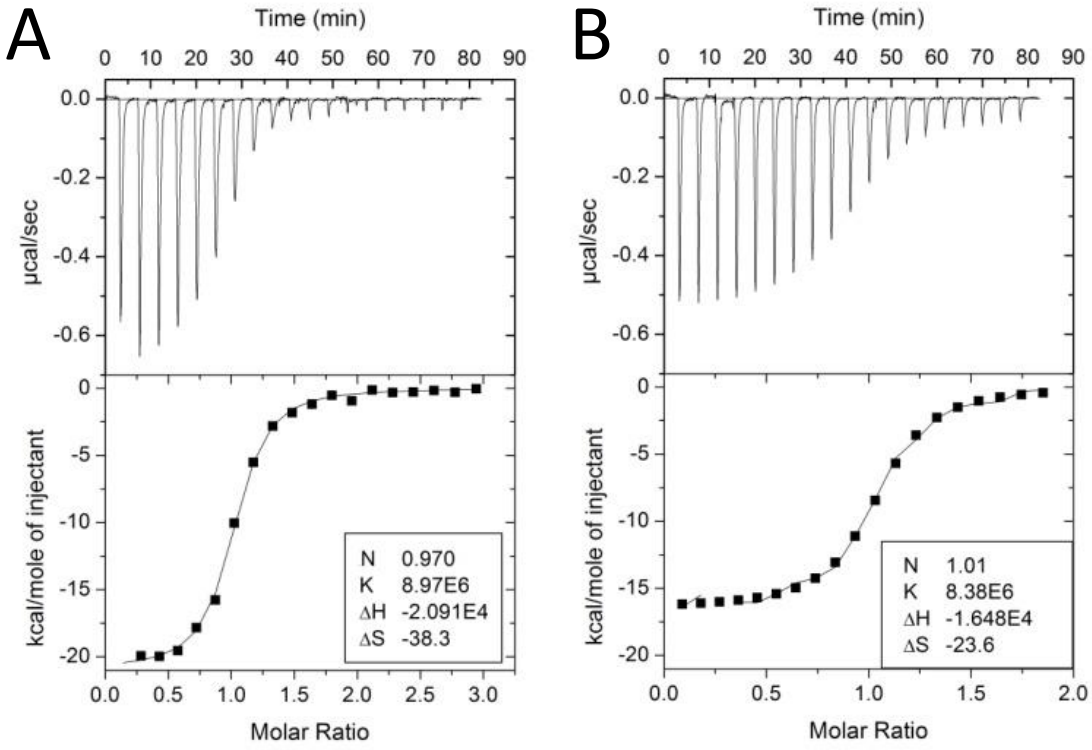

Figure 2.4: ITC binding curves for 15 µL injections of a 70 µM aptamer solution binding to a 6.5 µM solution of thrombin (A) and to a 6.5 µM solution of PPACK-thrombin (B).

with a K_D of 1.7 nM as assessed by SPR (Figure 2.6) (Beach, 2009). Thus, it appears that fragments of TM do not provide a directly measurable thermodynamic signature of binding to exosite 1. In contrast, a DNA aptamer selected to bind to exosite 1 was highly exothermic with a ΔH of -20.2 kcal/mol and an equilibrium binding dissociation constant of 111 nM (Figure 2.1D, Table 1). These results show that different exosite 1 ligands have markedly different thermodynamic signatures.

2. Binding of the DNA aptamer to exosite 1 alters the thermodynamics of binding at the active site.

The binding of single ligands to either the active site or exosite 1 gave clear thermodynamic signatures that could be reproducibly measured by ITC. We next used these same ligands to probe the thermodynamic cross talk between exosite1 and the active site. In these experiments, a complex was pre-formed between thrombin and one of the ligands and then this complex was titrated in the ITC with the other ligand. The amount of the first ligand added to form the complex was determined from the ITC titrations shown in Figure 1 and a sufficient excess was added so that the thrombin was completely bound. We first probed the effects of binding the DNA aptamer to exosite 1 prior to titrating the active site with DAPA. The results showed that when the DNA aptamer was bound, the heat released (ΔH) upon binding DAPA was significantly reduced from -5.9 kcal/mol upon binding DAPA to free thrombin to only to only -4.2 kcal/mol upon binding DAPA to the aptamer-thrombin complex (Figure 2.3). Remarkably, the binding affinity was nearly the same with a ΔG of -10.4

kcal/mol for DAPA binding to free thrombin *vs*. a ΔG of -10.5 for DAPA binding to the aptamer-thrombin complex (Table 2.1). The reason for the large difference in heat released compared to the small difference in ΔG between the two binding reactions is accounted for by a compensating difference in the entropy change upon binding. We report the entropy change as –TΔS so that it can be directly compared to the ΔH and ΔG. For DAPA binding to thrombin, the -TΔS was -4.4 kcal/mol whereas the –TΔS was -6.4 kcal/mol for DAPA binding to the aptamer-thrombin complex (Table 1). Use of DAPA as the ligand in these experiments was convenient because its K_A is in a good range of c values so that the stoichiometry and K_A could be reliably obtained directly from the ITC experiment. The value of ΔG was then obtained from the ITC measurement of K_A, and finally the value of -TΔS was computed from ΔG-ΔH.

3. Binding of the DNA aptamer to free thrombin has a different thermodynamic signature from binding of the DNA aptamer to PPACK-thrombin.

To ascertain whether the alteration in thermodynamic signature "goes both ways" in thrombin, we next compared the thermodynamics of binding of the DNA aptamer to free thrombin *vs*. PPACK-thrombin. Again, the heat released upon binding of the DNA aptamer to PPACK-thrombin was significantly less than for binding of the DNA aptamer to free thrombin (Figure 2.4). In this case, the overall ΔG for these two binding events was very similar (-9.7 *vs*. -9.4 kcal/mol) and the difference in the entropy change upon binding again compensated for the difference in heat released (Table 1).

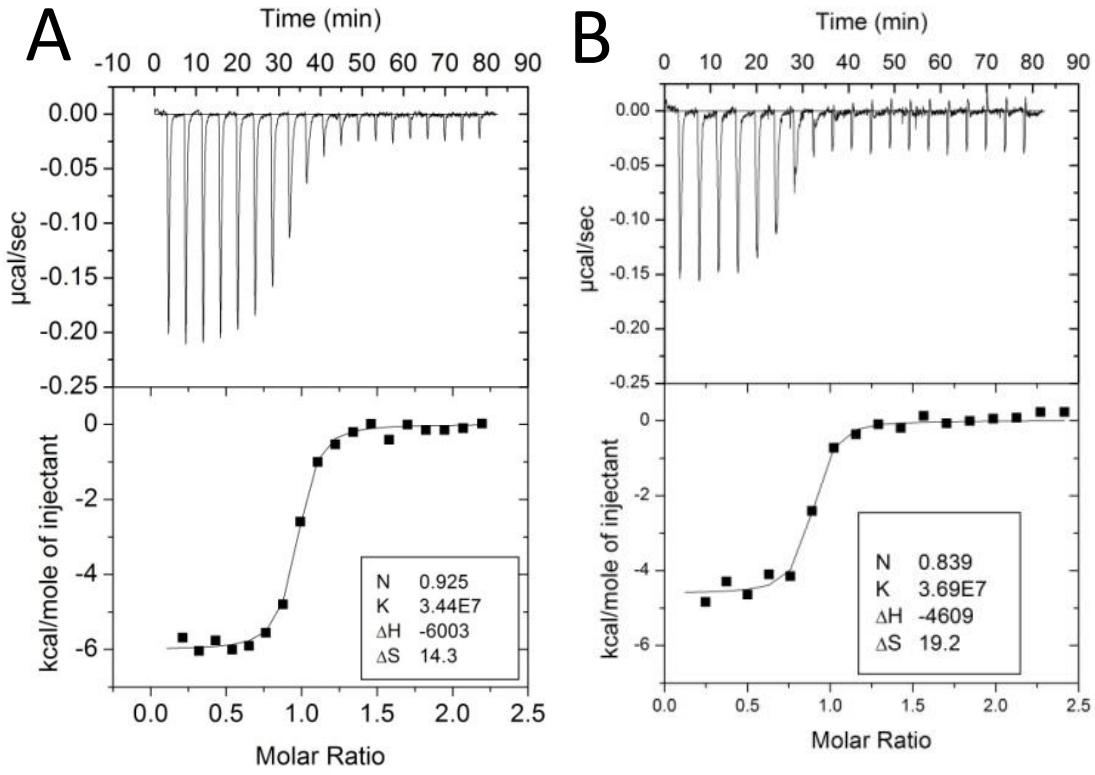

Figure 2.5: ITC binding curves for 15 µL injections of a 70 µM solution of DAPA binding to thrombin alone (6.5 µM in the cell) (A) and to TM45-thrombin (6.5 µM thrombin with 32.5 µM TM45) (B).

4. Effect of TMEGF45 on the thermodynamics of DAPA binding to thrombin

To test whether TM binding also affects ligand binding at the active site, binding of DAPA to free thrombin was compared to binding of DAPA to the thrombin-TMEGF45 complex. As with the aptamer, the ΔH upon DAPA binding to free thrombin was significantly more favorable than the ΔH upon DAPA binding to the thrombin-TMEGF45 complex (Figure 2.5). The enthalpy change upon binding was reduced from -5.9 kcal/mol to -4.5 kcal/mol and the entropy change again fully compensated for the difference so that the difference in binding free energy between the two experiments was negligible (Table 2.1). This result was all the more remarkable considering the completely different thermodynamic signature of the aptamer binding (highly favorable ΔH) compared to TMEGF45 binding (no observable binding ΔH).

5. Effects of calcium on the binding thermodynamics of ligand binding

Although thrombin is not thought to have a calcium-binding site, experiments on TM binding to thrombin are usually carried out in buffer containing calcium because both TM and protein C are known to bind calcium (Colpitts, 1995, Light, *et al.*, 1999). We thus repeated all of the experiments already described in buffer containing 2.5 mM $CaCl_2$ (Table 2.1). The thermodynamic signature of DAPA binding to thrombin was within error the same whether the buffer contained calcium or not (Table 2.1). Consistent with the ionic nature of the interaction between the

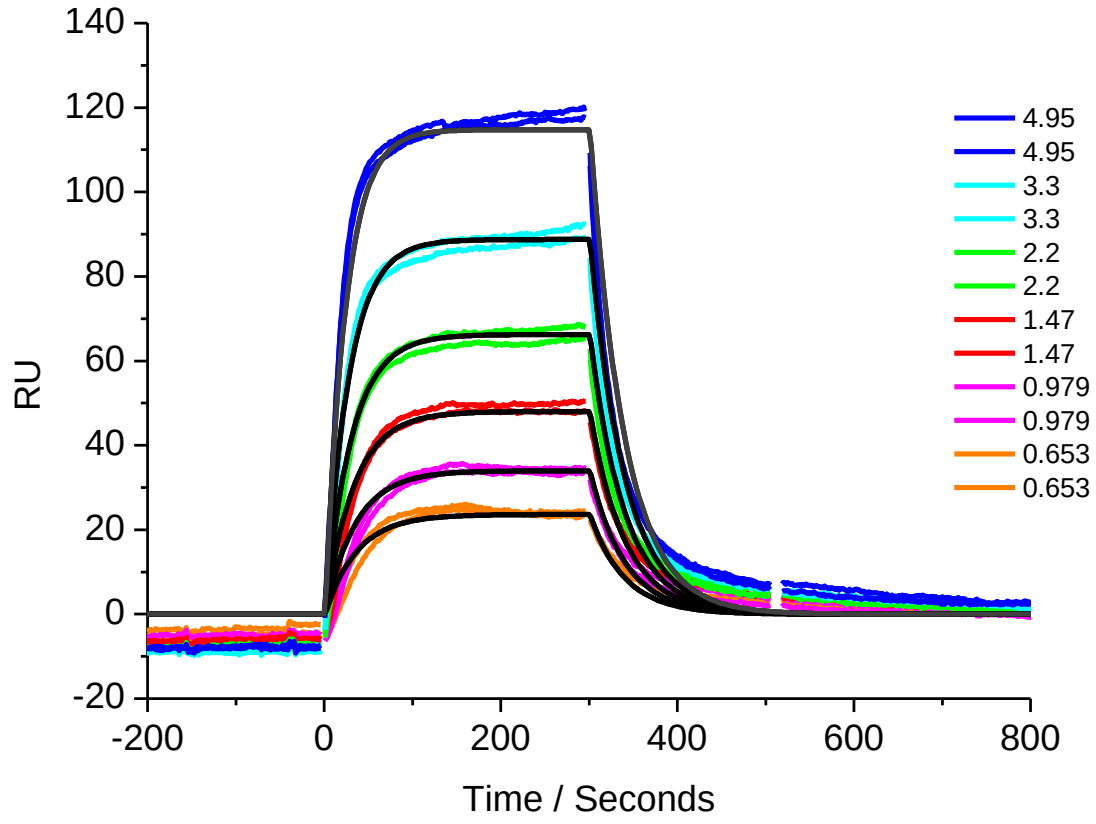

Figure 2.6: Surface Plasmon Resonance binding data for TM 56 binding to thrombin. The k_a was 3.6 x 10^6 (compare to 5.4 x 10^6 for TM456), the k_d was 0.26 s^{-1} (compare to 0.23 s^{-1} for TM 456), and the K_D was 7 x 10^{-9} M (compare to 4 x 10^{-9} for TM456)

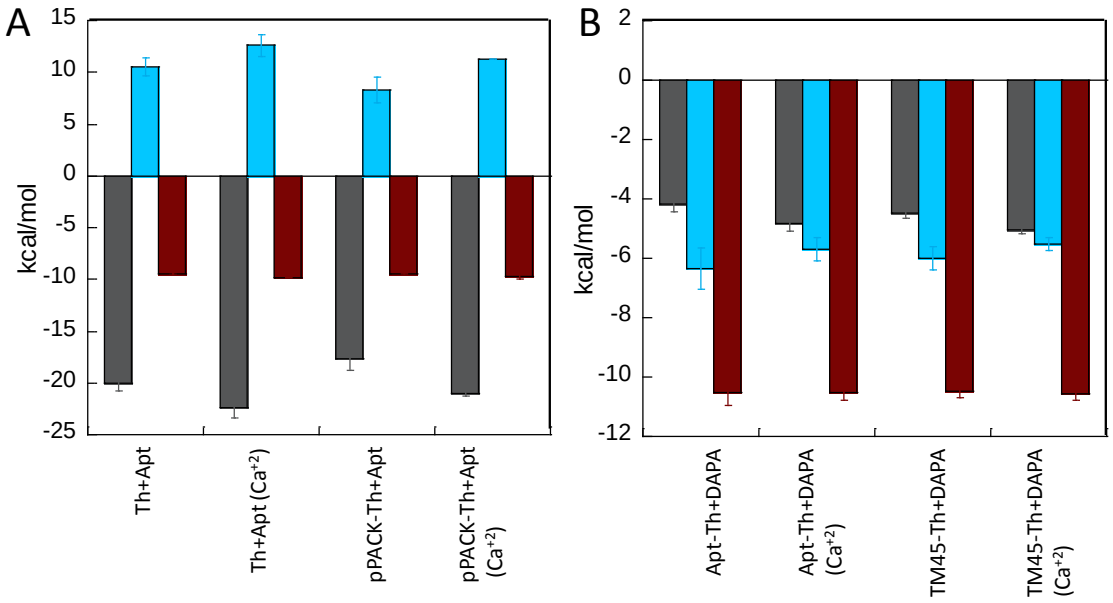

Figure 2.7: (A) Thermodynamic parameters for Thrombin and PPACK-thrombin titrated with aptamer with and without Ca^{2+} present. (B) Thermodynamic parameters for aptamer-thrombin and TM45-thrombin with and without Ca^{2+} present. For both figures, ΔH is shown in gray, $-T\Delta S$ is shown in blue, and ΔG is shown in dark red.

DNA aptamer and exosite 1 of thrombin, the thermodynamic signature for the aptamer binding changed slightly so that the binding ΔH was slightly more favorable and the -TΔS was slightly less favorable. These differences were only slightly outside of the experimental error, and were judged to be insignificant. We also compared the differences between each thermodynamic parameter measured in the presence and absence of calcium for the ternary interactions (Figure 2.7). These results showed again that the enthalpy-entropy compensation is nearly complete also in the presence of calcium. In all cases, the same trends were observed for the ternary interactions in the presence or absence of calcium. For example, pre-binding of the DNA aptamer caused the ΔH to be somewhat more favorable and the –TΔS to be somewhat less favorable for DAPA binding, and this trend was also seen in the presence of calcium (Figure 2.7A). Pre-binding of TMEGF45 also showed similar trends (Figure 2.7B). Attempts to measure a change in heat upon addition of calcium to thrombin in the cell showed no measurable direct binding indicating that the calcium effects are most likely secondary ionic effects most likely influencing binding at exosite 1.

6. Relationship between binding and overall thrombin stabilization

One explanation for the decreased entropic penalty for binding a ligand at one site when a ligand is already bound at another site is that the first ligand reduces the dynamics of the protein so that a smaller conformational entropy change occurs upon binding the second ligand (Tsai, 2008). We previously showed that when PPACK is bound at the active site of thrombin the backbone dynamics are reduced throughout

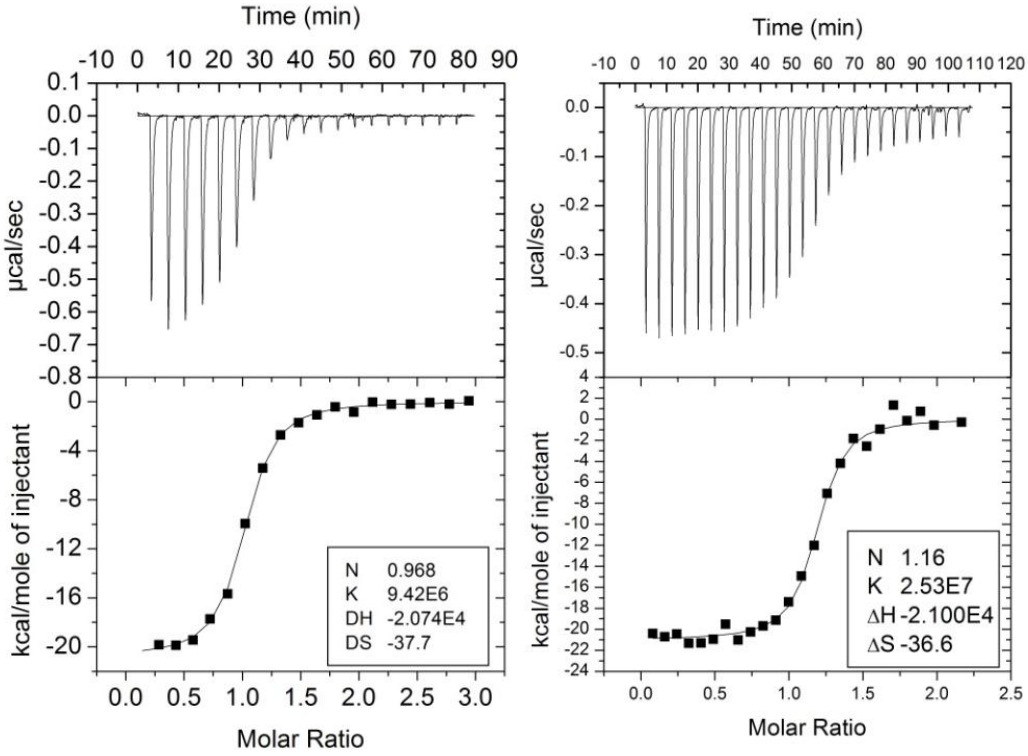

Figure 2.8: Comparison of aptamer binding to bovine thrombin (A) and to human thrombin (B). Even though the experiments were not performed using the same number and size of injections, the values of ΔH and ΔS are within error.

the protein (Koeppe & Komives, 2006). The reduced dynamics are accompanied by a large increase in stabilization; the T_m increases from 57^{o}C to 70^{o}C as measured by DSC (Croy, *et al.*, 2004). To probe whether something similar happens when ligands bind to exosite 1, we performed DSC experiments to compare the stability of thrombin alone to thrombin bound with the aptamer or TMEGF45 at exosite 1. Both the aptamer and TMEGF45 caused a small but measureable increase in melting temperature (57.9^{o}C) as compared to thrombin alone (56.9^{o}C) (Figure 2.9A) however the change was much smaller than that observed for PPACK binding to the active site (Croy, *et al.*, 2004). Thus, the thermodynamic coupling between exosite 1 and the active site may be partially, but not completely attributed to alterations of conformational dynamics.

D. Discussion

Direct thermodynamic measurement of binding allostery in thrombin has been a difficult goal to achieve for several reasons. First, the concentration of thrombin required for ITC measurements is relatively high, and under these conditions, thrombin autolysis is expected to be significant. We circumvented this problem by using freshly-prepared thrombin that was stored briefly at -80^{o}C at pH 6.5 with 5mM benzamidine, then re-purified by size exclusion chromatography and rapidly concentrated immediately before the ITC experiment was performed. These "heroic" measures ensured that all of the thrombin was fully binding competent making the measured stoichiometry and heat released upon binding accurate. As reviewed in the introduction, previous work by us and others, particularly focused on the binding of

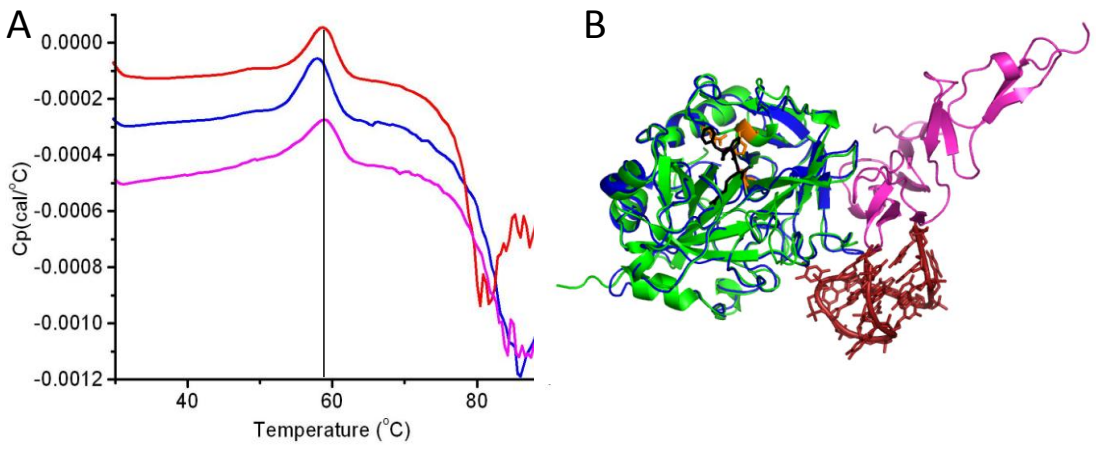

Figure 2.9: (A) DSC thermal denaturation data for thrombin alone (25 μM, blue), aptamer-thrombin (25 μM thrombin with 75 μM aptamer, red), and TMEGF45-thrombin (25 μM thrombin with 100 μM TMEGF45, magenta). The denaturation temperatures are 57.9°C, 58.7°C, and 58.9°C respectively. (B) Overlay of the crystal structures of thrombin complexed with aptamer (thrombin - blue, aptamer - red) (PDB 1HUT (Padmanabhan, *et al.*, 1993)) and of thrombin complexed with TM456 (thrombin - green, TMEGF456 - magenta) (PDB 1DX5 (Fuentes-Prior, *et al.*, 2000)).

TM fragments to exosite 1, suggested that binding at exosite 1 somehow changes the active site of thrombin (Ye, *et al.*, 1991, Koeppe, *et al.*, 2005). Although these results hinted that the binding sites may engage in "allosteric communication", binding affinities (K_D) measured by SPR were exactly the same for active thrombin binding to TMEGF456 vs. PPACK-inactivated thrombin binding to TMEGF456 (Baerga-Ortiz, *et al.*, 2000, Baerga-Ortiz, *et al.*, 2004). As allostery is traditionally defined as a change in ΔG of binding at one site when the allosteric site is occupied, this result should be interpreted as the absence of allostery between exosite 1 and the active site.

The results we present here definitely demonstrate thermodynamic coupling between exosite 1 and the active site, however the coupling does not result in a change in ΔG as would be expected for traditional allostery. Instead what is observed is a near perfect enthalpy-entropy compensation. Two different ligands, a DNA aptamer and a TM fragment were used as ligands at exosite 1. Two different ligands, a covalent PPACK modification at Ser 195 and a non-covalent ligand, DAPA, were used to probe binding at the active site. To look for allostery, we measured the difference in binding thermodynamics at the one site in the presence or absence of a ligand pre-bound at the other site. These experiments revealed, as expected, that the allosteric coupling "runs in both directions". That is, if a ligand is bound at exosite 1, the binding ΔH at the active site is reduced, but also the entropic cost is lower so the overall binding ΔG doesn't change. Similarly, if a ligand was bound at the active site, the heat released

upon binding a ligand at exosite 1 was reduced and the entropic cost lowered so that again the binding ΔG doesn't change.

Such an enthalpy-entropy compensation mechanism is most often seen in protein folding reactions where a the protein adopts a large number of conformations in the unfolded state (high entropy) and when the protein folds to a single native state this entropy is exchanged for the favorable enthalpy of specific side chain interactions in the folded structure. It is tantalizing to speculate that ligand binding to either site on thrombin in effect further folds the protein and that this is what we are observing in the binding experiments. It is well-known that thrombin is highly dynamic. Indeed, ligand binding to either exosite 1 or the active site reduced amide hydrogen exchange throughout thrombin (Koeppe, *et al.*, 2005, Koeppe & Komives, 2006). Recent NMR experiments also showed that some resonances that were presumably exchange-broadened in free thrombin could be observed in the ligand-bound states (Lectenberg, *et al.*, 2010). One interpretation of both of these results is that ligand binding changes the energy landscape of thrombin towards a more folded structure. This interpretation is bolstered by the finding that thrombin is highly stabilized towards thermal denaturation by ligand binding as measured by DSC (Koeppe & Komives, 2006).

Probably the most fascinating part of the story, however, is that it doesn't seem to matter what the ligand is. The two ligands that bound to exosite 1 had completely different thermodynamic signatures; the DNA aptamer bound with a highly favorable ΔH and a highly unfavorable -TΔS whereas the TMEGF45 showed no change in enthalpy upon binding and presumably bound with a favorable -TΔS. It is worth emphasizing that even though we did not directly observe a change in heat upon

TMEGF45 binding, the large difference in binding enthalpy when DAPA was bound to free thrombin *vs*. the TMEGF45-thrombin complex is clear evidence that the TMEGF45 was, in fact, bound. Despite the completely different thermodynamic signatures, and even the completely different bound structures (Figure 6B), both of these ligands induced the same effects on DAPA binding. Both reduced the favorable binding ΔH and in both cases this was compensated by a reduced entropic cost so that the overall binding ΔG was the same. The fact that such different ligands could induce the same thermodynamic changes in the active site strongly argues that they both caused similar folding changes in thrombin.

Chapter II, in full, is a reprint that the dissertation author was the principal researcher and author of. The material appears in *Biochemistry*. (**Treuheit, N.A.,** Smith, M., and Komives, E. A., Thermodynamic compensation upon binding to exosite 1 and the active site of thrombin, *Biochemistry* (2011) 50(21))

E. References

[1] Ayala YM, Cantwell, A. M., Rose T., Bush, L. A., Arosio D., and Di Cera, E. (2001) Molecular Mapping of Thrombin-Receptor Interactions. *Proteins: Struct Funct Genet* **45**: 107-116.

[2] Baerga-Ortiz A, Rezaie AR & Komives EA (2000) Electrostatic dependence of the thrombin-thrombomodulin interaction. *J Mol Biol* **296**: 651-658.

[3] Baerga-Ortiz A, Bergqvist SP, Mandell JG & Komives EA (2004) Two different proteins that compete for binding to thrombin have opposite kinetic and thermodynamic profiles. *Protein Sci* **13**: 166-176.

[4] Beach M (2009) Thermodynamics of the Thrombin-Thrombomodulin Interaction. *Ph. D Thesis, Department of Chemistry and Biochemistry, UC San Diego*.

[5] Bode W, Mayr I, Baumann U, Huber R, Stone S & Hofsteenge J (1989) The refined 1.9 A crystal structure of human alpha-thrombin: interaction with D-Phe-Pro-Arg chloromethyl ketone and significance or the Tyr-Pro-Pro-Trp insertion segment. *Embo Journal* **8**: 3467-3475.

[6] Colpitts T, Prorok, M., Castellino, FJ (1995) Binding of Calcium to Individual Gamma-Carboxyglutamic Acid Residues of Human Protein C. *Biochemistry* **34**: 2424-2430.

[7] Croy CH, Koeppe JR, Bergqvist S & Komives EA (2004) Allosteric Changes in Solvent Accessibility Observed in Thrombin upon Active Site Occupation. *Biochemistry* **43**: 5246-5255.

[8] De Cristofaro R & Landolfi R (1999) Allosteric modulation of BPTI interaction with human alpha- and zeta-thrombin. *Eur. J. Biochem.* **260**: 97-102.

[9] Esmon CT (2000) Regulation of blood coagulation. *Biochimica et Biophysica Acta* **1477**: 349-360.

[10] Fuentes-Prior P, Iwanaga Y, Huber R, *et al.* (2000) Structural basis for the anticoagulant activity of the thrombin-thrombomodulin complex. *Nature* **404**: 518-525.

[11] Hayashi T, Zushi M, Yamamoto S & Suzuki K (1990) Further localization of binding sites for thrombin and protein C in human thrombomodulin. *J Biol Chem* **265**: 20156-20159.

[12] Kamath P, Huntington JA & Krishnaswamy S (2010) Ligand Binding Shuttles Thrombin along a Continuum of Zymogen- and Proteinase-like States. *J Biol Chem* **285**: 28651-28658.

[13] Koeppe J & Komives E (2006) Amide H/2H exchange reveals a mechanism of thrombin activation. *Biochemistry* **45**: 7724-7732.

[14] Koeppe J, Beach, M., Baerga-Ortiz, A., Kerns, J., and Komives, E. (2008) Mutations in the fourth EGF-like domain affect thrombomodulin-induced changes in the active site of thrombin. *Biochemistry* **47**: 10933-10939.

[15] Koeppe JR, Seitova A, Mather T & Komives E (2005) Thrombomodulin tightens the thrombin active site loops to promote protein C activation. *Biochemistry* **44**: 14784-14791.

[16] Kurosawa S, Stearns DJ, Jackson KW & Esmon CT (1988) A 10-kDa cyanogen bromide fragment from the epidermal growth factor homology domain of rabbit thrombomodulin contains the primary thrombin binding site. *J Biol Chem* **263**: 5993-5996.

[17] Lectenberg B, Johnson D, Freund S & Huntington J (2010) NMR Resonance Assignments of Thrombin Reveal the Conformational and Dynamic Effects of Ligation. *Proc Natl Acad Sci U S A* **107**: 14087-14092.

[18] Light DR, Glaser CB, Betts M, *et al.* (1999) The interaction of thrombomodulin with Ca2+. *Eur J Biochem* **262**: 522-533.

[19] Macaya R, Waldron J, Beutel B, *et al.* (1995) Structural and Functional Characterization of Potent Antithrombotic Oligonucleotides Possessing both Quadruplex and Duplex Motifs. *Biochemistry* **34**: 4478-4492.

[20] Mandell JG, Baerga-Ortiz A, Akashi S, Takio K & Komives EA (2001) Solvent accessibility of the thrombin-thrombomodulin interface. *J Mol Biol* **306**: 575-589.

[21] Myles T, Church F, Whinna H, Monard D & Stone SR (1998) Role of thrombin anion-binding exosite-I in the formation of thrombin-serpin complexes. *J Biol Chem* **273**: 31203-31208.

[22] Nesheim M, Prendergast F & Mann K (1979) Interactions of a fluorescent active-site-directed inhibitor of thrombin: Dansylarginine N-(3-ethyl-1,5-pentanediyl)amide. *Biochemistry* **18**: 8.

[23] Ni F, Konishi Y & Scheraga HA (1990) Thrombin-bound conformation of the C-terminal fragments of hirudin determined by transferred nuclear Overhauser effects. *Biochemistry* **29**: 4479-4489.

[24] Padmanabhan K, Parmanabhan K, Ferrara J, Sadler J & Tulinsky A (1993) The structure of alpha-thrombin inhibited by a 15-mer single stranded DNA aptamer. *J Biol Chem* **268**: 17651-17654.

[25] Rezaie AR, He X & Esmon CT (1998) Thrombomodulin increases the rate of thrombin inhibition by BPTI. *Biochemistry* **37**: 693-699.

[26] Rezaie AR, Cooper ST, Church FC & Esmon CT (1995) Protein C inhibitor is a potent inhibitor of the thrombin-thrombomodulin complex. *J Biol Chem* **270**: 25336-25339.

[27] Stearns DJ, Kurosawa S & Esmon CT (1989) Microthrombomodulin. Residues 310-486 from the epidermal growth factor precursor homology domain of thrombomodulin will accelerate protein C activation. *J Biol Chem* **264**: 3352-3356.

[28] Tsai C, del Sol, A., Nussinov, R. (2008) Allostery: Absence of a Change in Shape Does Not Imply that Allostery is not at Play. *J Mol Biol* **378**: 1-11.

[29] van de Locht A, Bode W, Huber R, Le Bonniec BF, Stone SR, Esmon CT & Stubbs MT (1997) The thrombin E192Q-BPTI complex reveals gross structural rearrangements: implications for the interaction with antithrombin and thrombomodulin. *EMBO J* **16**: 2977-2984.

[30] White CE, Hunter MJ, Meininger DP, White LR & Komives EA (1995) Large-scale expression, purification and characterization of small fragments of thrombomodulin: the roles of the sixth domain and of methionine 388. *Protein Eng* **8**: 1177-1187.

[31] Wood MJ & Komives EA (1999) Production of large quantities of isotopically labeled protein in Pichia pastoris by fermentation. *J Biomol NMR* **13**: 149-159.

[32] Wu Q, Tsiang M & Sadler JE (1992) Localization of the Single-Stranded DNA Binding Site in the Thrombin Anion-Binding Exosite. *J Biol Chem* **267**: 24408-24412.

[33] Xu H, Bush LA, Pineda AO, Caccia S & Di Cera E (2005) Thrombomodulin changes the molecular surface of interaction and the rate of complex formation between thrombin and protein C. *J Biol Chem* **280**: 7956-7961.

[34] Ye J, Esmon NL, Esmon CT & Johnson AE (1991) The active site of thrombin is altered upon binding to Thrombomodulin. *J Biol Chem* **266**: 23016-23021.

Chapter III

Creation and Characterization of TM456m and TM456t – Improved Versions of TM45

A. Introduction

The role of thrombin is well established as a critical part of the coagulation cascade and maintaining hemostasis. Furthermore, the interaction between free thrombin and fibrinogen has been extensively characterized, showing that distant binding of fibrinogen to ABE1 of thrombin is required to correctly present the cleavage site of fibrinopeptides A and B for cleavage. (Stubbs, *et al.*, 1992, Pechik, *et al.*, 2004) This is one of the hallmark processes in the pro-coagulation pathway, summarized in Figure 1.1, where fibrin polymers ultimately form the bulk of any blood clot.

Regulation of the coagulation pathway is achieved by thrombin's binding partner, thrombomodulin (TM), which serves a critical function in not only preventing further fibrinogen cleavage, but also in dramatically improving the activation of PC by thrombin (Esmon, 2000). In the previous chapter, we characterized the thermodynamics of various ligands binding to thrombin. However, this behavior with respect to thrombin is still very hard to explain as a result of a number of difficulties in studying the thrombin-TM interaction. First, any allosteric changes in thrombin as a result of TM binding are not observed in crystallographic studies, perhaps because of the requirement for addition of a covalently bound active site inhibitor to prevent autoproteolysis during concentration and crystallization, see Figure 1.3. Second, natural TM is extremely difficult to purify and TM expression is hindered by the high number of disulfide bonds within each EGF-like domain and the need for

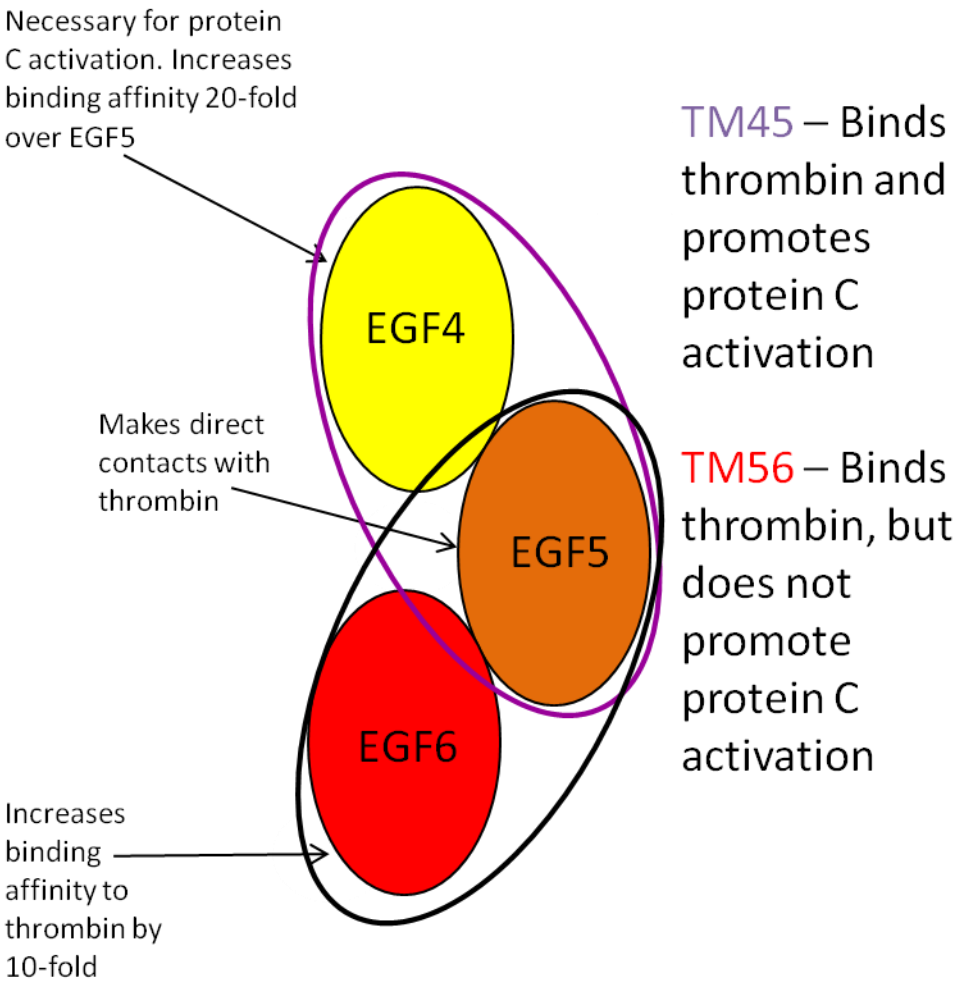

Figure 3.1: Schematic showing the two main constructs of TM studied previously and their effects on thrombin

glycosylation at two different sites to aid solubility (White, *et al.*, 1995). The void left by the lack of conclusive crystallographic evidence however, can be filled by using solution-based experiments, which allow for better analysis of the dynamic behavior of thrombin. But, in order to continue developing our understanding of this interaction it is necessary to improve the tools available for eliciting changes in thrombin

Only a small part of full, naturally expressed TM is necessary to recreate the cofactor activity of the full protein. In fact, TM456, a construct of TM containing EGF-like domains 4, 5, and 6, is enough to mimic the complete activity of full TM. (Zushi, *et al.*, 1989) But, TM456 is a poorly behaved protein in solution, prone to aggregation at the higher concentrations required for solution studies (Komives lab, unpublished). However, it has been shown previously that the construct TM45, combining only the 4^{th} and 5^{th} EGF-like domains, is sufficient to promote the activation of protein C by thrombin, although it has significantly reduced affinity compared to TM456, see Figure 3.1 (White, *et al.*, 1995). On the other hand, the 5^{th} and 6^{th} EGF domains combine to yield a construct with complete thrombin binding, but TM56 is unable to alter the activity of thrombin toward PC. Previous work, from other labs (Rezaie, *et al.*, 1995, van de Locht, *et al.*, 1997, Myles, *et al.*, 1998, Rezaie, *et al.*, 1998, De Cristofaro & Landolfi, 1999)as well as our own (Mandell, *et al.*, 2001, Koeppe, 2005), has shown that not only does the 4^{th} domain have an allosteric effect on inhibitors in the active site, but it also affects the catalytic activity.

However, understanding the specific effects of the 6^{th} EGF domain of TM has been difficult. NMR binding experiments analyzing the changes in transferred NOE signals in various short TM peptides upon binding to thrombin (Tolkatchev, *et al.*,

2000). One 28 residue peptide in particular comprised the linker between the 5th and 6th domain as well as a large portion of the 6th domain, residues T422-G449 of human TM. When allowed to mix and bind with thrombin, differential resonance perturbations as well as transferred NOEs were observed in the TM peptide, suggest both binding to thrombin as well as structuring upon binding.

Combining this research with our own previous observations has lead us to hypothesize that it may be possible to improve the anticoagulant cofactor activity of TM45 by attempting to add some portion of the 6th domain to more closely mimic TM456.

There is abundant potential use for high stability constructs of TM because they are gaining traction as potential anticoagulation therapies. The construct Solulin, which contains all of the extracellular domains of TM and some favorable mutations, is currently progressing through clinical trials as a coagulation inhibitor (van Lersel, *et al.*, 2011) that apparently binds and inhibits thrombin generation without increasing the levels of aPC/PCI complex.

Here, we will present purification and activity data on two new constructs of TM that add increasing portions of the 6th EGF-like domain of TM onto TM45. TM456mini, or TM456m, adds the first 23 residues of the 6th EGF-like domain onto TM45 and TM456truncation, or TM456t, adds the next 7 residues of the 6th EGF-like domain to the end of TM456m. These constructs have increased binding affinity towards thrombin, and also better anticoagulant cofactor activity. These new TM derivatives can be purified by reversed-phase chromatography at neutral pH and show reasonable stability at the concentrations required for *in vitro* experimentation.

B. Materials and Methods

1. Expression of TM456m and TM456t

Subcloning

TM456m was subcloned from the TM456 gene, using a small sh4 shuttle vector. TM456t and its subsequent alanine point mutants, D347A, L350A, and R352A, were made using nucleotide addition by Quick Change Mutagenesis on the finished 456m gene. These constructs were all synthesized utilizing the *E. coli*-optimized codons used previously by Chris White and described by White *et al.* (White, *et al.*, 1995). Initially, DNA was cloned into the sh4 vector, a 4K base pair E. coli shuttle vector, which is suitable for PCR mutagenesis. The expression vectors for *Pichia* expression, pPic9a and pPic9K, are too large for efficient PCR mutagenesis, so the TM gene is manipulated in the smaller vector, psh4, and then transferred into pPic9a. XhoI and EcoRI sites are engineered a short distance beyond the 5' and 3' ends of the TM gene. However, a second XhoI site exists in the Pic9K vector in the kanamycin resistance gene, required for transformant selection. Thus, the gene fragment is first ligated into pPIC9a (which does not have the kanamycin resistance gene). To transfer the gene from pPIC9a to the final protein expression vector pPIC9K, a number of potential pairs of restriction enzyme can be used for subcloning, here we use BamHI and XbaI, but the SacI-SalI pair also works well for this. Spheroplasting, transformation, and transformant selection were performed according

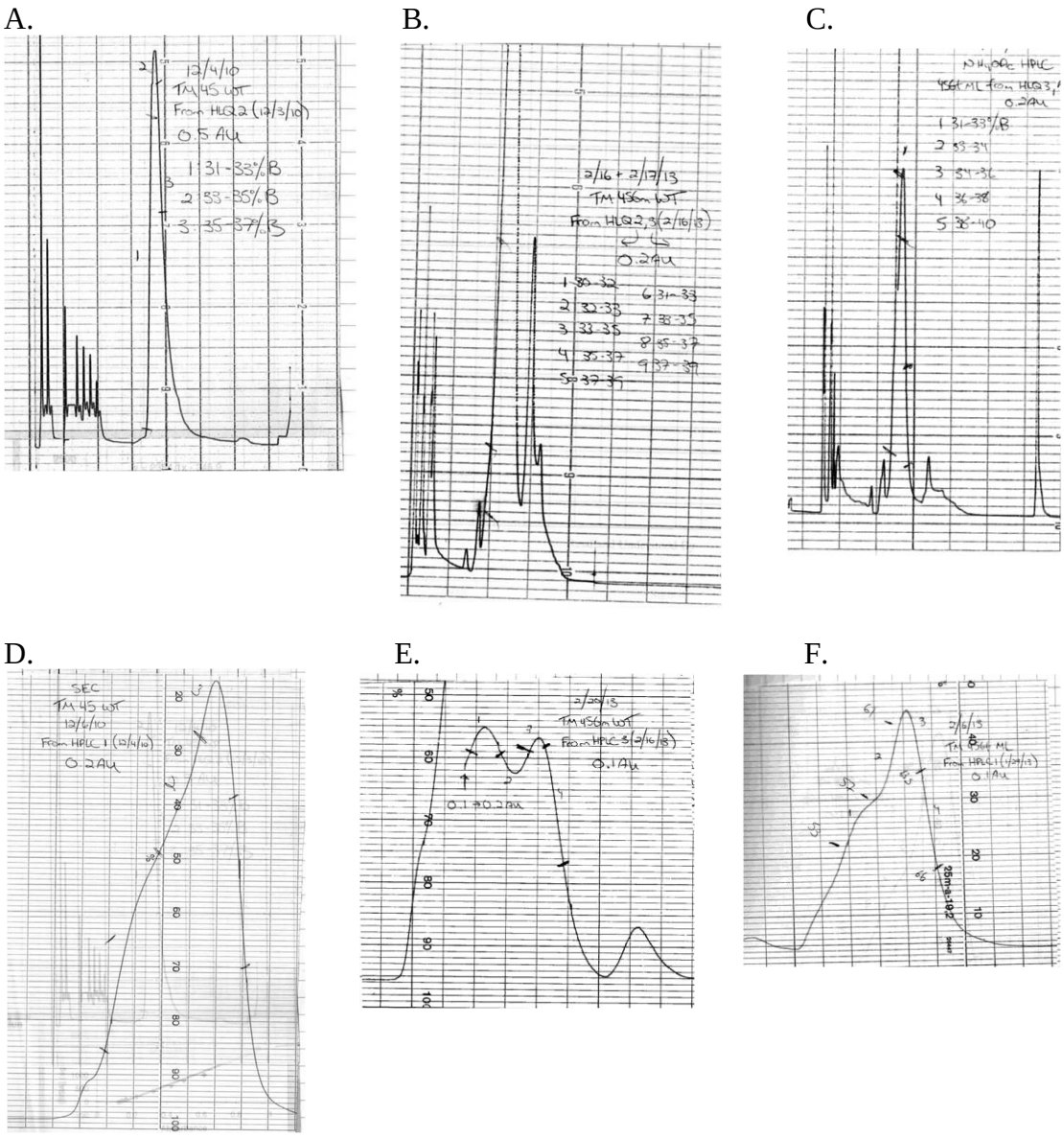

Figure 3.2: Representative purification traces for TM constructs. RP-HPLC traces for TM45 WT (A), TM456m WT (B), and TM456t ML (C) as well as SEC traces for TM45 WT (D), TM456m WT (E), and TM 456t ML (F) are shown here.

to the protocol used by White *et al.* (White, *et al.*, 1995). Briefly, Gene-clean purified pPic9K expression plasmid is linearized with BglII, and spheroplasts of the *P. pastoris* protease resistant strain, SMD1168, are transformed. This procedure results in multicopy insertion of the expression plasmid into the chromosomal DNA resulting in stable transformants. The multicopy transformants are then selected by replica plating onto high concentrations of G418, a kanamycin analog that penetrates *P. pastoris*. The SMD 1168 transformants that produced the highest level of TM expression were stored as glycerol freezes at -80^{0}C.

Protein Expression

Shake Flask Expression: A portion (10 μL) of a cell freeze was used to inoculate a 10 mL cultures of BMGY medium (1x YNB, 1% glycerol, 1% casamino acids, 0.4 mg biotin, pH 6.0), and allowed to shake at 30^{0}C and 300 RPM for two days. On day 3, the entire 10 mL culture was used to inoculate a 1L culture of BMGY in a sterile, 4L baffled flask, covered with 4 layers of sterile cheesecloth to further increase aeration and grown with continued shaking at 300 RPM and 30^{0}C. After another 48 hours, the cells consumed all of the glycerol present in the media and achieved a cell density usually around 50-60 Optical Density $(OD)_{600}$/mL. The cultures were collected by centrifugation (1500 g for 5 minutes) and each cell pellet was resuspended in 500 mL BMMY (Same as BMGY, but with 2% methanol instead of glycerol) and allowed to grow in the same manner for one final day. The final concentration step allows us to easily increase the cell density, which allows for improved protein production. Prior to purification, shake flask supernatant is filtered

through 0.8 μm followed by 0.2 μm filters to remove large contaminants prior to column loading in order to prevent column clogging in the first purification step.

Fermentation: Although shake flasks provide a convenient way to produce protein from *P. Pastoris*, fermentation allows for production of significantly larger amounts of protein. All fermentations were carried out in a BioFlo 3000 fermentor (New Brunswick Scientific, NJ) equipped with a 3L bioreactor containing 1.8L of Basal salts medium (13.3 mL/L phosphoric acid, 2.3 g/L calcium sulfate·$2H_20$, 14.3 g/L potassium sulfate, 11.7 g/L magnesium sulfate·$7H_20$, 3.9 g/L potassium hydroxide, and 40 mL/L glycerol) plus 4 mL/L PTM4 salts (2 g/L cupric sulfate·$5H_20$, 0.08 g/L sodium iodide, 3 g/L manganese sulfate, 0.2 g/L sodium molybdate·$2H_20$, 0.02 g/L boric acid, 0.5 g/L cobalt chloride, 7 g/L zinc chloride, 22 g/L ferrous sulfate·$7H_20$, and 5 mL/L sulfuric acid) and 4 mL/L of 10 mM biotin adjusted to pH 5.0 in the autoclave-sterilized fermenter vessel. A 10 mL culture is started similar to the shake flask preparation, but after 24 hours that culture is used to inoculate a 200 mL growth of BMGY. After another 24 hours at 30^0C and 300 RPM, the entire 200 mL culture was used to inoculate the fermenter vessel. During the fermentation, the growth was maintained at pH 5.0 by a controlled feed of 30% NH_4OH and the dissolved oxygen (DO) setpoint was maintained at 30% by a mixed feed of filtered air and pure O_2 supplied to the fermenter and adjusted automatically. After 20-24 hours of batch growth, the batch glycerol was depleted, shown by a corresponding increase, or spike, in the DO. A 1mL sample of the fermentation was separated at 3000 g for 1 minute and the Wet Cell Weight (WCW) was determined to be approximately 120 mg cell weight/mL culture. At this point, the glycerol fed-batch process was initiated,

where the feeding medium consisted of 50% glycerol and 12 mL/L of PTM4 salts and biotin at a feed rate of 10 mL/L/h. During the fed-batch process, the WCW increases to over 300. Optimal induction of protein production occurs when the induction phase starts at a WCW of approximately 320. The induction phase was initiated by first halting the glycerol feed and allowing a short period of time for the remaining glycerol to be metabolized, shown by another spike in the DO. The induction feed medium consisted first of 50% methanol with 12 mL/L of PTM4 salts and biotin and then after 24 hours 100% methanol with 12 mL/L of PTM4 salts and biotin. The induction was done in two phases, where the first phase is 50% methanol feed ramped from 1 mL/L/h to 10 mL/L/h over the course of 10 hours and then allowed to continue feeding at 10 mL/L/h for an additional 12 hours. After this, the 50% methanol is exchanged for 100% methanol and starting at a feed of 5 mL/L/h is ramped to 10 mL/L/h over 3 additional hours and allowed to continue at the maximum feed rate for 7 more hours. After this second period of induction, the fermenter supernatant was collected by centrifugation at 3000 g for 15 minutes and purified as described hereafter. A 24 to 36 hour induction appears to be the ideal period of time to make sufficiently large amounts of protein without the cell machinery or by products to begin to deteriorate and contaminate the final product, with the 100% methanol phase being entirely optional based upon observed stability of the fermentation itself and protein products.

TM Purification

The initial TM purification steps used here, including QAE Sephadex and Hi Load Q preparations are described in Chapter 2, and use methods outlined by White *et*

al. and Wood *et al.(Wood & Komives, 1999)*. However, recently changes have been made that provide improved purification of TM fragments beginning with reversed-phase HPLC. The partially purified TM from the HLQ was injected directly onto a Waters C18 reversed-phase prep column (19 x 300 mm) equilibrated with 20 mM NH_4OAc pH 5.75. TM was eluted in by a gradient of 90% NH_4OAc/ 10% ACN for 10 min, 10-50% over 30 min, and 50-90% over 20 min at a flow rate of 10 mL/min. The highest activity TM fragments normally eluted near 30% ACN and yields were approximately 50% in most cases. Fragments were lyophilized and stored at -20^0C. Finally, the fragments were reconstituted in DI H_2O and purified by HiLoad 16/60 Superdex 75 size-exclusion chromatography. (Amersham/GE Healthcare) in 50 mM Tris (pH 7.4), 150 mM NaCl. Representative traces of RP-HPLC and SEC purification steps for TM45 WT, TM456m WT, and TM456t ML are shown in Figure 3.2.

2. Protein C activation assay

Specific Activity Assay

In order to measure the thrombin-TM activation of protein C, or specific activity, we allowed a thrombin-TM complex to generate activated protein C (aPC) for a short amount of time and then after inactivating the thrombin with antithrombinIII, we measured the protease activity of the present activated protein C using an aPC-specific chromogenic substrate, S-2366 (Diapharma, West Chester, OH). A standard curve of aPC and chromogenic substrate versus time was generated previously by White *et al.* in order to convert the data to nmol aPC produced per minute, where 1 enzymatic unit

of activity, 1U, is equal to 1 nmol aPC produced per minute, and specific activity values are commonly reported in U/mg. This difference in production levels of aPC allows us to directly compare the activity of different TM constructs and mutants when experiments are performed at similar concentrations of thrombin. Typical specific activities for various TM constructs are reported in Figure 3.4.

The details of the assay procedure are as follows: stock solutions of 1x TBS (20 mM Tris, 100 mM NaCl, pH 7.4), BSA/Ca^{2+} (55 mg BSA, 28 mM $CaCl_2$ in 10 mL 1x TBS), and Enzyme Dilution Buffer or EDB (2 mL of BSA/Ca^{2+} solution in 9 mL of 1x TBS) were made. A solution of active thrombin was made just prior to beginning the assay, by mixing 4 μL of active thrombin from a stock solution of active thrombin, 0.2 mg/mL aliquots, stored at -80^{0}C with 196 μL of EDB (final thrombin concentration of 0.004 mg/mL or 108 nM). TM solutions were made ranging from 0.001-0.01 mg/mL depending upon expected activity. First, 20 μL of BSA/Ca^{2+} and 90 μL of 1x TBS are placed in different wells of a 96-well plate, then 15 μL of thrombin solution is added and finally 10 μL of each TM solutions. After 10 min of incubation at 25^{0}C, 20 μL of 60 μg/mL human protein C (Haematologic Technologies, Essex Junction, VT, diluted in EDB immediately before use) is added to each well. After incubation for an additional 20 minutes at 25^{0}C, the aPC production is quenched by adding 40 μL of Heparin-Antithrombin III solution (70 μg/mL ATIII, Haematologic Technologies, Essex Junction, VT with 82 μg/mL heparin and 2.7 μg/mL BSA in 1x TBS). After incubation for a further 10 min to completely inactivate thrombin, the pH was adjusted by addition of 20 μL of 100 mM Tris (pH 8) per well, and finally the amount of activated protein C was determined with the addition of 15 uL of the aPC-

specific chromogenic substrate, S-2366 (12.5 mg/mL in water, stored frozen at -20^{0}C until use).

Kinetic Protein C Assay

The determination of kinetic constants for TM binding to thrombin and subsequent binding and activation of PC is possible using a version of the specific activity assay above, but with three modifications (White, *et al.*, 1995). The first significant difference was the use of an enzymatically limiting amount of thrombin in the reaction. Instead of the excess used above, a starting solution of 40 ng/mL or 1 nM thrombin was used in each well, effectively making thrombin the limiting reagent in these kinetic assays in the range of [TM] used in these experiments. The other modifications were in the setup required for the determination of the Michaelis-Menten binding constants. Two sets of experiments were performed to calculate the Michaelis constants for TM and PC to thrombin, or $K_{M,TM}$ was $K_{M,PC,}$ respectively. $K_{M,TM}$ was determined by using a range of [TM] concentrations (0.8 μM to 7.75 μM) at a fixed [PC] (7.75 μM), in the assay, and $K_{M,TM}$ was calculated at the concentration of $V_{max,app}/2$ on the corresponding Michaelis-Menten curve. Second, $K_{M,PC}$ was determined by a similar assay, but the [TM] was held constant at the determined $K_{M,TM}$ and a range of [PC] was used (7.75 μM to 77.5 μM), and it was calculated at the concentration of $V_{max,app}/2$ on the corresponding Michaelis-Menten curve as well. First, the apparent V_{max} is obtained from the hyperbolic first using Equation 1 and 3 to determine $K_{M,TM}$ and $K_{M,PC}$. Then, the true V_{max} was calculated by correcting for the $K_{M,TM}$ and $K_{M,PC}$ Equations 2 and 4). Finally, the true V_{max} was used to calculate k_{cat}.

$$V_{TM} = \frac{V_{max}[TM]}{K_{M,TM}\frac{1+K_{M,PC}}{[PC]} + [TM]\frac{1+K_{M,PC}}{[PC]}}$$ Equation 1

$$V_{max} = V_{max,app}(TM)(1 + \frac{K_{M,PC}}{PC})$$ Equation 2

and

$$V_{PC} = \frac{V_{max}[PC]}{K_{M,PC}\frac{1+K_{M,TM}}{[TM]} + [PC]\frac{1+K_{M,TM}}{[TM]}}$$ Equation 3

$$V_{max} = V_{max,app}(PC)(1 + \frac{K_{M,TM}}{TM})$$ Equation 4

These equations represent the kinetics for an enzymatic process requiring an activator molecule, which in this case is the TM.

C. RESULTS

1. TM456m Construct and its Activity

A new construct of TM45 was made that also incorporated a portion of the sixth EGF-like domain. This construct added the first 23 residues of the sixth EGF-like domain of TM to the previously used fragment, TM45. However this truncates C462 which forms the 3rd disulfide bond in the 6th domain with C448. Thus, to avoid the potential protein stability problems caused by a free thiol from unbound C448, this residue was conservatively mutated to a serine. We have named this construct TM456-mini or TM456m, and its sequence is shown in Figure 3.3, with the additional residues added from the 6th domain shown in blue. Additionally, the resides are highlighted on the crystal structure of TM456-thrombin in Figure 3.4 to show their position relative to both the 5th domain of TM and the binding interface with thrombin. As shown, the

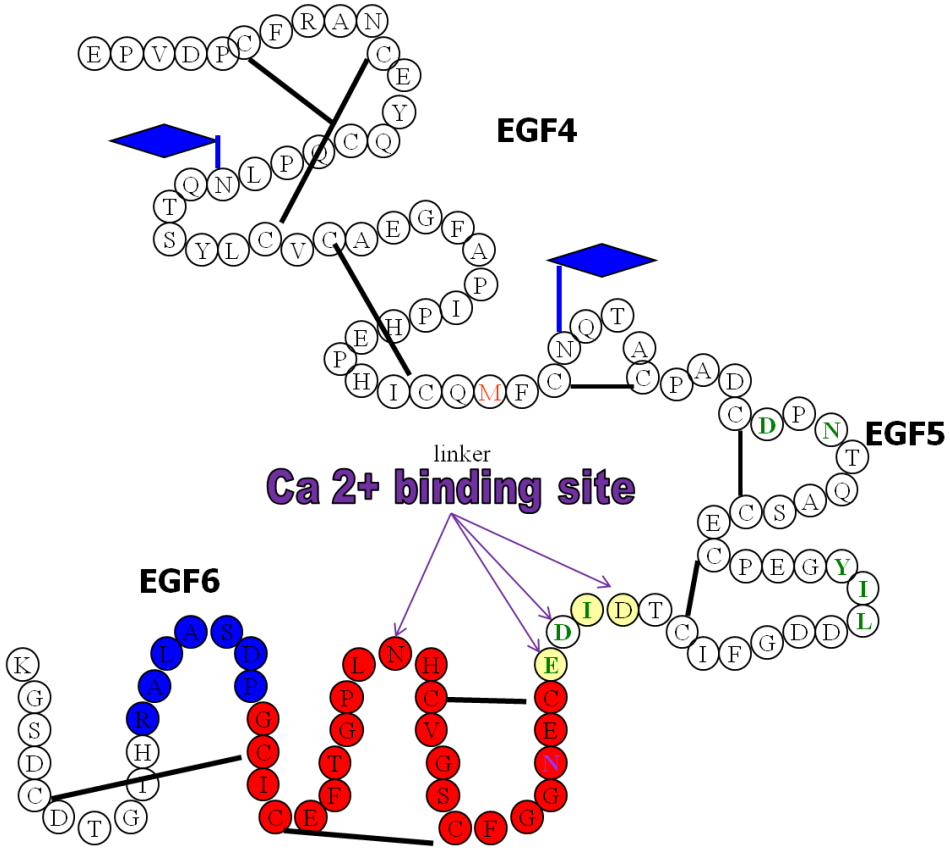

Figure 3.3: Full schematic of TM456. Disulfide bonds shown are black lines and glycosylation sites are shown by blue diamonds. The first 23 residues of 6th domain filled in red, the 24th to 30th residues of the 6th domain are filled in blue. The Ca^{2+} binding residues are highlighted in purple.

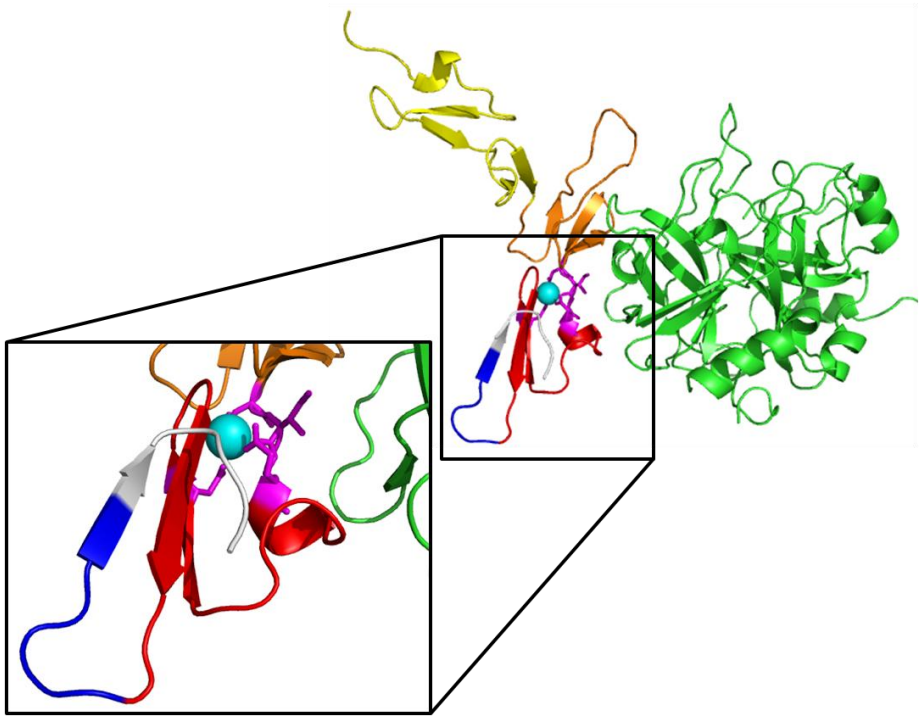

Figure 3.4: Crystal structure of TM456 complexed with Thrombin (green, PDB 1DX5). The 4th EGF domain is in yellow, the 5th domain is in orange, the first 23 residues are colored in red, the next 7 are colored in blue, and the rest of the available structure is white. The Ca^{2+} coordinated between the 5th and 6th domains is colored in cyan.

first two disulfide bonds in the 6th domain are kept intact and would indicate that the structure near TM5 and the binding interface would be largely unchanged. TM456m purified from *P. Pastoris* by both shake flask and fermenter growths, showed both high production quantities and fair activity in the crude product. Final yields were typically on the order of 5-10 mg of pure protein.

TM456t ML Construct and its Activity

TM456m exhibited low activity, but strong stability, so in continuing to expand upon TM456m, we attempted to expand the incorporation of 6th domain residues into our construct. We added the next seven residues of the 6th domain to our 456m construct, yielding 75% of the 6th domain, or more than 90% of full TM456. We have named this construct TM 456t, and it is shown in Figure 3.3, with the additional 7 residues colored in red. As with TM 456m, TM456t includes the C448S mutation. Additionally, our experiments here also incorporate the M388L mutation in the linker between the 4th and 5th domains of TM. This methionine was originally shown to decrease cofactor activity by 75-90% upon oxidation (Glaser, *et al.*, 1992), and mutation to leucine successfully increases protein stability by eliminating the potential for oxidation. Additionally, this mutation also increases the cofactor activity of thrombin towards PC by approximately 2 fold (White, *et al.*, 1995). TM 456t ML was purified from *P. Pastoris* by both shake flask and fermenter preparations, with similar activity levels obtained from each. Table 3.4 shows a summary of the purification steps for TM 456t ML, with total protein amounts and corresponding TM

Table 3.1: Purification summary for TM 456t ML. Each step shows typical protein yield and specific activity.

Purification Step	Specific Activity – Scheme 1 (U/mL)	Specific Activity – Scheme 2 (U/mL)	Protein Yield (mg)
QAE Sephadex	8×10^4	8×10^4	100 mg
Hi Load Q	1.5×10^5	1.5×10^5	24 mg
HPLC (0.1% TFA)	1×10^5		6 mg
HPLC (20 mM NH_4OAc)		3.5×10^5	6 mg
Size Exclusion	1.5×10^5	9×10^5	2 mg

activities at each step in the purification. The raw activity for TM 456t ML increased dramatically with each step in the purification, although only small portions of each peak show high activity. During the purification of TM 456t ML, a large portion of the protein was being inactivated during reversed-phase HPLC in 0.1% TFA. Active protein from the Hi Load Q was effectively inactivated by the low pH gradient in the HPLC. However, protein activity was effectively preserved and even dramatically increased by using 20 mM NH_4OAC pH 5.75 instead of 0.1% TFA. The activity gains for each purification step as well as the difference between the HPLC purification conditions are illustrated by the JBC activity table in Table 3.1. The specific activity for TM456t ML is shown in Table 3.2 and compared to various other TM constructs including TM45 and TM456.

TM456t ML also shows improved stability in solution. It maintained full activity in the size exclusion buffer, 1X TBS, after storage for more than one week at 4^0 C. Also, compared to TM456 which cannot be successfully concentrated for solution experiments, TM456t ML can be successfully concentrated beyond 1mM (12 mg/mL) without aggregation or loss of activity.

With the improved purification scheme for TM456t, we purified a new sample of TM456m using the improved HPLC conditions. There was a dramatic increase in specific activity after both HPLC and size-exclusion chromatography using 20 mM NH_4OAC vs. 0.1% TFA. Table 3.4 reflects the improved specific activity for TM456m WT: 6×10^5.

3. TM Calcium Binding

Table 3.2: This table summarizes the specific activities for various TM constructs. *-values were previously reported values by White *et al. (White, et al., 1995).*

TM Construct	**Specific Activity (nmol aPC*min^{-1}*mg^{-1})**
Rabbit TM*	1.7×10^6
TM 45 WT	1.7×10^5
TM 45 ML*	3.5×10^5
TM 456 ML*	3.5×10^6
TM 456m WT	6×10^5
TM 456t ML	9×10^5
TM 456t ML (pH 2)	7.4×10^5 (82%)
TM 456m WT (pH 2)	5.2×10^5 (87%)
TM 456t ML (Chelex)	4.9×10^5 (54%)
TM 456m WT (Chelex)	2.8×10^5 (46%)

In trying to understand why reversed-phase HPLC of TM45 in 0.1% TFA resulted in high activity protein whereas constructs containing part of the 6^{th} domain were reduced in activity levels close to those of TM45, we hypothesized that the low pH might be partially removing the calcium ion that is known to be bound very tightly in TM (Light, *et al.*, 1999). In these experiments from Light *et* al. it was shown by equilibrium dialysis that there is one tight calcium binding site in TM456 ($K_d \sim 2\ \mu M$) that can only be depleted by EDTA. Furthermore, when this calcium was removed, they found that the binding affinity of thrombin for TM was decreased by 75-fold, as measured by BIAcore. This Ca^{2+} binding site is located between the 5^{th} and 6^{th} domains of TM and it is highlighted in Figures 3.3 and 3.4 (Ca^{2+} is shown in cyan and suspected binding residues are highlighted in magenta). In order to test the effects of Ca^{2+} binding, we attempted to remove the Ca^{2+} from both TM456m and TM456t ML using Chelex-100 Resin (BioRad), a chelating resin that can be quickly and easily separated from solution by centrifugation. We incubated TM samples with 50 mg/mL of Chelex 100 resin at room temperature with moderate agitiation in order to maintain the suspension of resin. Samples of each TM were removed hourly and analyzed using the specific activity Protein C Assay. There was a small reduction in activity within the first hour, but the activity remained essentially constant over the following 5 hours. We allowed the samples to continue shaking overnight and an additional three days after that. There was another small reduction in activity for both TM constructs after the overnight incubation, but no further reduction after multiple days of incubation. We also used a room temperature control of TM without resin that showed almost no loss of activity under the same agitation conditions as these Chelex samples. The

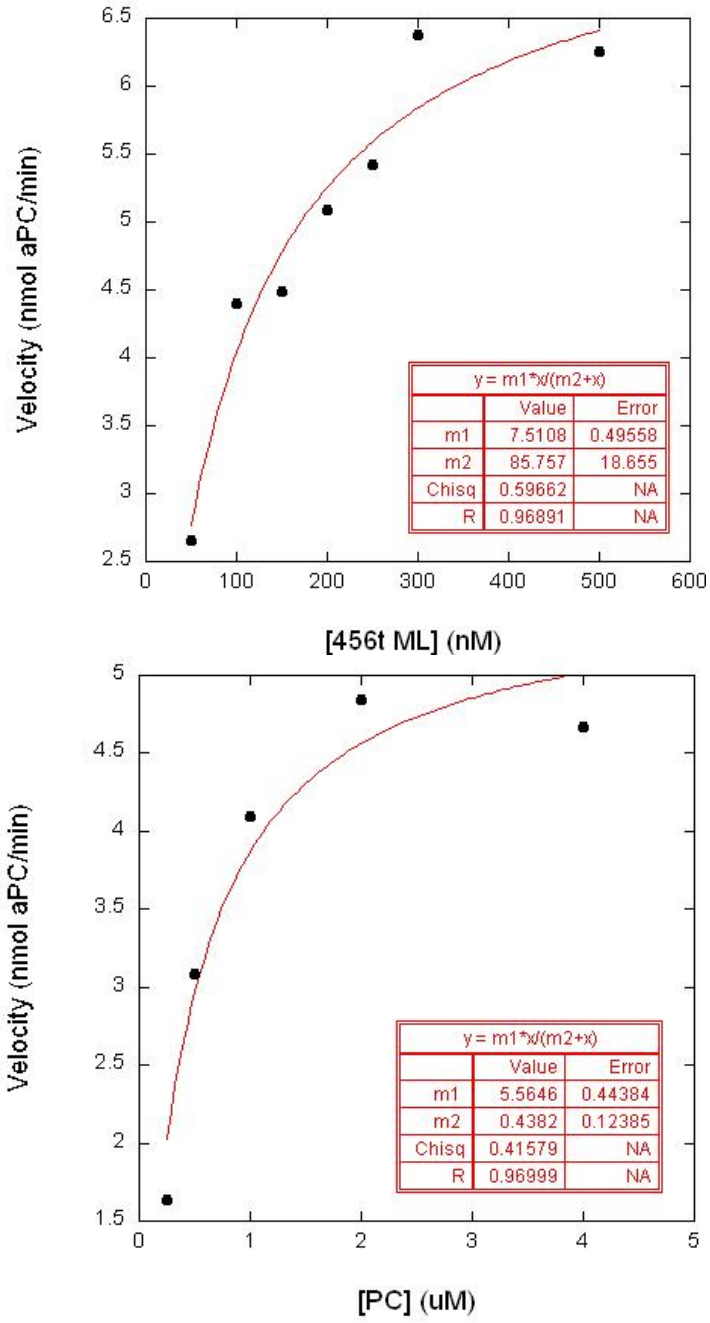

Figure 3.5: Representative plots for kinetic PC assays to find $K_{M,\,TM}$, $K_{M,\,PC}$, and k_{cat} for TM 456t ML. Both graphs show reaction velocity V, on the y-axis, plotted against variable concentration of the reagent. The left plot uses variable [TM] to derive $K_{M,TM}$ and the right plot uses variable [PC] to calculate $K_{M,PC}$. The table summarizes the experiments with the average for the data shown with its standard deviation.

activity data for these TM samples is shown in Table 3.2 for both TM456t ML and TM456m WT (Chelex) along with the percent activity compared to their unaltered forms. Additionally, we tested the effects of low pH conditions upon TM activity by making a dilution of TM456m and TM456t ML into 0.1% TFA (pH 2) and agitating at 25^0C for the same timepoints used above for chelex incubations. The activity data for these samples is also shown in Table 3.4 for both TM 456t ML and TM 456m WT (pH 2), and there was a much smaller reduction in activity compared to the Chelex incubated samples.

4. TM Construct Kinetic Constants

In order to fully contrast the effects of TM 456t ML with TM 45, it was important to establish the $K_{M,TM}$, $K_{M,PC}$, and k_{cat}. These parameters were established previously by White *et al.* for TM 45, and more recently for a number of TM 45 point mutants by Koeppe *et al.* (Koeppe, 2008). Using the kinetic protein C assay, we found the Michaelis-Menten constants for TM456t ML. Figure 3.5 shows representative plots of these experiments for both $K_{M,TM}$, and $K_{M,PC}$, as well as the specific activity, k_{cat}, and $k_{cat}/K_{M,PC}$.

After the improved purification of TM456t, and application of this technique to purify TM456m, we established the $K_{M,TM}$, $K_{M,PC}$, and k_{cat} for it as well. Figure 3.6 shows representative plots from these experiments, similar to Figure 3.5 for TM456t ML.

D. Discussion

1. New TM constructs improve the activity of TM45

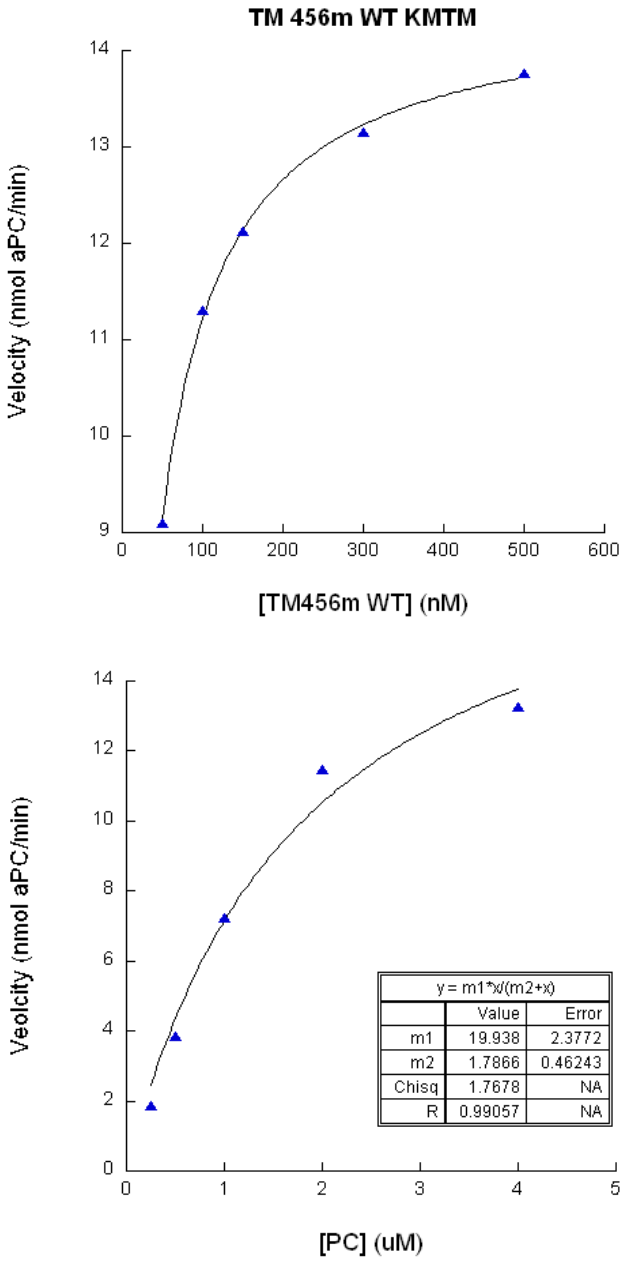

Figure 3.6: Representative plots for kinetic PC assays to find $K_{M,\,TM}$, $K_{M,\,PC}$, and k_{cat} for TM 456m WT. Both graphs show reaction velocity V, on the y-axis, plotted against variable concentration of the reagent. The left plot uses variable [TM] to derive $K_{M,TM}$ and the right plot uses variable [PC] to calculate $K_{M,PC}$. The table summarizes the experiments with the average for the data shown with its standard deviation.

The initial specific activity for TM456m WT suggested that it was essentially the same as TM45. A multitude of protein preps and attempts at purification yielded low activity protein that quickly deteriorated. Our initial hypothesis was that this first portion of the 6th domain was insufficient to recapitulate the activity gains from inclusion of the 6th domain

However, the activity of TM456m was dramatically improved by increasing the pH of the HPLC conditions. Even though we could not demonstrate that Chelex-100 treatment or treatment with 0.1% TFA in the absence of C18 chromatography completely reversed the activity against, we believe that the activity improves when the calcium binding site is retained. This belief is partly based on previous results from out lab (unpublished) and from Light *et al.* that show that the calcium is extremely tightly bound and difficult to remove.

The initial specific activity for TM456t ML was extremely high, almost 80% of the activity for full TM456. However, using the same initial purification strategy for TM45 shown previously was very inconsistent, typically resulting in poorly active protein and only rarely giving protein with noticeably higher specific activity than TM45. We hypothesize that the difference in initial activities between TM456m and TM456t is that the extra residues allowed for a small enough improvement in Ca^{2+} binding that some small portion of the protein could rarely be purified in active form. However, this inconsistency made it appear that TM456t was ineffective as a substitute for TM45, showing low stability and high purification difficulty, but those few successful purifications hinted at the potential success for this construct. All successful and unsuccessful purifications showed similar specific activities after both

the QAE and Hi Load Q columns, an example is shown in Figure 3.4. Then, protein purified by RP-HPLC in 0.1% TFA not only failed to increase specific activity, but actually lost activity in comparison to the Hi Load Q purified protein. Although protein had previously been successfully purified in these conditions, this data strongly suggested that either the column or method was causing the activity loss, or that it was the conditions themselves. This suggests the importance of Ca^{2+} binding facilitated by multiple aspartic acid residues and a glutamic acid around the binding site. The pK_a's for both aspartic acid and glutamic acid are approximately 4, and at pH 2, its side chain will be ~99% protonated. The protonated forms of Asp and Glu eliminate the negative charges, which appear to be critical in maintaining the charge interaction holding Ca^{2+} in the 5^{th} domain. Thus, we used another mobile phase condition at a higher pH: 20 mM NH_4OAc, pH 5.75. This adjustment significantly increased the activity of TM456t ML, and allowed for an even larger activity increase after size-exclusion purification. Furthermore, multiple different protein preparations showed consistently high activity under these conditions. Active TM45 was easily purified at low pH in 0.1% TFA on the HPLC, but the added portion of the 6^{th} domain makes maintaining overall cofactor activity more difficult. Thus, the improved purification scheme now yields pure TM456t ML that shows activity at approximately 53% of full length TM456, compared to 10% for TM45.

2. Pure TM456t ML and TM456m WT show high solution stability

Previous experimental research has shown that full length TM456 is very unstable in solution, particularly when concentrated, whereas TM45 is extremely well-behaved. Although our initial data suggested that the new TM constructs were similar in behavior to TM456, improved purification has dramatically improved both their activity and stability. Previously, White *et al.* also used a higher pH for purification of TM456, but their purifications were inconsistent and typically gave low yields and rarely high activity. After purification, TM456t and 456m can be successfully concentrated to >10 mg/mL (800 μM) and stored at 4^0C for days to weeks with little to no loss in activity. Furthermore, at < 1mg/mL these TM constructs can be stored at 4^0C in TBS (pH 7.4) for more than a month with no loss in activity. These stability studies suggest that TM456t and 456m are very stable at a number of conditions and demonstrate a significant improvement over full length TM456.

3. Kinetic data suggests that TM456t and TM456m bind to thrombin more tightly than TM45

We have created these two constructs based on research that seemed to show that the portion of the 6^{th} domain of thrombomodulin necessary for thrombin binding was contained primarily in residues T422-G449 of human TM, based upon peptide-binding NMR binding experiments analyzing transferred NOEs and residue chemical shifts (Tolkatchev, *et al.*, 2000). The kinetic binding assay data for both TM456t ML and TM456m WT is summarized in figures 3.4 and 3.5. $K_{M,TM}$ serves as a pseudo binding constant for TM and thrombin and both constructs show significant (~4-fold) improvement in binding compared to TM45 (data not shown). This increase in binding

Table 3.3: Michaelis-menten parameters for TM45 WT, TM456t ML, and TM456m WT as determined by kinetic protein C assays. *-values are taken from White *et al.*

TM Construct	**$K_{M, TM}$ (nM)**	**$K_{M, PC}$ (μM)**	**k_{cat} (s^{-1})**	**$k_{cat}/K_{M,PC}$ (s^{-1} μM^{-1})**	**Specific Activity**
TM45 WT	350	1.5	2	1.3	1.7×10^5
TM456m WT	44	1.8	6	3.2	6×10^5

affinity strongly supports our hypothesis that these residues are an important component for overall binding of TM to thrombin. Furthermore, we suggest that one of the keys for this improvement in activity and binding is contained in the suspected calcium-binding domain of the 6th EGF-like domain shown in Figure 3.2, with the bound calcium shown in cyan, and the specific residues involved are highlighted in purple in Figure 3.3. We tested the basis for this activity by using Chelex 100 Chelating Ion Resin (BioRad) to remove the bound calcium from TM456m WT and TM456t ML. We incubated TM-Chelex samples both overnight and for multiple days at room temperature as well as testing the effects of long term incubation at acidic pH, as a mimic of our initial RP-HPLC conditions, by incubating protein in 0.1% TFA, pH 2 for the same time points as our Chelex samples. After incubation under various conditions we tested the specific activity of these samples; the results are summarized in Figure 3.10. We found that simple storage at low pH had a small effect on the specific activity of either TM construct, but incubation with Chelex resin caused a significant reduction in thrombomodulin activity. However, this effect of calcium chelation was insufficient to bring TM456m and TM456t completely back to the level of TM45. Data are summarized in Figure 3.4 along with the percent activity compared to normal TM456t ML and TM456m WT. We suggest that the effect of low pH and hydrophobic binding to a C18 RP-HPLC column combine to most effectively decimate the specific activity of our new TM constructs.

Based on our data presented here, TM456m and TM456t ML show similar cofactor activity levels after adjusting for the improvement resulting from the M388L

mutation. Thus, the additional 7 residues in the 6th domain added to TM456m to create TM456t do not appear to improve the overall cofactor activity, but we believe that those residues may play some small role in helping maintain the calcium binding site between the 5th and 6th domains, suggested by the initial stability gains of TM456t versus TM456m.

E. Conclusions

We have presented experiments here to express, purify, and begin characterization of two improved constructs of TM45. Both TM456t ML and TM456m WT show significantly increased specific activity compared to TM45, 6-fold and 4-fold respectively. Additionally, they do not show any of the poor stability problems found in full length TM456, but our point mutations presented here offer a small insight into some destabilizing factors in our new constructs. One of the main limitations for biophysical characterization of the TM45-thrombin interaction has been the low binding affinity, but the much higher activity and affinity of TM456m and TM456t allows for a broader spectrum of biophysical experiments that require stronger binding than was previously available. Finally, the greater efficiency of these constructs and the relative ease of both their expression and purification present new opportunities for *in vivo* applications to clot management. Current expression methods for Solulin and other soluble TM analogs are dependent on mammalian expression systems (Gomi, *et al.*, 1990) that have much lower economic efficiency compared to both the ease of use and high protein production qualities of *P. pastoris*. Thus, the

possibility of using a TM construct that is amenable to yeast expression creates the chance to make new TM-based drugs in high quantities with relatively low cost: ideal attributes for potential drug molecules.

F. References

[1] De Cristofaro R & Landolfi R (1999) Allosteric modulation of BPTI interaction with human alpha- and zeta-thrombin. *Eur J Biochem* **260**: 97-102.

[2] Esmon CT (2000) Regulation of blood coagulation. *Biochimica et Biophysica Acta* **1477**: 349-360.

[3] Glaser CB, Morser J, Clarke JH, *et al.* (1992) Oxidation of a Specific Methionine in Thrombomodulin by Activated Neutrophil Products Blocks Cofactor Activity. *J Clin Invest* **90**: 2565-2573.

[4] Gomi K, Zushi M, Honda G, *et al.* (1990) Antithrombotic Effect of Recombinant Human Thrombomodulin on Thrombin-Induced Thromboembolism in Mice. *Blood* **7**: 1396-1399.

[5] Koeppe J, Beach, M., Baerga-Ortiz, A., Kerns, J., and Komives, E. (2008) Mutations in the fourth EGF-like domain affect thrombomodulin-induced changes in the active site of thrombin. *Biochemistry* **47**: 10933-10939.

[6] Koeppe JR, Seitova, A., Mather, T., Komives, E. (2005) Thrombomodulin tightens the thrombin active site loops to promote protein C activation. *Biochemistry* **44**: 14784-14791.

[7] Light DR, Glaser CB, Betts M, *et al.* (1999) The interaction of thrombomodulin with Ca2+. *Eur. J. Biochem.* **262**: 522-533.

[8] Mandell JG, Baerga-Ortiz A, Akashi S, Takio K & Komives EA (2001) Solvent accessibility of the thrombin-thrombomodulin interface. *J Mol Biol* **306**: 575-589.

[9] Myles T, Church F, Whinna H, Monard D & Stone SR (1998) Role of thrombin anion-binding exosite-I in the formation of thrombin-serpin complexes. *J Biol Chem* **273**: 31203-31208.

[10] Pechik I, Madrazo J, Mosesson MW, Hernandez I, Gilliland GL & Medved L (2004) Crystal structure of the complex between thrombin and the central "E" region of fibrin. *PNAS* **101**: 2718-2723.

[11] Rezaie AR, He X & Esmon CT (1998) Thrombomodulin increases the rate of thrombin inhibition by BPTI. *Biochemistry* **37**: 693-699.

[12] Rezaie AR, Cooper ST, Church FC & Esmon CT (1995) Protein C inhibitor is a potent inhibitor of the thrombin-thrombomodulin complex. *J Biol Chem* **270**: 25336-25339.

[13] Stubbs MT, Oschkinat H, Mayr I, Huber R, Angliker H, Stone SR & Bode W (1992) The interaction of thrombin with fibrinogen. *Eur. J. Biochem.* **206**: 187-195.

[14] Tolkatchev D, Ng A, Zhu B & Ni F (2000) Identification of a Thrombin-Binding Region in the Sixth Epidermal Growth Factor-like Repeat of Human Thrombomodulin. *Biochemistry* **39**: 10365-10372.

[15] van de Locht A, Bode W, Huber R, Le Bonniec BF, Stone SR, Esmon CT & Stubbs MT (1997) The thrombin E192Q-BPTI complex reveals gross structural rearrangements: implications for the interaction with antithrombin and thrombomodulin. *EMBO J* **16**: 2977-2984.

[16] van Lersel T, Stroissniq H, Giesen P, Wemer J & Wilhelm-Ogunbiyi K (2011) Phase I study of Solulin, a novel recombinant soluble human thrombomodulin analogue. *Thromb. Haemost.* **105**: 302-312.

[17] White CE, Hunter MJ, Meininger DP, White LR & Komives EA (1995) Large-scale expression, purification and characterization of small fragments of thrombomodulin: the roles of the sixth domain and of methionine 388. *Protein Engineering* **8**: 1177-1187.

[18] Wood MJ & Komives EA (1999) Production of large quantities of isotopically labeled protein in Pichia pastoris by fermentation. *J. Biomol. NMR* **13**: 149-159.

[19] Zushi M, Gomi K, Yamamoto S, Maruyama I, Hayashi T & Suzuki K (1989) The last three consecutive epidermal growth factor-like structures of human thrombomodulin comprise the minimum functional domain for protein C-activating cofactor activity and anticoagulant activity. *Journal of Biological Chemistry* **264**: 10351-10353.

Chapter IV

Hydrogen-Deuterium Exchange Mass Spectrometry to Probe the Thrombin-TM456t Interaction

A. Introduction

The protease activity of thrombin is highly dependent upon many subtle motions in a variety of different timescales. This dynamic behavior can provide a number of benefits to its activity, such as increased enzymatic turnover and flexibility with substrate binding. One of the manifestations of these dynamic effects can be seen in allosteric changes upon ligand binding at the anion binding exosite I (ABEI). Although changes were not evident in a myriad of crystallographic studies, they have been shown in solution based studies previously in our lab via H/D exchange mass spectrometry (Koeppe, 2005) as well as by isothermal titration calorimetry (Treuheit, *et al.*, 2011). Furthermore, recent advances have been made in the bacterial expression of thrombin, which allows for production of both ^{13}C and ^{15}N isotopically labeled thrombin. This ability to produce labeled protein has opened new avenues for studying thrombin motions on multiple timescales in solution using NMR spectroscopy (Lechtenberg, *et al.*, 2010, Fuglestad, *et al.*, 2012). This research has allowed for much deeper insight into the dynamic fluctuations of thrombin, hinting at an ensemble of structures that may explain the solution behavior of the protein. Fuglestad *et al.* (Fuglestad, *et al.*, 2012) compared residual dipolar coupling data from NMR experiments with RDCs computed from crystallographic data or from structural ensembles generated from molecular dynamics (MD) simulations. The strongest agreement between the NMR experimental data from thrombin in solution and computational data was achieved by using an ensemble average from an accelerated MD simulation. Additionally, Gasper *et al.* performed accelerated MD simulations

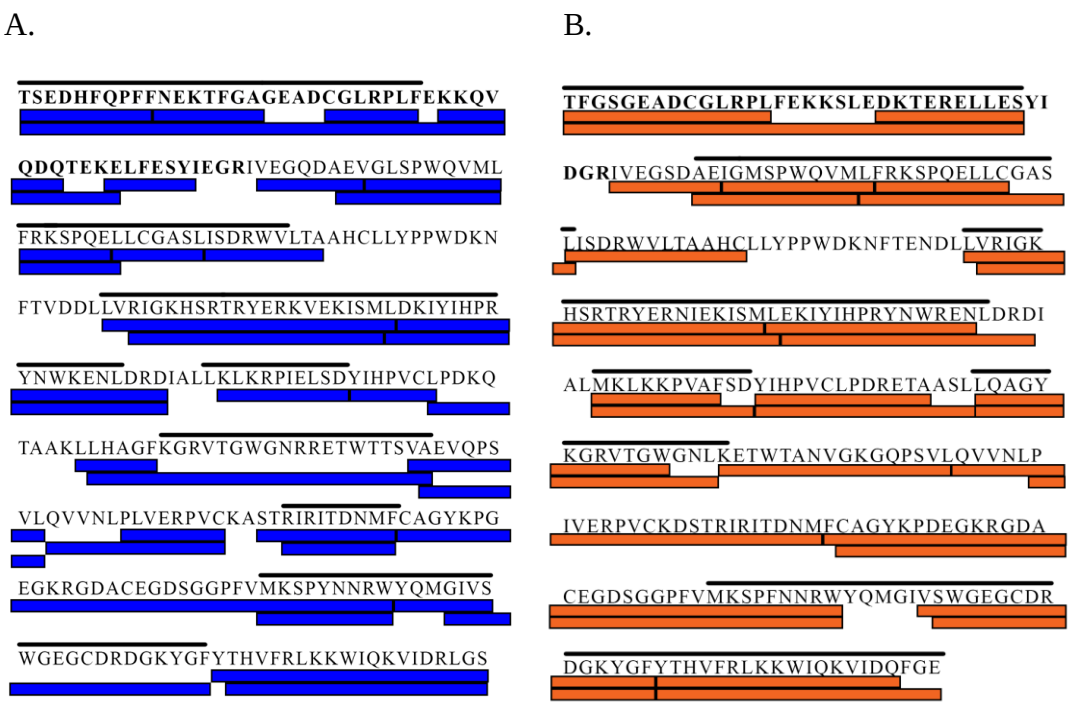

Figure 4.1: Peptide coverage maps for A. bovine thrombin (peptides shown in blue) and B. human thrombin (peptides shown in orange). For both proteins the light chain is shown in bold and heavy chain is in normal typeface. Solid lines above the sequence represent the prevences coverage regions obtained by Koeppe *et al. {Koeppe, 2005 #6}.*

A.

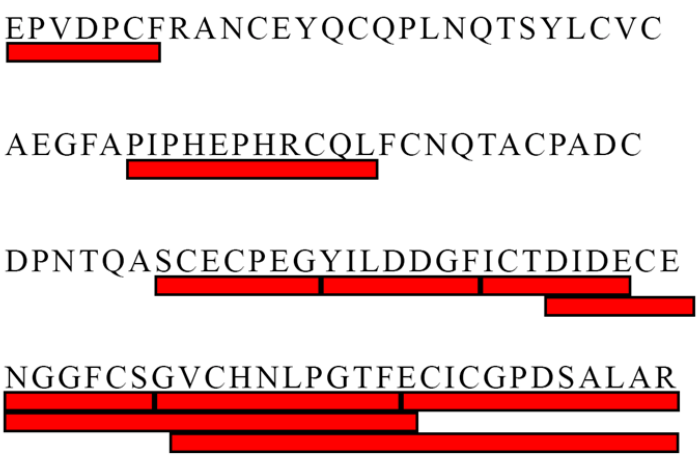

B.

Figure 4.2: (A) Peptide coverage map for TM456t ML. (B) Diagram mapping covered regions (red) and uncovered regions (gray) on to the crystal structure of TM456 (PDB: 1DX5) with glycosylation sites highlighted in purple.

simulations that show significant molecular motion as well as allosteric pathways that help account for both the effects of thrombomodulin (TM)-binding and the effects propagated by the 4th EGF-like domain that seems to have specific effects on the active site loops of thrombin (Gasper, *et al.*, 2012).

With the advent of new constructs of TM presented in Chapter 3 that show both high thrombin binding affinity and cofactor activity towards thrombin, we wanted to revisit previous H/D exchange mass spectrometry (HDXMS) experiments done previously with thrombin (Koeppe, 2005, Koeppe, 2008). Furthermore, the new Synapt G2 mass spectrometer combined with the LEAP-robotic HDX system (Waters) we have used in collaboration with researchers at Eli Lilly (Lilly Biotechnology, San Diego, CA) promised better sequence coverage. Using this system, we were able to analyze the HDX effects for both bovine and human thrombin in the presence or absence of TM456t. Here, we present the dramatic improvement in sequence coverage for both human and bovine thrombin, and new regions of the protein that show differences in H/D exchange upon binding as well as regions that are unchanged. Additionally, we are now able to generate and identify digestion products from TM using LC separation of samples treated with a high concentration of TCEP to reduce the disulfide bonds, from thrombomodulin, which was not possible in previous MALDI-TOF HDX experiments.

B. Materials and Methods

1. Proteins

Bovine thrombin was purified as described previously in Chapters 2 and 3. After purification, bovine thrombin was buffer exchanged into 25 mM NaH_2PO_4, 100 mM NaCl, pH 6.5 using 10 kDa molecular weight cutoff centrifugal concentrators (Amicon, 4 mL capacity) and then lyophilized in 2.7 nmol aliquots. These samples were stored at -80^oC until immediately before they were required, when they were reconstituted in either 40 μL of water for thrombin alone or 40 μL TM456t ML solution to create thrombin-TM456t ML complex for the exchange experiments

TM456t ML was purified as described in Chapter 3, where the final purification step yielded active protein by size exclusion chromatography into 50 mM Tris, 150 mM NaCl, pH 7.4. Active protein was buffer exchanged and concentrated to at least 2 mg/mL in 25 mM NaH_2PO_4, 100 mM NaCl, pH 6.5, again using 10kDa molecular weight cutoff centrifugal concentrators. This protein can be safely stored at 4^oC without any significant activity loss, as discussed previously, so these samples were made and stored the day before experiments were planned. Before complexing it with thrombin or analyzing TM alone, it was diluted with water to a final concentration of 135 μM. This provided very good peptide signal in the MS data at a reasonable protein concentration for these experiments.

Previous experiments in our lab have used human thrombin in addition to bovine thrombin for the purpose of increased sequence coverage as well as finding subtle differences in protein activity (Koeppe, 2006). Human α-thrombin was obtained from Haematologic Technologies (Essex Junction, VT). Activity was tested by a fibrinogen clotting assay and protein concentration was determined by absorbance at 280 nm ($\varepsilon = 1.92$ cm mL unit^{-1} mg^{-1}). Protein was also buffer exchanged into 25 mM

NaH_2PO_4, 100 mM NaCl, pH 6.5 and concentrated to ~2 mg/mL. 2.7 nmol aliquots were lyophilized and stored at -80^oC until immediately before use.

2. Mass Spectrometry

a. System Specifications

Mass spectrometry (MS) experiments were performed at Lilly Biotechnology (San Diego, CA) on a Waters Synapt G2S Mass Spectrometry system coupled to a LEAP-robotic HDX system. Digestion was achieved using an online POROS pepsin column (2.1 x 30 mm) at 16^oC, and peptides were separated by direct injection into a nanoACQUITY-UPLC BEH 21 x 5 mm C18 column with 1.2 μm resin and fully eluted over a 12 min gradient of formic acid/acetonitrile. Mass spectra were acquired by electrospray ionization of the column eluent onto a G2S Q-TOF mass spectrometer equipped with eloctrospray ionization. Mass spectra were collected in MS^E mode, with mass calibration using a Glu-Fibrinogen peptide. Peptides were identified using ProteinLynx Global Server software (Waters), and the HDX data were analyzed using the DynamX 2.0 software (Waters).

b. Amide H/D Exchange Experiments

For free bovine- and human-thrombin exchange experiments, lyophilized aliquots were reconstituted in 40 μL of H_2O immediately before beginning a set of exchange timepoints. Thrombin-TM complex experiments required two different concentration ratios to ensure the existence of completely bound thrombin and TM in

A.

B.

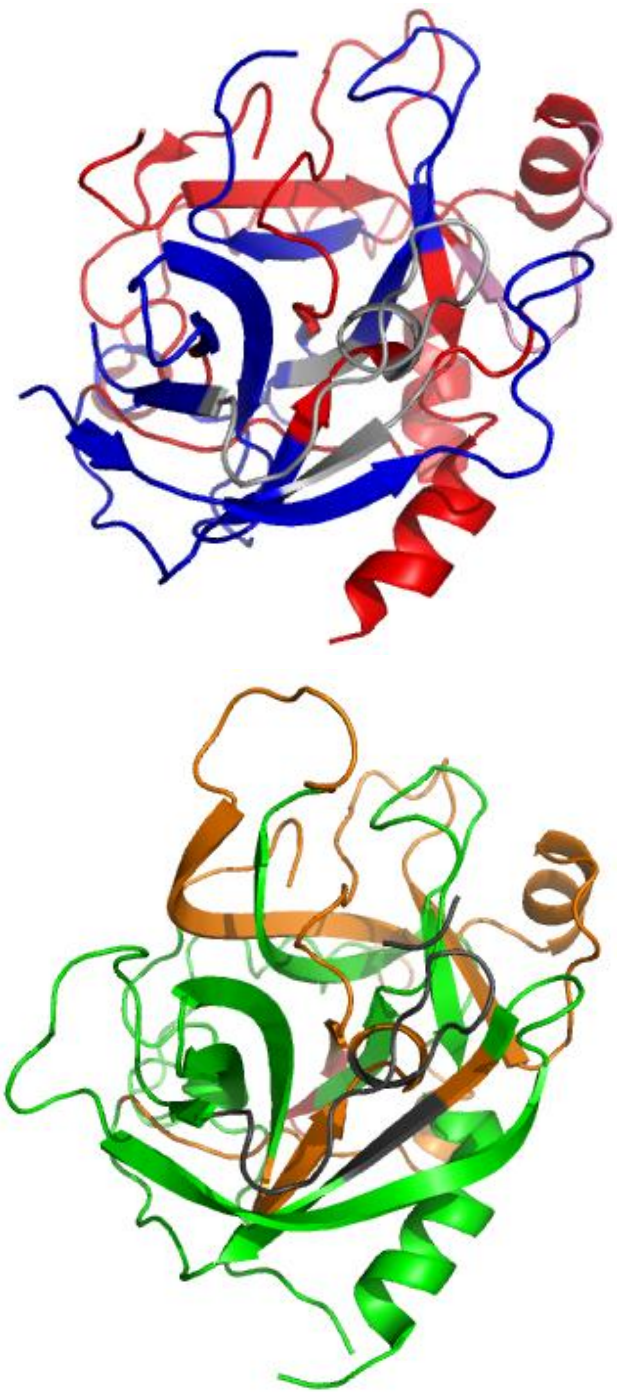

Figure 4.3: A. Coverage diagram for bovine thrombin (PDB 3PMA) where previously covered regions by Koeppe *et al.* are highlighted in blue, new coverage is shown in red, and still uncovered regions are shown in grey. B. Coverage maps for human thrombin (PDB 1PPB) where previously covered regions by Koeppe *et al.* are highlighted in green, new coverage is shown in orange, and uncovered regions are shown in gray.

each experiment. Lyophilized thrombin samples were reconstituted in 40 μL of 135 μM TM456t ML, giving a 1:2 ratio of thrombin:TM456t ML. To create fully bound TM, the same amount of TM solution was used to reconstitute 4 lyophilized fractions of thrombin, resulting in a 2:1 ratio of thrombin:TM456tML. For deuterium on-exchange experiments, 5 μL of thrombin or thrombin-TM complex was added to 45 μL of D_2O for varying exchange times (10 seconds to 20 minutes), samples were quenched and diluted by further addition of 5 μL of exchange sample to 45 μL of reducing quench solution: 25 mM H_3PO_4, 250 mM TCEP, pH 2.5. After 5 minutes of quench, 10 μL of sample was injected into the pepsin column, followed by UPLC separation and injection into the synapt for MS^E analysis.

C. RESULTS

1. Identification of peptides from pepsin digests

The Protein Lynx Global Server software for peptide identification requires digestion data without deuterium exchange first, in order to effectively find and catalog all fully hydrogenated peptides that are generated by pepsin digestion. We did each of these experiments individually for bovine thrombin, human thrombin, and TM456t ML. Each protein was "exchanged" into H_2O instead of D_2O in order to maintain the same protein concentrations between the 0 s, or non exchanged, sample and the other deuterium exchanged samples. All samples were "quenched" with a 10-fold excess of 100 mM H_3PO_4, 250 mM TCEP, pH 2.5 for 5 min to allow for significant reduction of buried disulfide bonds. We obtained 91% coverage for bovine

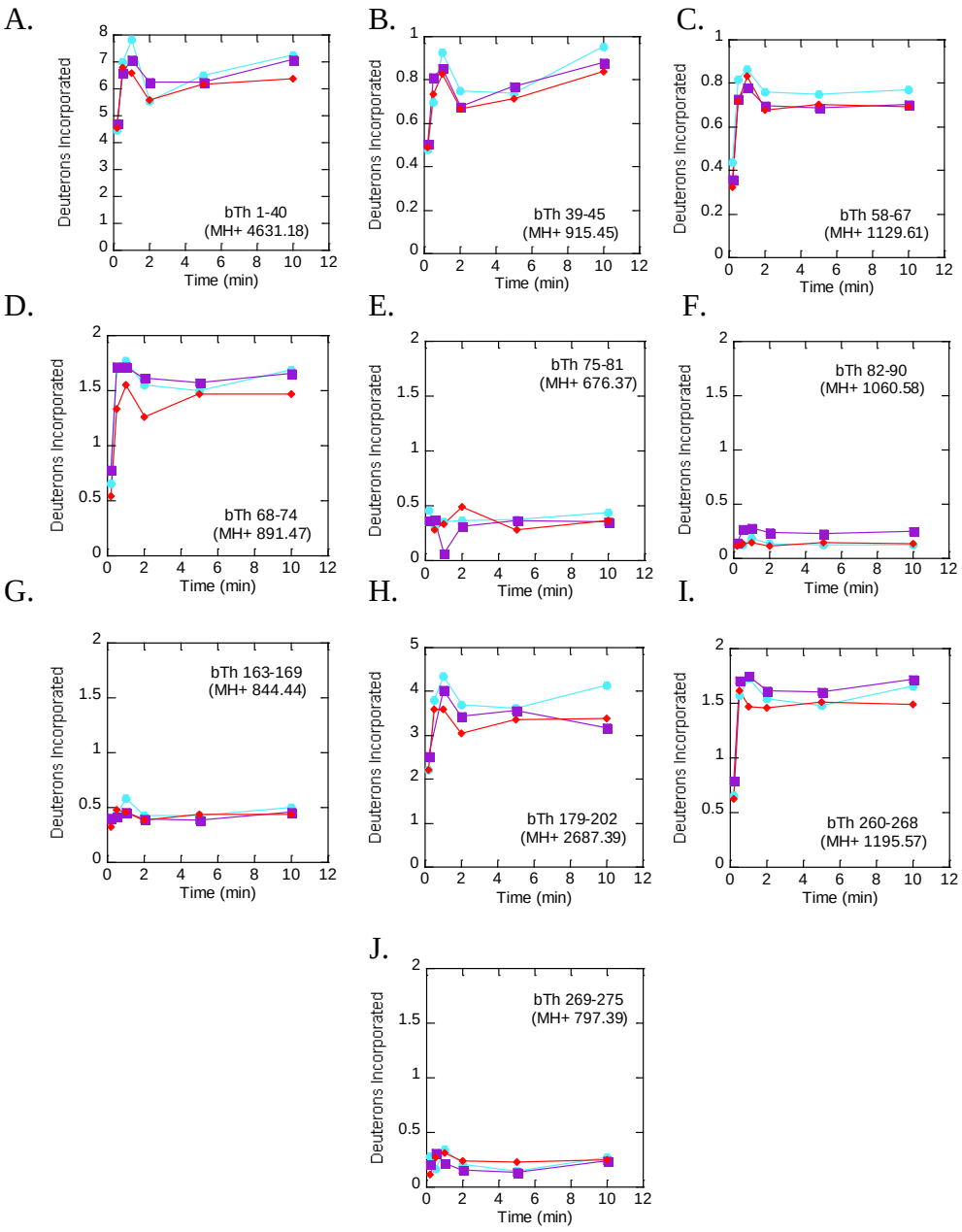

Figure 4.4: Deuterium exchange data for regions of bovine thrombin that show no protection upon TM binding: bTh alone (cyan), 1:1 bTh:TM456t ML (purple), 1:2 bTh:TM456t ML (red). Peptides by sequential numbering: Residues 1-40 (A), 39-45 (B), 58-67 (C), 68-74 (D), 75-81 (E), 82-90 (F), 163-169 (G), 179-202 (H), 260-268 (I), and 269-275 (J).

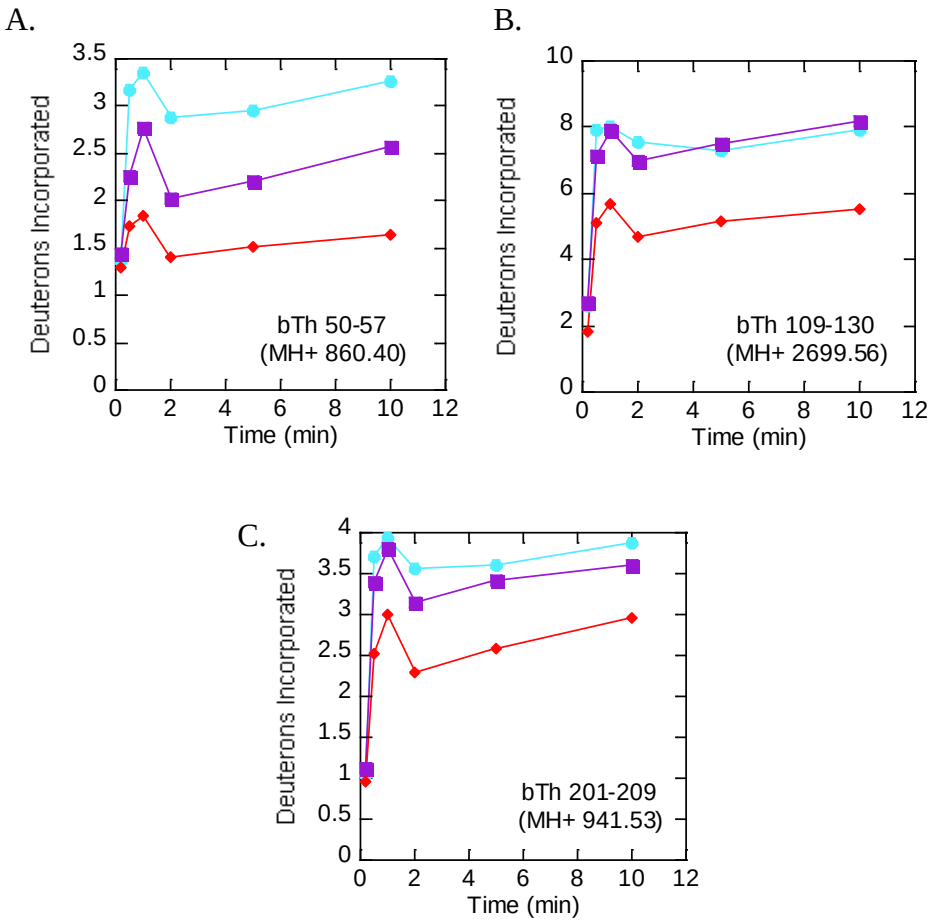

Figure 4.5: Deuterium exchange data for regions of bovine thrombin that show heavy protection upon TM binding: bTh alone (cyan), 1:1 bTh:TM456t ML (purple), 1:2 bTh:TM456t ML (red). Peptides by sequential numbering: Residues 50-57 (A), 109-130 (B), 201-209 (C).

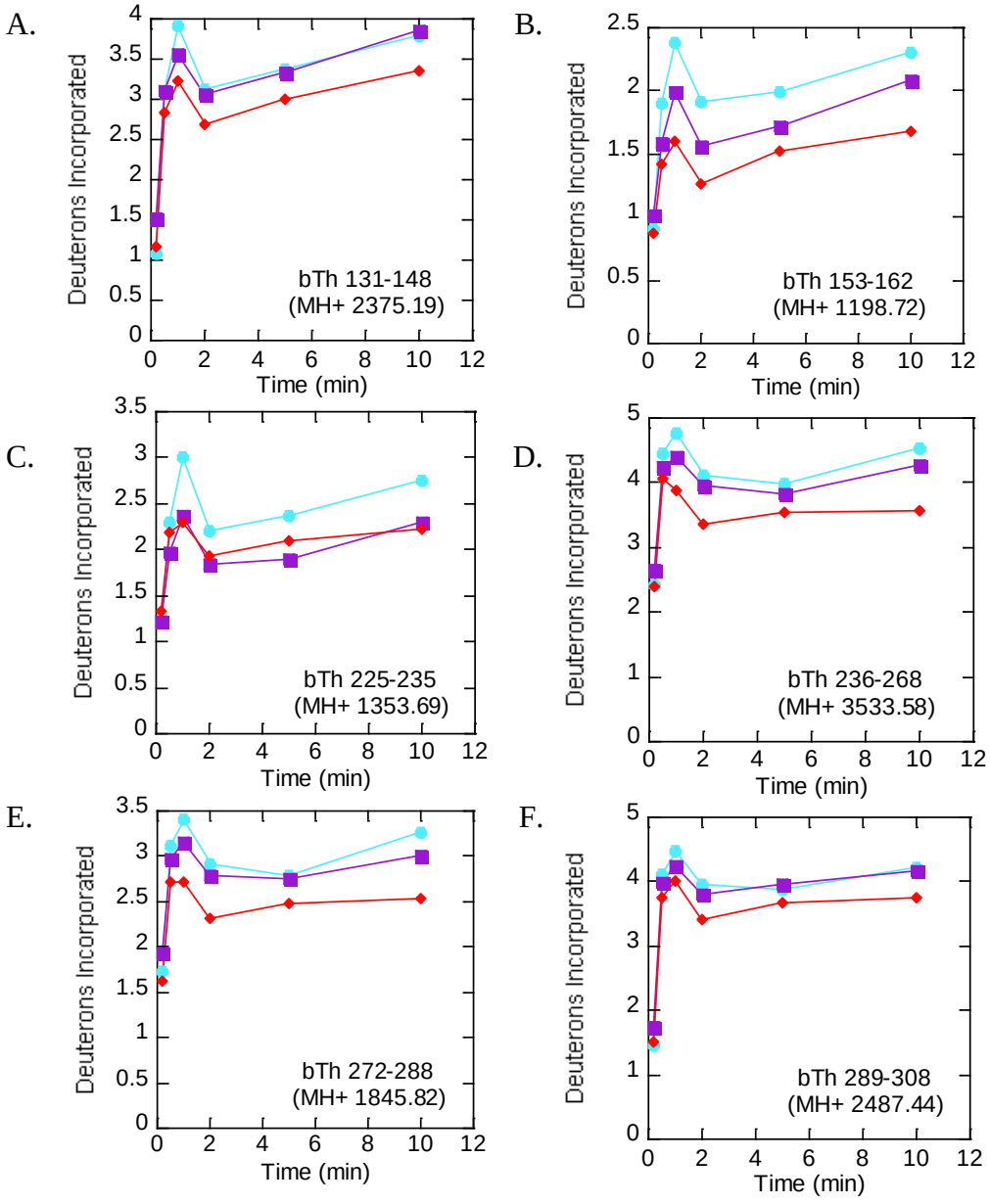

Figure 4.6: Deuterium exchange data for regions of bovine thrombin that show light protection upon TM binding: bTh alone (cyan), 1:1 bTh:TM456t ML (purple), 1:2 bTh:TM456t ML (red). Peptides by sequential numbering: Residues 1-40 (A), 131-148 (B), 153-162 (C), and 179-202 (D), 225-235 (E), 272-288 (F), 289-308 (G).

thrombin, 91% coverage for human thrombin, and 62.5% coverage for TM456t ML, with the coverage maps shown in Figure 4.1 for thrombin and Figure 4.2 for TM456t ML.

2. Bovine thrombin-TM456t ML complex exchange data

Using both 1:1 and 1:2 bTh:TM456t ML complexes, we obtained H/D exchange data at various timepoints as described in the Materials and Methods section. Previously, Mandell *et al*. (Mandell, *et al.*, 1998) showed the 70s loop and the 30s loop that form anion-binding exosite 1 (ABE1) were protected upon TM binding and Koeppe *et al.* (Koeppe, 2005) have probed thrombin allostery. Both of these studies used a TM fragment, TM45 and MALDI-TOF HDXMS. The TM45 binds with a 10-fold weaker affinity, and therefore a 5-7 fold excess of TM fragment was required in the experiments. The coverage of the thrombin sequence from the MALDI-TOF MS data was approximately 50%. To increase sequence coverage Koeppe *et al.* used both human and bovine thrombin for their experiments, proteins that are 86% identical and more than 95% similar, meaning that they effectively behave as the same protein, but small sequence differences allow for different peptides to be observed and an increase in protein sequence coverage. Here we present new peptides resulting from our significantly improved sequence coverage. First, we show significantly improved coverage of the light chain, which previously had 57% coverage, now we have overlapping peptides that cover the 45 of the 49 residues (92%) in the light chain. A similar improvement was seen for the heavy chain as well. Figure 4.2a highlights the improvements in sequence coverage by mapping new and old peptides on to the

A.

B.

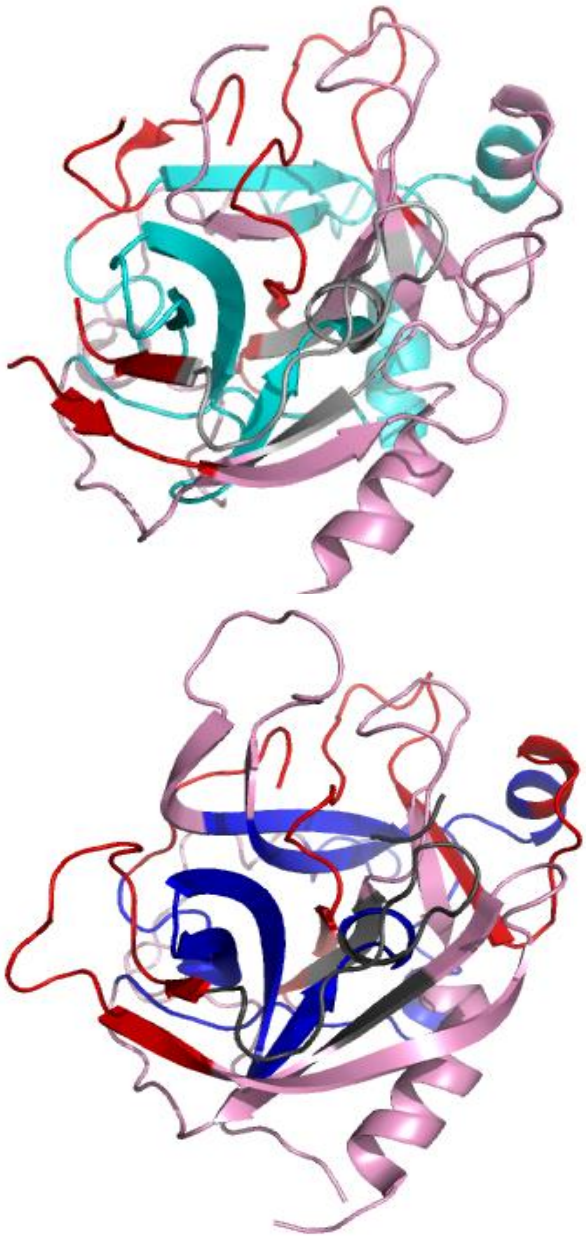

Figure 4.7: (A) Peptide protection map shown on bovine thrombin crystal structure (PDB 3PMA). Peptides showing no protection upon thrombin binding to TM are shown in cyan, peptides showing small protection are shown in pink, and peptides showing large effects are shown in red, and uncovered regions shown in light gray. (B) Peptide protection map shown on human thrombin crystal structure (PDB 1PPB). Peptides showing no protection upon thrombin binding to TM are shown in blue, peptides showing small protection are shown in pink, and peptides showing large effects are shown in red, and uncovered regions shown in dark gray.

crystal structure of bovine thrombin, with old and new overlapping peptides shown in blue, new peptides in red, and still uncovered regions shown in grey. There is only one large uncovered sequence in both bovine and human thrombin that can be readily explained because it also covers the N-X-S/T glycosylation site in thrombin.

Deuterium exchange data for the light chain of bovine thrombin is shown in Figure 4.3. Five small peptides and one large peptide cover 91.8% of the light chain, with a combination of low and medium solvent accessibility, and these peptides agree with the previous data suggesting a small protection at the N-terminus upon TM binding and no effect at the C-terminus.

New peptides in the heavy chain show a much wider variety of solvent accessibility and effects from TM protection. Figure 4.4 summarizes new data for four peptides that do not show a protective effect upon TM binding. Figure 4.5 shows data for two newly covered peptides, the N-terminus of the heavy chain and an α-helix near ABE II, that show significant protection upon TM binding. Both sets of new peptides are highlighted in Figure 4.6 on the crystal structure of bovine thrombin.

3. Human thrombin-TM456t ML complex data

In a similar experiment to the exchanges above, we obtained H/D exchange data at various time points for both human thrombin alone and 1:2 hTh:TM456t ML complex. We also found a significant increase in overall protein coverage, where we now have 100% coverage of the light chain of thrombin compared to 86.1% previously and 91.1% coverage of the heavy chain compared to approximately 60% previously. This ultimately yielded a significant improvement over the total sequence coverage from 65% to 92.2%. There were 2 very short regions that we failed to cover:

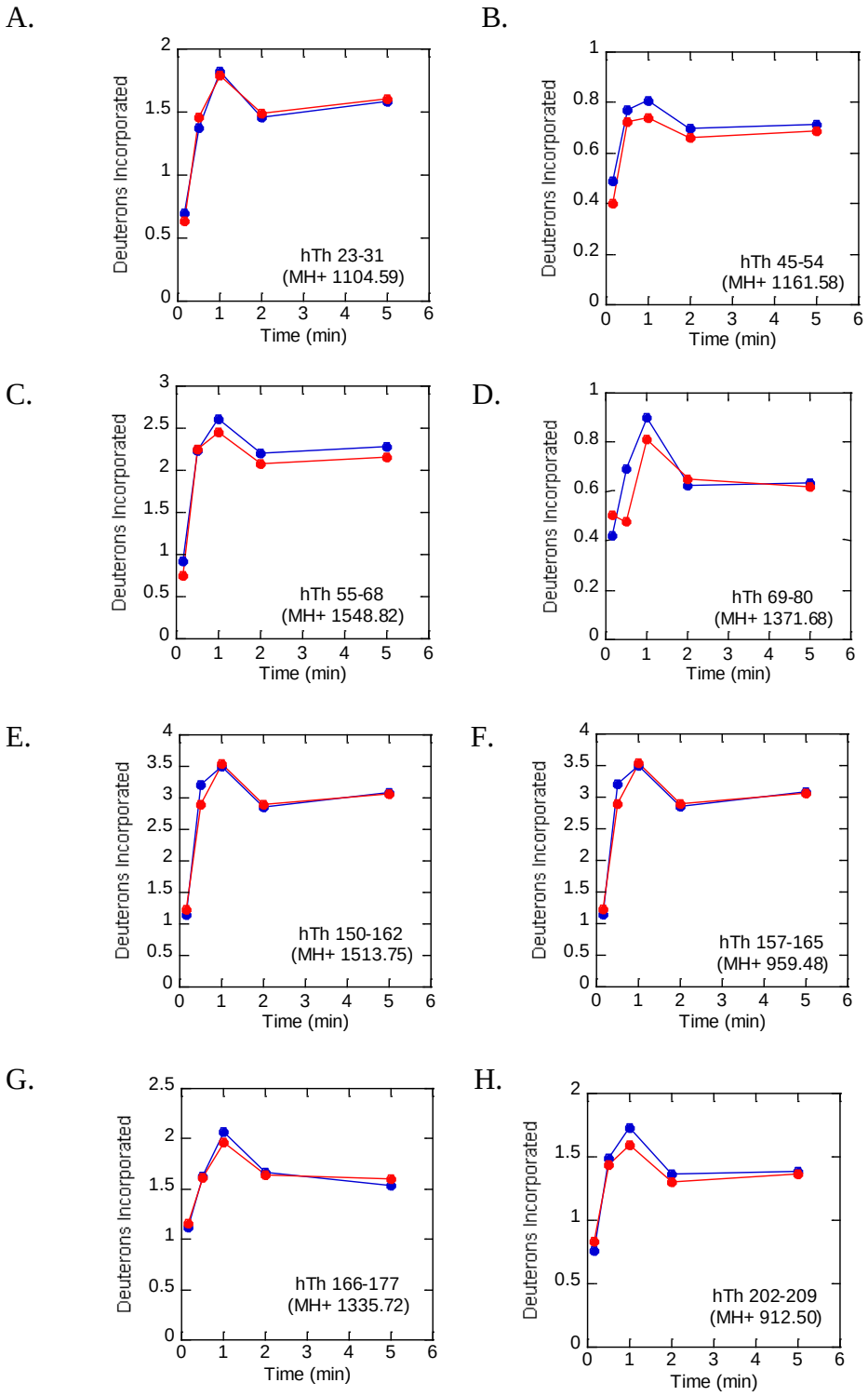

Figure 4.8: Deuterium exchange data for newly covered regions in the light and heavy chains of human thrombin that do not show protection: hTh alone (blue), 1:2 hTh:TM456t ML (red). Peptides covering these regions by sequential numbering are: Residues 23-31 (A), 45-54 (B), 55-68 (C), 69-80 (D), 150-162 (E), 166-177 (F), 202-209 (G).

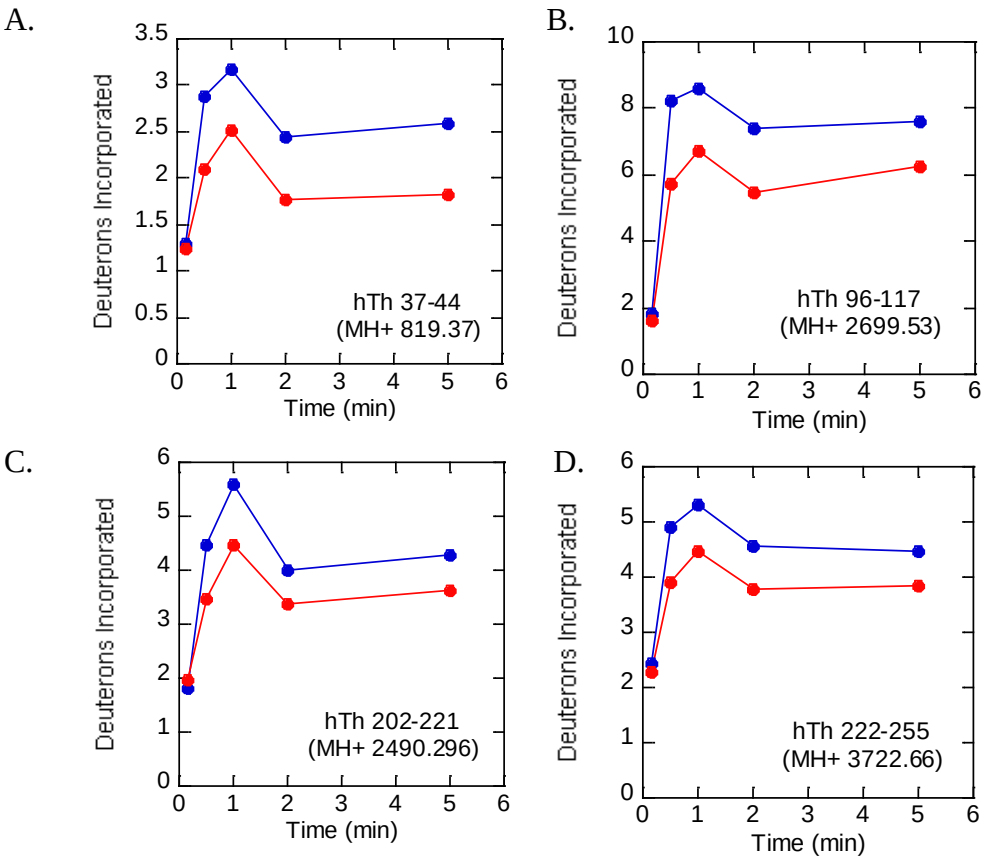

Figure 4.9: Deuterium exchange data for newly covered regions in the light and heavy chains of human thrombin that show heavy protection: hTh alone (blue), 1:2 hTh:TM456t ML (red). Peptides and residues covering these regions are: 37-44 (A), 96-117 (B), 202-221 (C), and 222-255 (D).

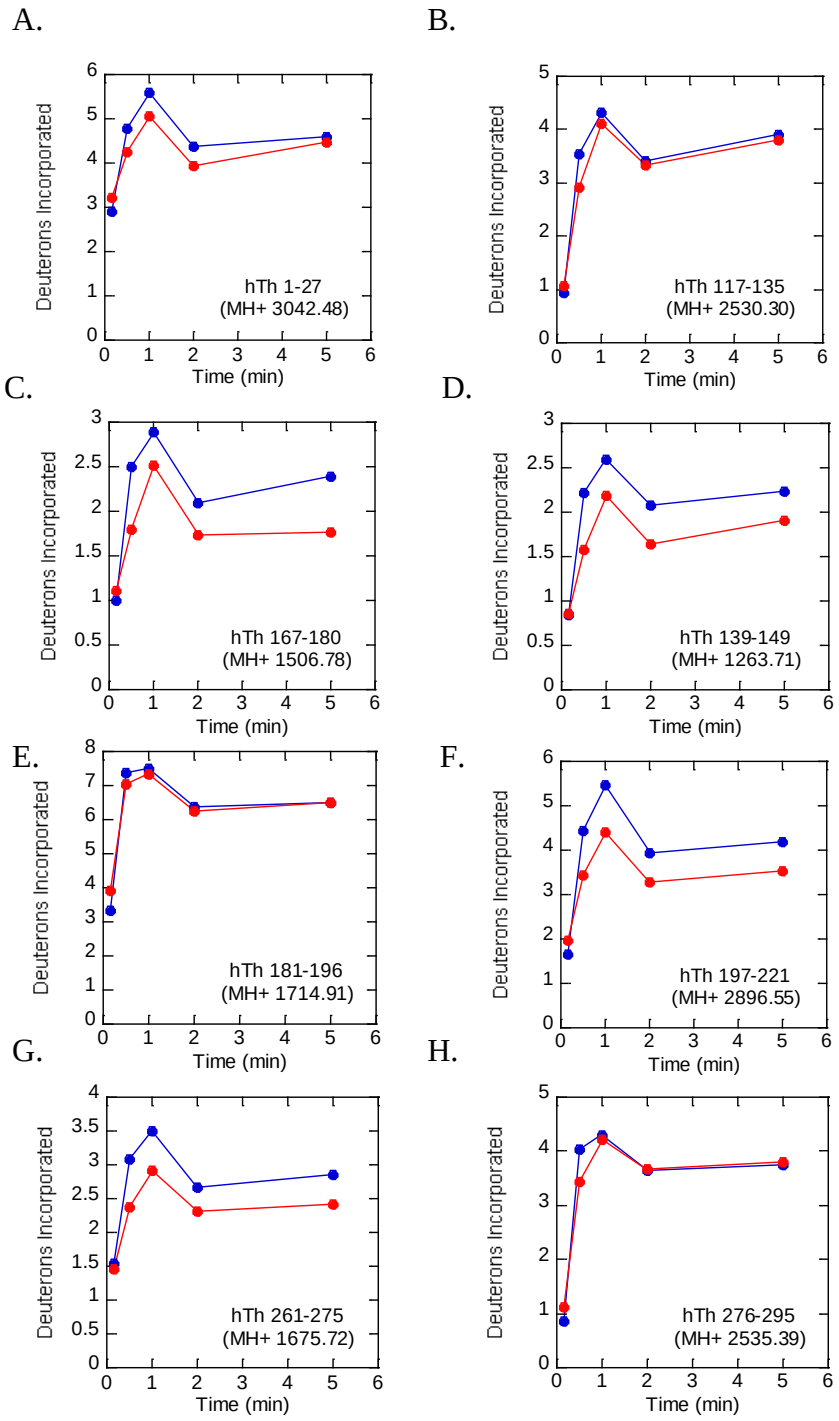

Figure 4.10: Deuterium exchange data for newly covered regions in the light and heavy chains of human thrombin that light protection: hTh alone (blue), 1:2 hTh:TM456t ML (red). Peptides and residues covering these regions are: 1-27 (A), 117-135 (B), 167-180 (C), 139-149 (D), 181-196 (E), 197-221 (F), 261-275 (G), 276-295 (H).

residues 136-138 (103_{CT}-105_{CT}) and residues 256-260 (208_{CT}-212_{CT}) and 1 large region spanning residues 81-95 (60_{CT}-64_{CT}). These are very similar to the uncovered regions of bovine thrombin, and the large region again corresponds to the single glycosylation site in thrombin, making it difficult to identify. Figure 4.2a shows highlights the improvements in sequence coverage compared to Koeppe *et al.*, with old and new overlapping peptides shown in green, new peptides in orange, and still uncovered regions shown in red.

Deuterium exchange data for the light chain of human thrombin is shown in Figure 4.X. A number of peptides span the full sequence of the light chain, and small protection can be seen in most of the light chain except for the c-terminal region, where this protection is highlighted in pink compared to the unprotected region in blue.

New peptides in the heavy chain also show a much wider variety of solvent exposure and effects from TM protection. Figure 4.X shows new regions covered that show little to no protective effects upon TM binding. Figure 4.X shows H/D exchange data for newly covered peptides, including the N-terminus of the heavy chain and other regions all throughout human thrombin, where lighter protection is highlighted in pink and stronger protection is highlighted in red. All these sets of peptides are highlighted in Figure 4.6b on the crystal structure of human thrombin.

D. Discussion

1. New portions of bovine thrombin show varied solvent accessibility

The data presented here allows us to build on previous experiments and it suggests that thrombin is even more structurally dynamic than formerly shown in H/D experiments. We have found a number of heretofore unseen peptides after TCEP reduction, pepsin digestion, and electrospray ionization into the Waters G2S Q-TOF mass spectrometer. These peptides have given us greater insight into the dynamic behavior of thrombin in solution. Some of these new peptides show little deuterium exchange under any condition and do not have a noticeable protective effect, as summarized in Figures 4.4 and 4.8. These peptides are also shown in blue in Figure 4.7 and mostly appear to either be found within the core of the protein or protected by secondary structure elements along the surface.

However, there are also a number of new peptides that show both light and heavy protective effect upon TM binding to thrombin. These data are summarized in Figures 4.5 and 4.9 (heavy) and Figures 4.6 and 4.10 (light), and also shown in the diagram in Figure 4.7. These protected residues are highlighted in pink (low protection) and red (high protection). These new peptides cover multiple, distant parts of the protein as well as being far from the binding site for TM, ABEI. This strongly suggests that a number of structural changes happen throughout thrombin upon binding to TM, all of which could contribute to the dramatically altered PC activation kinetics.

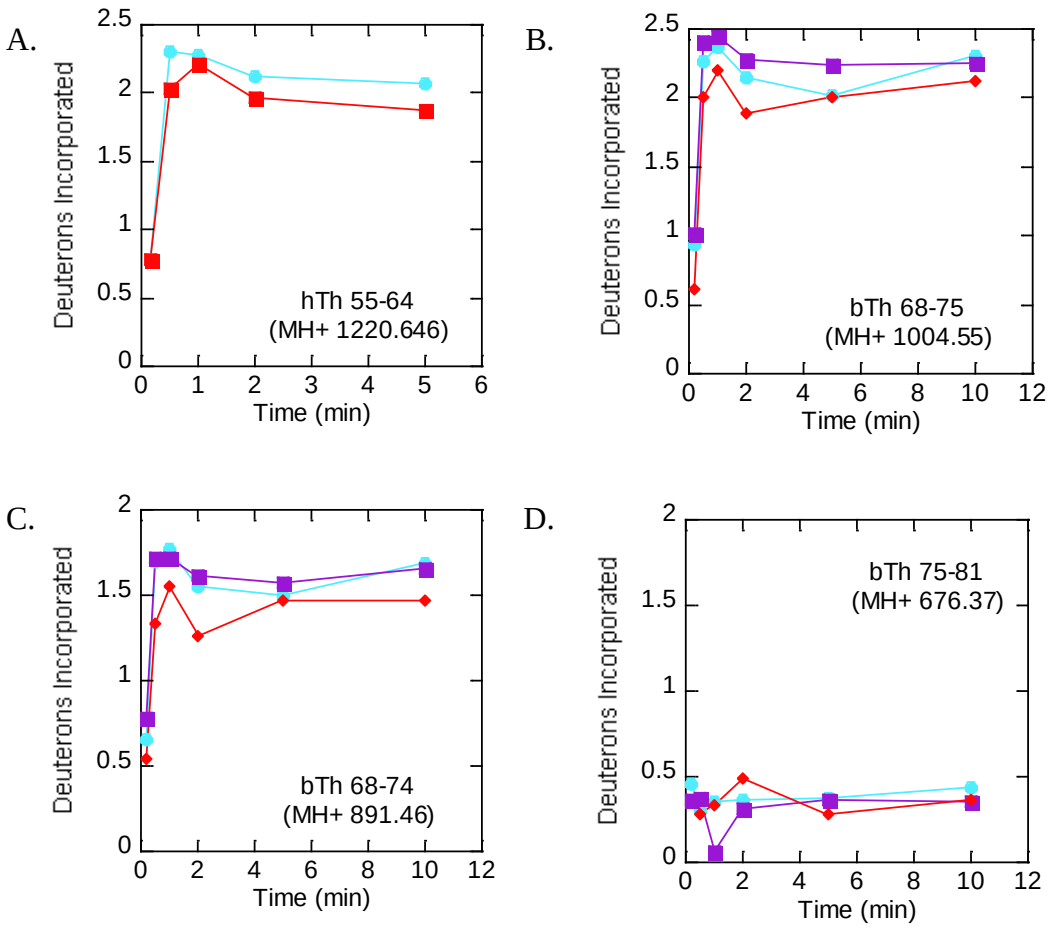

Figure 4.11: HD exchange data for FRKSPQELLC in both human and bovine thrombin. Human thrombin (A) and bovine thrombin (B,C, and D) are shown with thrombin alone in cyan, 1:1 thrombin:TM456t ML in purple, and 1:2 thrombin:TM456t ML in red.

Additionally, one short region near the N-terminus of the heavy chain of both bovine and human thrombin showed very light protection previously, and we a similar effect in our data here. These peptides are summarized in Figure 4.11 and help show further agreement with previous data, even for subtle protection effects.

Accelerated MD simulations had previously shown that a number of regions of thrombin are expected to have decreased motions on the ms-ms time scale upon TM binding. On slow time-scales thrombin:TM456 exhibits remarkably more reorientation dynamics in the active site loop regions; the 90_{CT} loop (residues 122 to 132), the 148_{CT} loop (residues 184 to 192), the 170_{CT} loop (residues 213 to 221), the 186_{CT} loop (residues 228 to 234) and the 220_{CT} loop (residues 265 to 274). In the AMD simulation, these regions actually showed more reorientation dynamics on slow time scales. When this paper was published, it didn't make sense to us that in previous HDXMS work, we had seen a small difference, where the 90_{CT} loop (residues 122 to 132) showed less amide exchange in the TM-bound form as compared to thrombin alone. Now we have the same phenomenon going on across several regions of thrombin. In fact, there is an amazing correlation between those regions that show decreased amide exchange in the TM-bound form, and those regions identified as undergoing more reorientation dynamics on slow time scales (Figure 4.12). These motions are correlated to motions in TM, according to the AMD simulations, and apparently the HDXMS is picking up these small differences in the redistribution dynamics.

A remarkable new result from the HDXMS is the strong protection of the first eight residues of the heavy chain. It is well-known that when serine proteases are

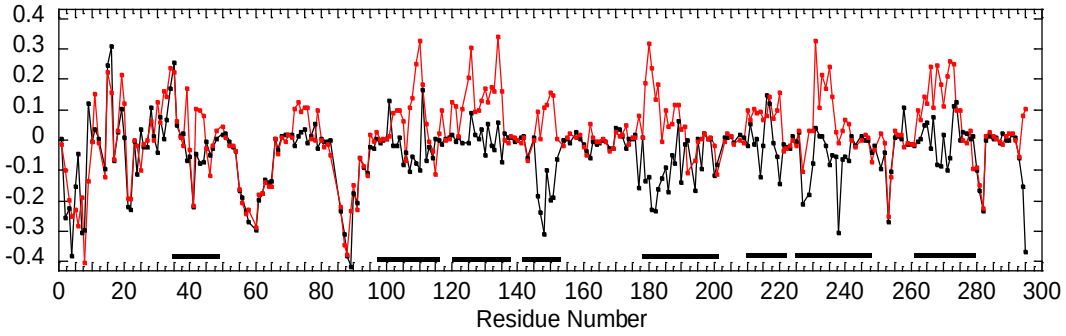

Figure 4.12: Differences in order parameters calculated from AMD simulations (to capture slow time scale motions) between thrombin-TM456 (red) and thrombin-TM56 (black) compared to the regions that show protection when TM456 is bound. The regions that show protection in the HDXMS are marked with black lines. There is a remarkable correlation between those regions that are specifically responding to TM456 binding in the AMD simulations and those regions showing protection in the HDXMS experiments.

activated by cleavage resulting in the two-chain form containing the light chain and the heavy chain, the newly generated N-terminus (usually called the N-terminus of the heavy chain) inserts into the core of the protease. This insertion is thought to be critical for proper formation of the active site for catalysis. The N-terminus is always seen in crystal structures of thrombin as well-inserted, but that may be because the structures always have an active site ligand in them. Since no one has really been able to observe a structure of the TM-bound thrombin in the absence of an active site ligand, this has not been seen before. This result would predict that, in fact, the highly improved kcat for protein C activation may directly result from TM-mediated positioning of active site residues for optimal catalysis.

E. Conclusions

Using new tools for H/D exchange mass spectrometry, we have re-analyzed the interaction of thrombin with TM in solution. We have been able to illuminate the dynamic motions of entirely new portions of the protein, finding areas with new protective allosteric effects as well as unchanging portions of the protein that were previously unseen. Furthermore, we can now see a significant portion of TM that was once invisible. We can use this information, combined with previous experiments by our colleagues as well as new ongoing experiments to continue working to improve our understand of the activity of thrombin in solution and its interactions with TM.

F. References

[1] Fuglestad B, Gasper PM, Tonelli M, McCammon JA, Markwick PRL & Komives EA (2012) The dynamic structure of thrombin in solution. *Biophysical Journal* **103**: 79-88.

[2] Gasper PM, Fuglestad B, Komives EA, Markwick PRL & McCammon JA (2012) Allosteric networks in thrombin distinguish procoagulant vs anticoagulant activities. *Proc Natl Acad USA* **109**: 21216-21222.

[3] Koeppe J, Beach, M., Baerga-Ortiz, A., Kerns, J., and Komives, E. (2008) Mutations in the fourth EGF-like domain affect thrombomodulin-induced changes in the active site of thrombin. *Biochemistry* **47**: 10933-10939.

[4] Koeppe J, Komives, EA (2006) Amide H/2H exchange reveals a mechanism of thrombin activation. *Biochemistry* **45**: 7724-7732.

[5] Koeppe JR, Seitova, A., Mather, T., Komives, E. (2005) Thrombomodulin tightens the thrombin active site loops to promote protein C activation. *Biochemistry* **44**: 14784-14791.

[6] Lechtenberg BC, Johnson DJ, Freund SM & Huntington JA (2010) NMR resonance assignments of thrombin reveal the conformational and dynamic effects of ligation. *Proc Natl Acad USA* **107**: 14087-14092.

[7] Mandell JG, Falick AM & Komives EA (1998) Identification of protein-protein interfaces by decreased amide proton solvent accessibility. *Proc Natl Acad USA* **95**: 14705-14710.

[8] Treuheit NA, Smith MA & Komives EA (2011) Thermodynamic compensation upon binding to exosite I and the active site of thrombin. *Biochemistry* **50**: 4590-4596.

Chapter V

Agouti-Related Protein as a Handle for Targeting TM to Activated Platelets

A. Introduction

Integrins are the large, complex family of proteins responsible for the management of cell-cell adhesion. Integrins generally are αβ heterodimers, with 24 distinct combinations of 8 distinct β and 18 α subunits in mammals (Hynes, 2002). These large (~1600 amino acid) proteins exist almost entirely on cell surfaces, with a single transmembrane domain, and a short (20-50 amino acid) cytoplasmic tail. They play critical roles in development, immune response, cancer and other human diseases, and of particular interest here, hemostasis (Hynes, 2002). Furthermore, most integrins are typically expressed in inactive states, requiring some sort of signal to trigger their activation. This signal commonly comes in the form of "inside-out" activation, where a signal molecule binds to the cytoplasmic tail, and an allosteric change is propagated through the transmembrane domain to the large extracellular domain, which can open up and bind assorted ligands.

Cell-cell adhesion is a central component for a number of critical processes, and one excellent example of this property is in the middle of a blood clot. Two of the main components in a blood clot are fibrin and activated platelets, and at the interface of these activated platelets is $\alpha_{IIb}\beta_3$ integrin (Bennett, 1996). The $\alpha_{IIb}\beta_3$ integrin has two conformations: a closed, inactive conformation and an open, ligand-binding conformation (Takagi, *et al.*, 2002).

The $\alpha_{IIb}\beta_3$ integrin, in its active conformation, provides a unique target that is exclusively present along the surface of blood clots. Thus, a molecule that is capable of binding to the $\alpha_{IIb}\beta_3$ integrin could be targeted toward active blood clots. However,

A.

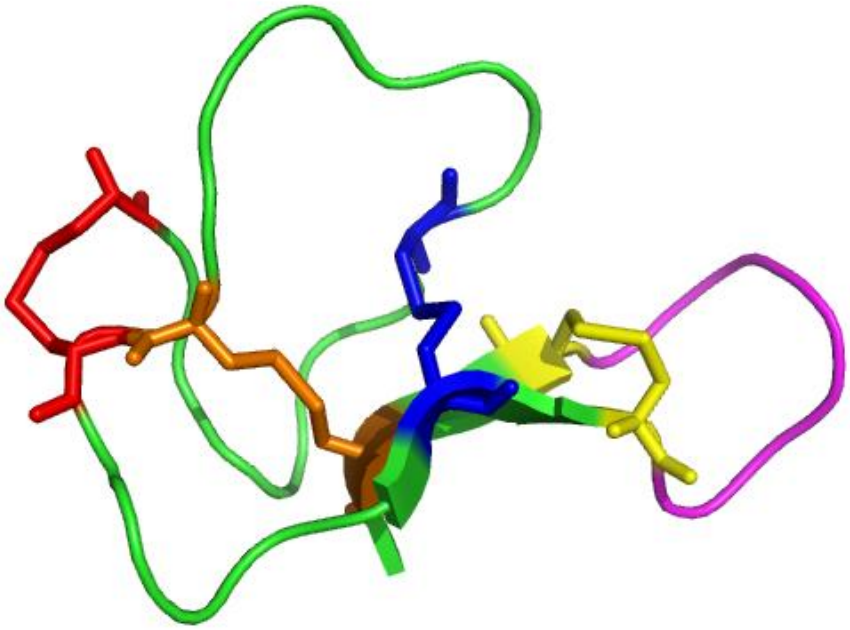

B.

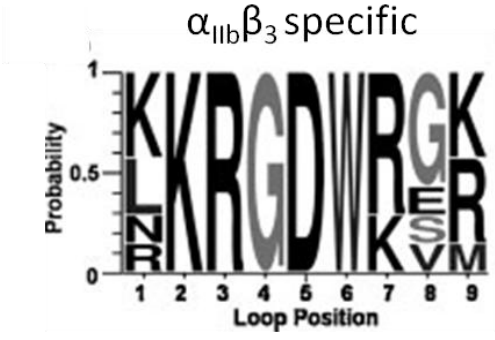

C.

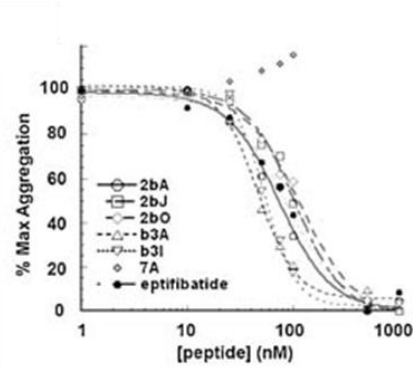

Figure 5.1: (A) Crystal structure of the C-terminal fragment of AgRP with the four disulfide bonds colored in red, blue, orange, and yellow, and the loop colored in purple was randomized with RDG peptide sequence to generate $\alpha_{IIb}\beta_3$ integrin binding partners. (PDB 1MR0) (B) Summarizes the sequences found for the randomized loop that successfully bound to $\alpha_{IIb}\beta_3$ integrin. (C) Platelet aggregation assay using various AgRP constructs to bind $\alpha_{IIb}\beta_3$ integrin and inhibit platelet aggregation. Figures B and C are taken from Silverman *et al. (Silverman, et al., 2011).*

since most integrins bind an RGD tripeptide motif(Li, *et al.*, 2003), it is challenging to find molecules that bind to a single integrin and not to other family members. For example, the $\alpha_5\beta_3$ integrin uses a very similar binding motif to $\alpha_{IIb}\beta_3$ integrin, but where $\alpha_{IIb}\beta_3$ integrin is involved in blood clotting, $\alpha_V\beta_3$ integrin has generated significant interest as a cancer target based on its potential involvement with tumor invasiveness (Brooks, *et al.*, 1994, Alghisi & Ruegg, 2006). In the end, strong specificity of potential binding partners is required with these integrins before they can be used to target drugs to specific cell types *in vivo*.

This problem was solved in principle by Silverman *et al.* (Silverman, *et al.*, 2009) by using a variant of the C-terminal domain of the human Agouti-related protein (AgRP). This truncated form of AgRP is a small, cystine-knot protein that serves as a scaffold for protein engineering. This engineering was accomplished by replacing the fourth loop of AgRP with new, randomly generated 9 residue sequences containing the RGD integrin binding motif. In doing so, they were able to generate a variant that bound to the $\alpha_V\beta_5$ integrin with both high affinity and specificity. They continued to apply this technique in order to develop specific binding partners for other integrins, including $\alpha_{IIb}\beta_3$ integrin. Silverman *et al.* (Silverman, *et al.*, 2011) successfully developed another variant of AgRP that bound to $\alpha_{IIb}\beta_3$ integrin with high affinity and specificity. The crystal structure of the C-terminal portion of AgRP protein used as the scaffold for protein binding studies is shown in Figure 5.1A, with its four disulfide bonds in various colors and the loop used to generate randomized RGD binding colors shown in purple. The sequences of successful $\alpha_{IIb}\beta_3$ integrin binding partners is

summarized in Figure 5.1B, and the platelet aggregation inhibition assay for those proteins is shown in Figure 5.1C. Thus, they have successfully

We thought that we might be able to use the selected AgRP that specifically targets the $\alpha_{IIb}\beta_3$ integrin to target TM to activated platelets. An advantage of this approach is that the AgRP derivative was expressed in *Pichia pastoris* because of the high number of disulfide bonds present in cystine knot proteins. Thus, we began a collaboration to attempt to fuse our new TM constructs with this AgRP protein designed to bind to $\alpha_{IIb}\beta_3$ integrin with the goal of creating a fusion protein that could both interfere with platelet aggregation and target TM to the surface of blood clots to inhibit further thrombin cleavage of fibrinogren and protease-activated receptors. Here, we will summarize our data and initial attempts to express, purify, and characterize new TM-AgRP fusion proteins for their ability to both activate thrombin and bind to the surface of platelets.

B. Materials and Methods

1. TM-AgRP Fusion Proteins

Multiple TM-AgRP fusion protein constructs were cloned into pPIC9K expression vectors for *P. Pastoris*, using the same methods described in Chapter 3. Four different constructs were made: N-terminal AgRP for AgRP-TM456t, C-terminal AgRP for TM456t-AgRP, and then two more constructs with a short G4S linker between the two proteins for AgRP-G4S-TM456t and TM456t-G4S-AgRP. The DNA and protein sequences for these fusion proteins are shown in Figure 5.2. These genes

A.

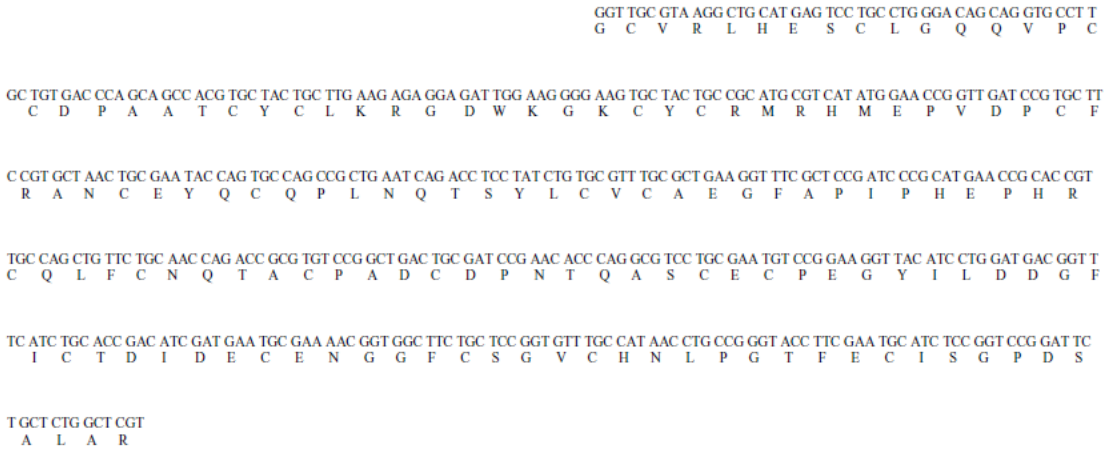

B.

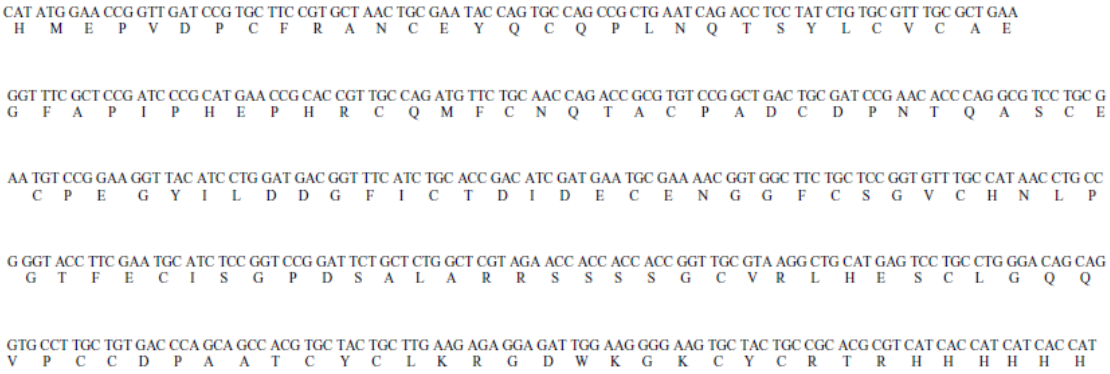

Figure 5.2: Protein and DNA sequences for TM-AgRP fusion constructs. (A) AgRP-TM456t ML fusion construct with no linker made in our lab. (B) Ag-RP-G4S-6H fusion construct with a GSSSS linker from the Cochran lab.

were cloned into SMD1168 cells, screened for activity and stored in aliquots at -80^{o}C. Protein was expressed and purified from both shake flask and fermenter purifications as described earlier.

C. RESULTS

TM Fusion Proteins show good expression, but poor activity

The various TM and AgRP fusion proteins were successfully expressed and purified from *P. Pastoris* supernatant. Specific activities from both shake flask purification and fermenter purifications are shown in Tables 5.1 and 5.2, with protein samples taken and analyzed from each purification step. In all cases, the overall TM cofactor activity in both protein purifications was significantly impaired as compared to the activity of TM456t, shown in the purification tables for comparison.

D. Discussion

Although the TM fusion proteins can be expressed and purified, it seems that some part of this protein combination is destabilizing the complex as a whole. Extremely low activity relative to TM456t alone characterizes the protein across its purification. This also applies to the multiple permutations of TM, AgRP, and linker combinations to make the fusion protein. An explanation for this loss in activity is not readily apparent because these are both proteins that can be successfully purified individually in *P.pastoris*, but attaching a new subunit to either end of TM is significantly reducing its cofactor activity. There was a slight gain in protein activity

Table 5.1: JBC activity table for purification of TM456t-3GS-AgRP from fermentation with activities and approximate protein yield at each step. Purification was performed with 0.1% TFA mobile phase in reversed-phase HPLC step.

TM456t-3GS-AgRP Purification Step	**Specific Activity (nmol aPC*min^{-1}*mL^{-1})**	**Protein Yield (mg)**
QAE Sephadex	9 x 10^3	100 mg
Hi Load Q	2.5 x 10^4	24 mg
HPLC (0.1% TFA)	4.9 x 10^4	6 mg
Size Exclusion	9 x 10^4	3 mg
TM 456t ML	9 x 10^5	

Table 5.2: JBC activity table for purification of AgRP-3GS-AgRP from shake flasks with activities and approximate protein yield at each step. Purification was performed with 0.1% TFA mobile phase in reversed-phase HPLC step.

Purification Step AgRP-3GS-TM456t	**Specific Activity (nmol aPC*min^{-1}*mL^{-1})**	**Protein Yield (mg)**
Hi Load Q	1 x 10^4	15 mg
HPLC (20 mM NH_4OAc)	1.8 x 10^4	5 mg
Size Exclusion	3 x 10^4	2 mg
TM 456t ML	9 x 10^5	

for fermenter-expressed protein versus shake flask-expressed protein, but it is still well below the level of even wild-type TM45. Higher pH reversed-phase HPLC conditions as described in Chapter 3 also failed to noticeably improve activity. Experiments done previously in our lab have shown that binding to the 4th domain has a noticeable effect on cofactor activity (Komives lab, unpublished), and it may also be that without the 3rd disulfide bond in the 6th domain, attaching a new protein subunit could begin to destabilize that region as well. It may be that the expression and purification of these fusion proteins requires more optimization, but our preliminary data suggests that fusion with AgRP proteins will not be a successful avenue for potential future delivery of TM to blood clots. However, the potential for our new high activity constructs TM456m and TM456t remains high because of both the relative ease of purification in high quantities as well as the activity at a level close to that of natural, full length TM456 and presents many interesting possibilities for future use in therapeutic treatments.

E. References

[1] Alghisi GC & Ruegg C (2006) Vascular integrins in tumor angiogenesis: mediators and therapeutic targets. *Endothelium* **13**: 2006.

[2] Bennett JS (1996) Strucutural biology of glycoprotein IIb-IIIa. *Trends Cardiovasc Med* **16**: 31-36.

[3] Brooks PC, Clark RA & Cheresh DA (1994) Requirement of vascular integrin aVB3 for angiogenesis. *Science* **264**: 569-571.

[4] Hynes RO (2002) Integrins: Bidirectional, Allosteric Signaling Machines. *Cell* **110**: 673-687.

[5] Li R, Hoess RH, Bennett JS & DeGrado WF (2003) Use of phage display to probe the evolution of binding specificity and affinity in integrins. *Protein Eng* **16**: 65-72.

[6] Silverman AP, Kariolis MS & Cochran JR (2011) Cystine-knot peptides engineered with specificites for αIIbβ3 or αIIbβ3 and α5β3 integrins are potent inhibitors of platelet aggregation. *J Mol Recognit* **24**: 127-135.

[7] Silverman AP, Levin AM, Lahti JL & Cochran JR (2009) Engineered cystine-knot peptides that bind alpha(V)beta93) integrin with antibody-like affinities. *J Mol Biol* **385**: 1064-1075.

[8] Takagi J, Petre BM, Walz T & Springer TA (2002) Global conformational rearrangements in integrin extracellular domains in outside-in and inside-out signaling. *Cell* **110**: 599-511.